ABSTRACT

USE OF EM-38 SOIL SURVEYS IN FORAGE FIELDS AT A SALINE DRAINAGE WATER REUSE SITE TO CALIBRATE A HYDRO-SALINITY MODEL FOR DECISION SUPPORT

Soil salinity is a major factor affecting irrigated agriculture in the western San Joaquin Valley of California. Soil salinity is a spatially and temporally dynamic property, and thus, mapping at the field scale requires a rapid and reliable means of taking geospatial measurements. EM-38 soil salinity surveys were conducted at the SJRIP (San Joaquin River Improvement Project) facility managed by the Panoche Water District (Los Banos, California) where subsurface drainage water is re-used on forages such as 'Jose' tall wheatgrass (*Thinopyrum ponticum* var. 'Jose') and alfalfa (*Medicago sativa*) to reduce drainage discharge and salt loading into the San Joaquin River. Soil samples taken to a depth of 120 cm (4 ft.) in 30 cm (1 ft.) increments for calibration of EM-38 data, were analyzed for pH, EC_e, gravimetric water content and saturation percentage. The average EC_e for spring and fall 2016 samples was 12.5 to 19.3 dS/m for tall wheatgrass (TWG) fields and 8.9 to 14.4 dS/m for alfalfa (ALF) fields. In 2017, the average ECe ranged from 14.4 to 18.6 ds/m and from 9.5 to 13.3 ds/m for TWG and ALF fields, respectively. GIS maps were developed depicting the spatial variability of salts in the fields. Data will be used to calibrate a computer model (CSUID) developed as a decision support tool to optimize soil leaching requirement guidelines for irrigation water of varying salinity levels, with the overall goal of improving the sustainability of forage production using saline waters in the SJRIP.

Amninder Singh
May 2018

USE OF EM-38 SOIL SURVEYS IN FORAGE FIELDS AT A SALINE DRAINAGE WATER REUSE SITE TO CALIBRATE A HYDRO-SALINITY MODEL FOR DECISION SUPPORT

by

Amninder Singh

A thesis

submitted in partial

fulfillment of the requirements for the degree of

Master of Science in Plant Science

in the Jordon College of Agricultural Sciences and Technology

California State University, Fresno

May 2018

APPROVED

For the Department of Plant Science:

We, the undersigned, certify that the thesis of the following student meets the required standards of scholarship, format, and style of the university and the student's graduate degree program for the awarding of the master's degree.

Amninder Singh
Thesis Author

Sharon E. Benes (Chair) Plant Science

Florence Cassel Sharma Plant Science

Nigel W.T. Quinn Berkeley National Laboratory, Berkeley, CA

For the University Graduate Committee:

Dean, Division of Graduate Studies

AUTHORIZATION FOR REPRODUCTION

OF MASTER'S THESIS

X I grant permission for the reproduction of this thesis in part or in its entirety without further authorization from me, on the condition that the person or agency requesting reproduction absorbs the cost and provides proper acknowledgment of authorship.

_____ Permission to reproduce this thesis in part or in its entirety must be obtained from me.

Signature of thesis author:_____

ACKNOWLEDGMENTS

I am very grateful and would like to acknowledge my thesis committee for their help and immense knowledge. Firstly, I would like to express my sincere gratitude to my thesis advisor, Dr. Sharon Benes for the unconditional support, mentorship, patience, and motivation. I could not have imagined having a better advisor and mentor for my M.S. study. Besides my advisor, I would like to thank Dr. Nigel Quinn and Dr. Florence Cassel for their meaningful insights, encouragement and continuous guidance throughout the research and thesis writing process.

The support of SJRIP staff who provided assistance with conducting EM38 soil surveys and collecting irrigation water samples is greatly appreciated. I would also like to thank Alan Penteriche, Lucas Ingold, Leandro Zambon, Ulysses Bottino Jr., Giuliano Galdi and Sangeeta Bansal for the stimulating discussions and help in collecting field data as well as lab analysis.

I would like to acknowledge the help from Dr. Denis Bacon, Charles Cochran, and Janet Robles at the Graduate Laboratory. Also, I thank Tim Jacobson from Center for Irrigation Technology (CIT) for helping with the setup of equipment for EM38 surveys. A very special gratitude goes to the professors, staff, and all the wonderful people I met at the Department of Plant Sciences.

Funding for this project was provided by California Department of Water Resources (DWR). I am genuinely grateful for the Harvey Scholarship/Jordan Assistantship from Jordan College of Agricultural Sciences and Technology.

Last but not the least, my greatest gratitude goes to my parents. This accomplishment would not have been possible without them.

Thank you.

TABLE OF CONTENTS

Page

Page

LIST OF TABLES

Page

LIST OF FIGURES

Page

Page

Page

INTRODUCTION

Soil salinity is a major limiting factor for irrigated agriculture, in arid and semi-arid regions of the world. An estimated 60 million ha (or 20 percent of the world's irrigated area) are affected by soil salinity - soil salinity problems take an estimated 0.3 to 1.5 million ha of farmland out of production each year and decrease the production potential of another 20 to 46 million ha (FAO, 2015). This is important because irrigated agriculture provides 40% of the world's total food and fiber production. There are historical examples which illustrate the severe impact that salinity can have agriculture: the flat wastelands of southwestern Iraq, once highly fertile and productive and called "the Fertile Crescent", have been barren since the 12th century (Jacobsen & Adams, 1958). Without a natural drainage outlet salinity increased which ultimately lead to their abandonment

The western San Joaquin Valley (WSJV) of California is a highly productive agricultural area affected by salinity and drainage problems (Letey, 2000). Although groundwater levels have dropped in recent years due to a reduction in available water supply and decreased irrigation applied water due to conversion to micro-irrigation and other water conserving technologies -soil salinity problems persist and are projected to increase due to a drier climate and increased use of saline waters for irrigation (Benes, 2013; Benes et al. 2014). Soil salinity impacts are not limited to farmlands where it impairs crop production, or to the environment, where the discharge of saline drainage waters has risks associated with wildlife, but it also impacts the regional economy. It is estimated that, if unmanaged, the accumulation of salinity in the Central Valley of California could cause a loss of $2.167 billion in the value of California's goods and services by 2030 (Howitt et al., 2009). Another reason salinity needs particular attention is

that, being a conservative constituent, salts will accumulate over time in the crop root zone if water supply is insufficient to provide dilution and drainage insufficient to provide long-term removal from the crop root zone and disposal. These significant, but slowly developing, problems are often overlooked and/or action is postponed.

Considered the need to double food production to feed a projected global population of 9 billion plus by 2050 (Gregory & George, 2011; Roberts, 2011; Tilman et al., 2011), there is a great likelihood that areas affected by salinity will be brought under cultivation and water resources previously deemed too saline or marginal will be used for irrigation. For this, water resources such as recycled water, treated effluent, desalinized water, and saline sodic drainage water could be employed (Assouline et al., 2015; Grattan et al., 2014; Weber et al., 2014). Reuse of saline-sodic drainage water (DW) to irrigate salt-tolerant forage crops is attractive and leads to greater irrigation water use efficiency because it reduces the volume of DW requiring disposal and the land area affected by salinity (Suyama et al., 2007a). This is suited for the WSJV because of the availability of such water and lack of disposal options. The sustainability of forage production using saline irrigation requires adequate leaching to transport accumulated salts below the crop root zone. Quantifying the amount of leaching required for various soils and for leaching water of variable quality requires the development of simulation models, specifically formulated to help soil and water management making for saline water reuse projects such as the San Joaquin River Improvement Project (SJRIP) operated by the Panoche Drainage District.

The SJRIP is a 6,000 acre drainage water reuse facility where salt tolerant forages like ‘Jose’ tall wheatgrass (TWG) and Alfalfa (ALF) are the dominant crop owing to their ability to provide economic return while fulfilling the facility’s

major goal of drainage disposal. Some acreage is also planted to pistachios. This facility has been providing drainage service to Grasslands (Bypass) drainage area (GDA) since 1998. The 1000,000 acre GDA has highly productive soils capable of producing high-value crops but it is limited in its ability to grow such crops because of soils that are naturally high in native salts and trace elements such as boron and selenium. Applied irrigation water, imported from the Sacramento-San Joaquin Delta, contains low levels of salinity which are concentrated by evapotranspiration (ET) of crops growing in the GDA. Drainage reuse at the SJRIP has been instrumental in reducing the mass of salt, boron and selenium discharged to the San Joaquin River, while maintaining agricultural production in the GDA. However, over time, soil salinity has increased in some fields in the SJRIP to levels above the crop salinity threshold, leading to yield reductions. Without active monitoring of soil salinity status these impacts are only realized at final harvest. Modeling offers a less expensive solution to active soil salinity monitoring– a well calibrated model can simulate a salinity mass balance in the crop root zone, providing management opportunities to remediate the soil salinity before it exceeds the threshold for yield loss. Assessing the spatial and temporal changes in root zone salinity provides essential data for calibration of such a model – an example being the transient hydro-salinity model CSUID.

Transient state models are highly parameterized as compared to the traditional steady-state models and it is often difficult to calibrate and validate these models against actual field data. With technological advances and the development of various tools and techniques, it is now possible to provide data with high spatial and temporal resolution that can help models like CSUID to perform simulations with greater precision, thereby making them more suitable to serve as decision support tools. Customized model user interfaces, such as the one

developed specifically for this project, are useful in making the model more accessible to the novice user. The 1-D version of the CSUID model code and a customized user interface, programmed in MATLAB, was used to develop the CSUID-II model used for this project.

Soil salinity mapping using the EM-38 electromagnetic sensor in selected forage fields (i.e. alfalfa and 'Jose' tall wheatgrass) irrigated with subsurface drainage water, proved to be a valuable tool to provide reliable field data for the model calibration. One limitation is that whereas the EM-38 is able to produce maps of soil salinity over entire fields at 4 discrete soil profile depths – the CSUID model simulates average conditions within each model profile layer.

Salinity in California

Surveys by the US. Department of Agriculture's Soil Conservation Service prior to 1984 indicated that salinity (ECe > 4ds/m) affects 4.18 million acres of the 55.6 million acres of nonfederal land in California and 2.9 million of the 10.1 million acres of irrigated land (Backlund & Hoppes, 1984). Fig. 1 shows the map with areas affected by salinity in California.

Western San Joaquin Valley (WSJV) of California

The San Joaquin valley is the southern half of the Central valley and is an alluvial plain created from erosional deposits from the Sierra Nevada and Coastal ranges. The alluvium on the east side is generally coarse textured containing few native salts or trace elements as it derives from the granite rocks of Sierra Nevada mountains. Whereas, the west side alluvial is finer in texture derived from the sedimentary coast range deposits. The soils of the WSJV are naturally high in salts as they are derived from the alluvium of marine origin (Letey et al., 2002).

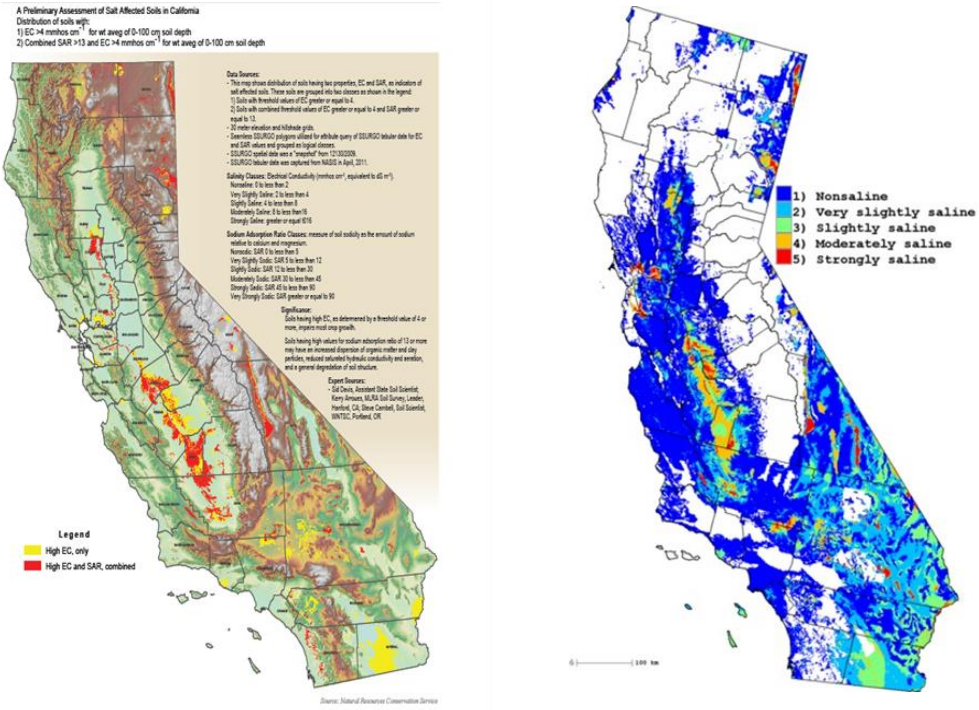

Figure 1. Maps showing areas of California affected by high salinity and/or sodicity (left - *California Water Plan update 2013*), and ECe map for California (right- *California Soil Resources Laboratory*).

Schoups et al. (2005) performed a long-term simulation (57 years) of soil salinity in western Fresno county in the WSJV using a regional groundwater and hydro-salinity model to simulate historic changes in soil salinity. The study showed how changes in the salinity of soils and the groundwater are dictated by spatial variations in soil hydrology, irrigation water source, droughts etc. They found that although long-term irrigation helped reduce root-zone salinity across the study area throughout the second half of the 20th century, there were concerns like increased storage of dissolved salts due to gypsum dissolution and increased salinization of deeper groundwater that might decrease the sustainability potential of current irrigation practices (Schoups et al., 2005). Moreover, there is also a risk that lower salinity trends in the root zone could reverse when irrigation ceases

such as when land is retired, resulting in rapid increase in salinity levels in lands with shallow groundwater, as observed by Corwin (2012)

According to a recent remote sensing study done by Scudiero et al. (2017) in WSJV, 0.78 million acres are salt affected (i.e., *ECe* > 4 dS/m), which represents 45% of the mapped farmland. The acreage under different subclasses of salinity is shown in Fig 2.

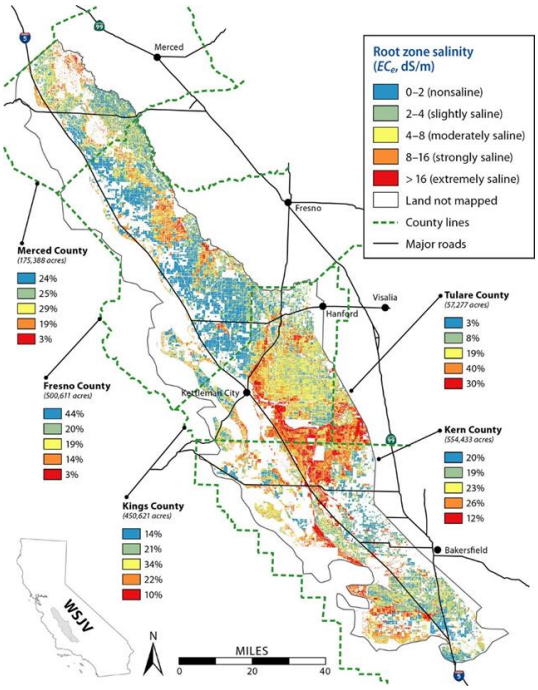

Figure 2. Remote-sensing estimations of root zone (0 to 4 feet) soil salinity for agricultural soils (orchards not included) of the WSJV. Boxes indicate the extent (in percentage) of soil salinity in the five counties of the WSJV (Scudiero et al., 2017).

Project Objectives

1. Monitor changes in spatial distribution of salinity within selected forage fields during the spring and fall seasons of 2016 and 2017.
2. Document irrigation water salinity levels applied to each field.
3. Develop datasets that could be used for calibration of the CSUID-II model.

4. Develop GIS maps depicting the spatial extent of salinity to help guide management practices within the SJRIP.

LITERATURE REVIEW

Salinity

Salinity refers to the presence of dissolved inorganic solutes in aqueous samples. The major solutes comprising dissolved mineral salts are the cations Na, Ca, Mg, and K and the anions Cl^-, SO_4^{2-}, HCO_3^-, CO_3^{2-}, and NO_3^-. Other constituents contributing toward salinity in hypersaline waters include B, Sr, Li, SiO_2, Rb, F, Mo, Mn, Ba, and Al ions (Tanji & Wallender, 2012). Soil is generally said to be saline if the EC_e (electrical conductivity of the solution extracted from a water saturated soil paste) is greater than 4 ds/m at 25^{o}C (USDA 1954). In a saline soil, salts have accumulated to an extent that it limits optimum plant growth and yield. According to Grattan and From (2006), the process of evapotranspiration (ET) concentrates salts in the soil: pure water is evaporated from wet soil surfaces and is transpired from crop leaves. Evapotranspiration (ET) is the sum of both evaporation and plant transpiration and is generally equal to the crop water demand. Nevertheless, the amount of salt that the plants take up is negligible relative to the amount of salts in the soil and that added by irrigation water and as a result, salts start to accumulate in the root zone. The salt concentration continues to increase if salts are not leached out of the crop root zone.

Sources of Salinity

Salinity problems usually tend to have both natural and human causes. The following are the primary sources of salinity.

Weathering

The main source of salts is the continuous geochemical weathering of rocks that form the upper portion of earth's crust (Suarez & Jurinak, 2012). Because most rocks have formed under high temperature and pressure, the constituent minerals are usually thermodynamically unstable when exposed to atmospheric conditions. Weathering is a natural process that transforms primary minerals into other minerals that are more stable at earth's surface. It is a continuous process that is also affected by other factors like atmospheric water, oxygen, carbon dioxide, and organic matter over time. Organic matter can serve as a reducing agent and a source of organic acids, both of which promote weathering.

Fossil or Secondary Deposits

Throughout geologic time, saline waters have inundated vast areas of our present-day continents, which were subsequently uplifted. The resulting geologic formations provide parent material for soils, which could also be a major source of salinity or sodicity. This is the case for the western San Joaquin Valley where prior to the uplifting of the Coastal Range, shallow seas were present and thus the parent material for these soils is marine in origin with higher concentrations of soluble salts, boron, and selenium (Letey et al., 2002).

Atmospheric Deposition

The atmospheric deposition of salts can be of localized importance. Dry and wet aerosol fallout contributes from 100 to 200 kg/ha/yr along sea coasts and from 10 kg/ha/yr to 20 kg/ha/yr in the interior (Suarez & Jurinak, 2012). The composition of atmospheric salt deposition varies with distance from the source. The salt is mainly NaCl at the coast, consistent with the composition of the oceans and becomes greater in Ca^{2+} and SO_4^{2-} ions as the air mass moves inland.

Anthropogenic Activities

Human activities like energy-related mining bring saline and sodic materials to the surface; which consequently can contribute to the salt loading of surface and shallow groundwaters. Industrialization has also increased the atmospheric loading of gaseous nitrogen and sulphur, which although acidic in nature, intensifies the soil mineral weathering rate.

A number of physical and chemical processes can be active depending upon California's natural geology, hydrology and geography resulting in a variety of salinity problems in different areas of the state. Sea-water intrusion into the coastal regions is a problem that leads to the increase of salinity in well waters. This problem could be exacerbated in future by climate change and projected sea level rise. The Tulare Lake Basin is a closed basin lacking any natural outlet. Thus, salt accumulates here after water moving downhill evaporates at the center of the basin leaving salt behind. Salination resulting from irrigation with saline water or from upward capillary flow from shallow saline water tables, are the most common causes of large-scale soil salination problems impacting irrigated agriculture (Maas et al., 1999).

Measurements of Salinity and Sodicity

Salinity is measured primarily as the electrical conductivity (EC) or as the total dissolved solids (TDS), while exchangeable sodium percentage (ESP) and the sodium adsorption ratio (SAR) are used to characterize soil sodicity. The electrical conductivity of the saturation paste extract of the soil, denoted as EC_e, is recommended as a general method for measurement of soil salinity (Rhoades & Chanduvi, 1999). A saturated soil paste is prepared by adding distilled water to a sample of air-dry soil while stirring, and then letting the mixture stand for overnight. The extract is obtained from the saturation paste by vacuum filtration.

Measurements for the concentration of individual ions like Na^{+}, Ca^{2+}, Mg^{2+}, K^{+}, Cl^{-}, SO_4^{2-}, HCO_3^{-}, CO_3^{2-} and boron can be done on the same solution extract.

Electrical Conductivity (EC)

The EC and the total salt concentration of the aqueous solution are closely related. Measuring the EC of the soil solution gives an indirect measurement of the salt content, as conductivity increases as more and more salt is dissolved in water. Pure water has no conductivity because of the absence of salts. EC is expressed as deciSemens per meter (dS/m) or microSiemens per centimeter (uS/cm).

Total Dissolved Solids (TDS)

It is the simplest method to determine the total amount of salts in the water. An aqueous solution is heated in a container until all the water has evaporated and only a dry residue remains. It is usually performed at a temperature of 180^{o}C. TDS is expressed as milligrams of solid residue per liter of water (mg/L).

Exchangeable Sodium Percentage (ESP)

It is defined as the percentage of available exchange sites on the clay surfaces occupied by sodium. It is expressed as:

ESP = (Exchangeable sodium, cmol/kg)/(Cation Exchange capacity, cmol/kg) x 100%.

Sodium Adsorption Ratio (SAR)

SAR gives information on the comparative concentration of Na^{+}, Ca^{2+}, Mg^{2+} in the soil solution. It is defined as follows:

$SAR = [Na]/\sqrt{([Ca]/2+[Mg]/2)}$

It is expressed in milliequivalents per liter (meq/l).

Soil Salinity Mapping

Another relatively rapid, reliable and easy method of measuring soil salinity on a large scale is by using Electrical Resistivity (ER) or Electromagnetic Induction (EMI) techniques (Corwin & Lesch, 2005a). Both these methods can be used to measure the apparent electrical conductivity of the soil (EC_a), which is later correlated with the EC_e values. ER is an invasive technique which involves measurement of the resistance to current flow across four electrodes inserted in a straight line on the soil surface at a specified distance between the electrodes. EMI is a non-invasive method of measuring apparent soil electrical conductivity, in which a transmitter coil located at one end of the instrument induces circular eddy current loops in the soil inducing a secondary electromagnetic field in the soil that is proportional to the concentration of salts in the soil. The secondary field is intercepted by the receiver coil in the instrument. The most commonly used EMI conductivity meter in agriculture is the EM-38 from Geonics Limited.

Remote Sensing

A popular approach to mapping salinity at a regional scale is the use of remote sensing technology. Accumulation of salts at the surface results in the formation of salt crusts which have different spectral reflectance properties as compared to non-saline soils. The presence of salts at the soil surface can be accessed using the remote-sensing (or direct) approach (Allbed & Kumar, 2013). However, if soil moisture is high, or the salt crust is invisible on the ground surface or mixed with other soil constituents (sparse vegetation, different textured soil, organic matter, etc.), this direct approach may yield unreliable results.

Canopy reflectance from remote sensing (indirect approach) is typically correlated with soil salinity in the root-zone (0-1 m) and not just salinity at the soil surface. Hence, this approach is more relevant to agricultural conditions. In order

to map soil salinity by observing the canopy reflectance, the effect of other stressors (e.g., water stress, pests) must be masked or eliminated so that soil salinity can be mapped efficiently. Some pioneering work in this area was performed by Lobell et al. (2010) and Lobell et al. (2007). They showed that under similar farming practices, the average salinity in the root zone remains relatively stable over multiple years (i.e., 5–7 years), while other stress factors are transient. Scudiero et al. (2015) used this approach to map soil salinity using multiple years of vegetation index data for farms in the San Joaquin Valley using the canopy reflectance data obtained from the Landsat 7 (L7) satellite at a 30 x 30m resolution.

Classes of Salt-Affected Soils

Problems related to salts include the increased concentration of salts (salinity) and the composition of sodium relative to calcium and magnesium (sodicity). The following are the three classes of salt-affected soils according to Brady & Weil (2008):

Saline Soils

The saturation extract of these soils has an electrical conductivity (EC) greater than 4 decisiemens per meter, and an exchangeable sodium percentage (ESP) below 15 (or SAR less than 13). Soil pH is ordinarily below 8.5. Saline soils are often referred to as “white alkali,” and are easily recognized by the white salt crust which forms at the surface as the soil dries. Given adequate water and drainage, these soils can be desalinized by leaching.

Sodic Soils

These are the soils in which the EC of the saturation extract is less than 4 dSm^{-1} and the ESP and SAR values exceed 15 and 13 respectively. The soil pH is generally above 8.5. These soils, often referred to as "black alkali" and are recognized by the absence of the white surface crust when the soil dries. High levels of sodium in these soils, combined with relatively low levels of calcium and magnesium, cause dispersion of clay particles. The result is a soil with poor structure and low water and air permeability.

Saline-Sodic Soils

The saturation extract of these soils has an EC greater than 4 dSm^{-1}, and ESP and SAR greater than 15 and 13 respectively. These soils have the limiting properties of both saline and sodic soils. Soil pH is seldom above 8.5. If existing soluble salts are leached downward while exchangeable sodium in the soil profile remains constant, soil properties are likely to closely resemble those of sodic soils. As long as soluble salts are present, these soils are more similar to saline soils in both appearance and physical properties. The concentration of neutral salts in these soils is high which moderates the dispersing influence of the sodium. Sodium becomes a problem when the neutral salts are leached from the crop root zone with excess water.

Effects of Salts on Soil

The effect of salinity and sodicity on soil is mostly related to the concentration of sodium and calcium in the soil solution. High concentration of calcium promotes aggregation of soil colloids, thus promoting good soil structure. Magnesium along with calcium is also considered beneficial for the soil structure. The USDA (1954) has grouped Mg and Ca together as similar ions – both

beneficial for enhancing soil structure. However, more recent work by Oster et al. (2016) points out that Mg and K, which tend to be elevated in recycled wastewaters, can be dispersive. For irrigation waters, they propose a new parameter (CROSS), a generalization of SAR, as a better predictor of the potential for soil permeability reduction; however, this water quality parameter has not been widely adopted to date.

In contrast, a high concentration of sodium (Na) causes dispersion of colloidal soil particles resulting in structural problems in the soil, reduced hydraulic conductivity and infiltration rate. Low overall concentration of electrolytes in the soil solution can be another reason for soil dispersion. The presence of high sodium in the soil solution causes soil infiltration and permeability problems because of the plugging of the pores by the dispersed clay particles. The exchangeable sodium percentage (ESP), or SAR, at which the soil hydraulic conductivity is appreciably reduced varies with the soil mineralogy, clay content, and bulk density (Frenkel et al., 1978). Reductions in the hydraulic conductivity of soils caused by increases in ESP, or decreases in electrolyte concentration, are greater for soils having higher clay content (McNeal et al., 1968). The deleterious effects of sodicity can be countered if the soil solution has a high electrolyte concentration because the dispersion of clay particles decreases as the electrolyte concentration increases. According to Shainberg & Letey (1984), soil permeability can be maintained even at high ESP if the electrolyte concentration of the water is above a threshold level.

When soil is irrigated, soil EC readings at the soil surface closely reflect the EC of the applied water, and soil ESP matches the SAR of the irrigation water closely– thus an equilibrium is established. Irrigation with a non-saline water or rainfall, however, can result in permeability problems because the number of

exchangeable ions (Ca and Mg) will be much lower than that required to replace exchangeable sodium on the soil complex (Ayers & Westcot, 1985; Oster, 1994). In other words, there are not enough ions in the soil solution to counteract the dispersive effect of sodium. This can result in the dispersion of soil particles which then fill the pore spaces, resulting in a loss of structural stability.

More recent work by Suarez and Jurinak (2012) and Suarez et al. (2006, 2008) points out the influence of soil pH, rainfall and vegetative cover (to protect from mechanical dispersion by water droplets striking the soil surface) on infiltration; these factors can influence soil permeability and infiltration for a given combination of SAR and ECe. The increase of SAR of the irrigation water will have an adverse impact on water infiltration because of high levels of sodium. This type of irrigation, when followed by rain, will result in a loss of soil structure for the reasons discussed above and breakdown of clods which can lead to the increased field runoff. As a result, less water will infiltrate into the soil for crop utilization.

Effects of Salts on Plants

The most dominant cations in saline soils are sodium (Na^{+}), calcium (Ca^{2+}), and magnesium (Mg^{2+}) while the most abundant anions are Chloride (Cl^{-}), sulfate (SO_4^{2-}) and bicarbonate (HCO_3-) (Läuchli & Grattan, 2007). Crops demand a minimum water supply for optimum growth which is called evapotranspiration (ET). It includes the evaporation of water from the soil surface and transpiration of water used by plants from the small pores on the underside of the leaves. The ET of a crop depends on its growth stage and various climatic factors (temperature, humidity, wind speed, radiation, etc.). It is also influenced by the availability of

water in the root zone and salinity. If there is limited water availability, ET will be reduced and crop growth will suffer.

High concentrations of salt in the soil solution affect plants by two processes which are: (a) osmotic potential and (b) specific-ion effects (Figure 3a; Munns, 2005). The osmotic process starts immediately as the roots are exposed to the increased salt concentration. Excess salts in the soil solution affect crop growth by creating an osmotic stress for the plant roots. Thus, plants have to spend more energy to extract water from the soil which, in turn, affects the yield (Ayers & Westcot, 1985). Reduction in the osmotic potential of the soil water is the primary reason for salinity stress. To overcome this, plants adjust by reducing its internal water potential, i.e., either by accumulating salts or by the synthesis of organic compounds such as sugars and organic acids.

Since NaCl is the most soluble and widespread salt, plants have evolved various mechanisms by roots to exclude Na^+ and Cl^- during water uptake from the soil (Munns & Tester, 2008). Plants vary widely in their tolerance to salinity (Fig. 3). Halophytes, which are plants that are well adapted to grow under high levels of salinity, are better able to maintain this exclusion as compared to glycophytes. However, the tolerance mechanisms to regulate salts is attributed mostly to their ability to adjust osmotically by the accumulation of salts absorbed from soil water (Hanson et al., 2006). Root cells of these plants accumulate salt to increase their osmotic potential (concentration of salts inside the root cell) in response to the increased salinity in the root zone, thus maintaining the flow of water from the soil to roots.

Glycophytes, on the other hand, are the plants that cannot tolerate the same high levels of salinity as halophytes and are affected by moderate soil salinity. However, within this group, salt tolerance varies widely, with plants such as

strawberry being very salt sensitive and other crops like barley, cotton, and sugarbeet being able to tolerate moderate levels of salinity (Maas et al., 1999). Most of the traditional crop plants belong to this group. These crops also adjust osmotically to the increase in salt concentrations in the soil water; but they do so by internally producing sugars and organic acids and not by the accumulation of salts like halophytes. The immediate effect of osmotic stress is stunted growth that can be observed by reduced height and size of leaves, although the plant otherwise appears healthy.

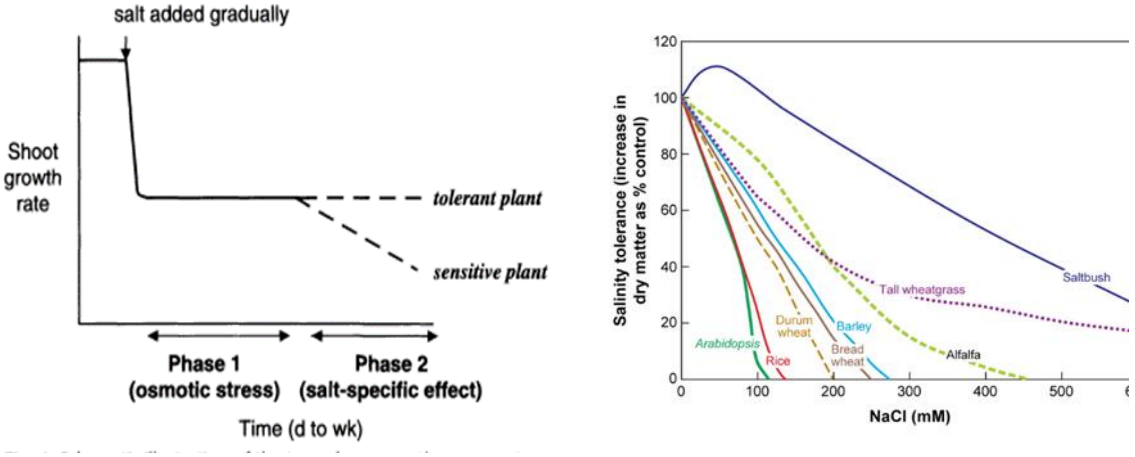

Figure 3. (a) two phase response to salinity of plants with different tolerance levels (left) and (b) salt tolerance of different species shown as increases in shoot dry matter after growth in sand culture containing NaCl for at least 3 weeks, relative to plant growth in the absence of NaCl (right) (Munns & Tester, 2008).

The second phase (specific-ion toxicity) is additive and appears at a later stage of plant growth when ions like Na^+, Cl^-, and B have accumulated in the stem and leaves to a toxic level because of prolonged exposure to salts. Specific-ion toxicities often result in symptoms like leaf burn appearing mostly on the tips and margins of the old leaves. Osmotic stress is still the dominant process as it appears immediately after plants are exposed to salt, and has a greater effect on growth than the specific-ion toxicity (Munns & Tester, 2008). This is particularly true for

annual crops where the growth period is not long enough for the accumulation of these ions to cause toxicity. Trees and vines are more prone to specific-ion effects and can become sensitive to salinity over the years. The use of saline water for sprinkler irrigation can also lead to accumulation of certain ions to toxic levels because of their absorption through the leaves. Benes et al. (1996a) showed that the leaf sap concentration of Na+ and Cl- in maize and barley increased more when applied through sprinkler irrigation as compared to soil salinity. Maize leaves were more selective in absorbing Na+ than Cl-; whereas barley leaves showed no selectivity. Post-washing with fresh water for brief periods was therefore recommended to avoid the uptake of salts through leaf surface (Benes et al., 1996b). Crops differ in their response to specific-ion accumulation in plant tissues. The following is an overview of the crop responses to the specific ions (Hanson et al., 2006; Maas et al., 1999):

Sodium (Na)

Although not an essential element, Na has some beneficial effects on the growth of some plants at concentrations below their salt tolerance threshold. Salt levels above the threshold may have direct and indirect negative effects on plants. Direct effects include the injury to plant parts, or leaf burn, due to the accumulation of toxic levels of sodium which is usually greatest in woody species.

Indirect effects include the deficiency of other elements like Ca^{2+} and Mg^{2+} due to the excess of Na^{+} in the soil solution, rendering the concentrations of Ca and Mg nutritionally inadequate. Usually, plants are selective in absorbing K^{+} over Na^{+}, but Na^{+} induced K deficiencies are also observed when under salinity stress (Grieve et al., 2004).

Chlorine (Cl)

Chlorine (Cl) is an essential micronutrient for plants which is relatively less toxic as compared to other micronutrients. Woody plants such as vines, avocado, citrus, and stone fruits are susceptible to high Cl^- concentrations. The major detrimental effect results from its contribution to the overall osmotic stress. Many tree crops are especially sensitive to Cl^- injury, but it varies among varieties and rootstocks within a species. Tolerance to Cl^- toxicity is controlled by the rootstock, which excludes the Cl- from the scion. In comparison, sensitive rootstocks readily absorb Cl- and transport this ion into the shoot.

Boron (B)

Boron is also an essential nutrient, but unlike Cl, it has a narrow concentration range between toxicity and deficiency. Like Na^+ and Cl^-, boron can also be absorbed through seeds when applied through sprinkler irrigation. Toxic concentrations are generally found in arid regions of the world. Boron toxicity can be observed in many deciduous fruit and nut trees as "twig die back". High boron concentrations were found to decreased the yield of tomatoes (Ben-Gal & Shani, 2002). These researchers also observed that increased soil salinity led to reduced boron accumulation in the leaves. The tomato yield response was better correlated with B concentration in irrigation water and the soil solution than to the B concentration in plant tissue (Ben-Gal, Shani, 2002). Soils with high pH are more prone to B deficiency; however, this is not the case in Western San Joaquin Valley soils because of the high B concentration in native soils.

Bicarbonate (HCO^-_3)

There is insufficient data on the toxic effects of soil HCO_3^- concentrations on plants. Sensitivity to HCO_3^- differs from crop to crop: for example, dalligrasss

is more sensitive than Rhodes grass and bean plants are more susceptible than beet plants.

Mechanisms of Salt Tolerance in Plants

Salinity tolerance in plants occurs by three mechanisms (Munns, 2005; Munns & Tester, 2008):

Tolerance to Osmotic Stress

One of the immediate effects of osmotic stress is that it reduces cell expansion in root tips and young leaves, and causes stomatal closure. A more limited response to osmotic stress results in greater leaf growth and stomatal conductance, although increased leaf area only benefits plants with sufficient available soil water. Greater leaf area expansion could be useful when irrigation provides the needed water, but it undesirable in water-limited systems, where soil water is depleted before the grain is fully mature.

Na+ Exclusion from Leaf Blades

Na^+ and Cl^- exclusion by roots ensures that these ions do not accumulate to toxic concentrations within leaves. A failure in Na^+ exclusion results in a gradual build-up in plants and toxic ion effects such as foliar injury and premature death of leaves after days or weeks, depending on the species.

Tissue Tolerance

Tissue tolerance is the ability of plant tissue to cope with accumulated Na^+, (or Cl^-). Tolerance requires compartmentalization of Na^+ and Cl^- at the cellular and intracellular levels to avoid toxic concentrations within the cytoplasm, especially in the mesophyll cells of the leaf. Toxicity occurs over time, after the leaf Na^+ concentration increases to the same high levels as in older leaves.

Salt Tolerance Assessment

There is a considerable variability in the ability of plants to tolerate salinity in the root zone (Fig. 4). All plants have an upper tolerance limit to the salinity beyond which the crop suffers damage and yield reduction. Salt tolerance can be characterized by plotting the relative yield of a crop as a continuous function of soil root zone salinity (EC_e). For most crops, this response function follows a sigmoidal relationship. However, some crops may die before their yield decreases to zero, thus eliminating the bottom part of the sigmoidal curve (Maas et al., 1999). According to Maas and Hoffman (1977), the response curve could be represented by two line segments: one, a tolerance plateau with a zero slope and the second, a concentration-dependent line whose slope indicates the yield reduction per unit increase of ECe. Thus, crop tolerance can be quantified by two parameters: a threshold beyond which yield begins to decline, theoretically and the slope (rate of yield decline), which are also referred to as the Maas and Hoffman coefficients (see Fig. 4). Maas et al. (1999) and Maas and Hoffman (1977) have provided salinity tolerance tables for most field and horticultural crops. The following formula can be used to calculate the estimated relative yield (Y) of any given crop when soil salinity exceeds the threshold value:

$$Y\,(\%) = 100 - B(ECe - A)$$

Where:

Y= relative yield (% of non-saline control).

A = salinity threshold (dS/m).

B= slope; percent yield decrease per unit of salinity (dS/m) when $EC_e > A$.

EC_e= electrical conductivity of the saturation paste extract of the soil.

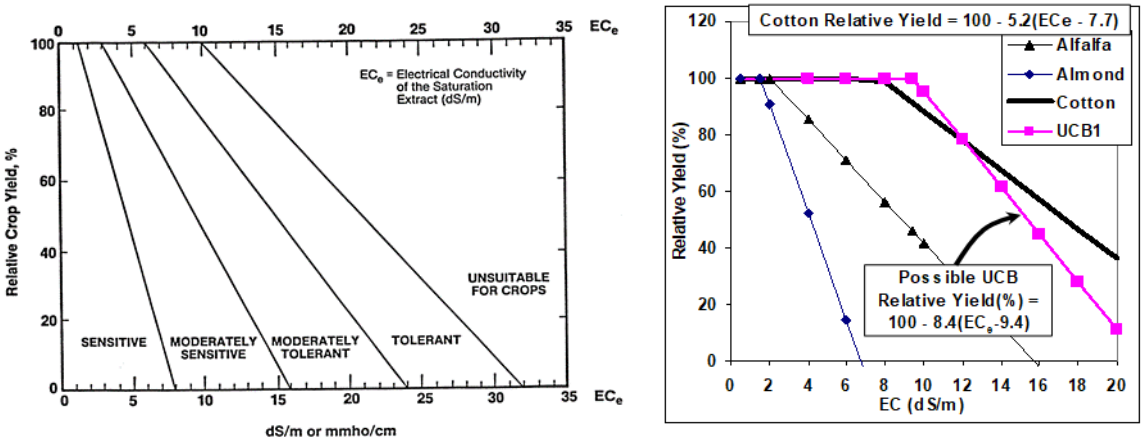

Figure 4. (a) Salinity tolerance classifications based on salt tolerance thresholds (left) (Maas et al.1999) and (b) salinity yield response curves for alfalfa, almond, cotton pistachio (right) (Blake Sanden, University of California Cooperative Extension, Kern Co.)

Drainage and Salinity

There is a close relationship between salinity management and drainage management: irrigation and drainage systems must be designed as an integrated water management system with specific management objectives. Major contributors to the drainage problem in the San Joaquin Valley are the salinity of imported water, its naturally saline soils, and the Valley's geological makeup which prevents effective natural drainage from some of the lands. Soils on the western side of the valley originate from uplifted marine sediments that comprise the coastal mountain range and are naturally elevated in salts and trace elements (Laird et al., 2015).

The problem of water logging and salinity in California's Central Valley was recognized by Hilgard (1889, 1893), who urged farmers and public agencies to construct a regional drainage system. Farmers began installing subsurface drains in fields with drainage problems by the late 1940s. By 1965, 330 miles of subsurface drains and 750 miles of open ditch drains were operational in the valley. For disposal of the saline drainage water produced by these system, a

Master Drain was suggested and designed by the US Bureau of Reclamation. The initial plan was to route the San Joaquin Valley master drain (San Luis Drain), from southwestern Kern County to the Sacramento-San Joaquin River Delta, with the Pacific Ocean serving as the ultimate sink (Fig. 5). However, due to financial and regulatory constraints, construction of the second phase of the master drain, linking the Kesterson regulating reservoir near Gustine to the Delta was abandoned in 1979. In 1981, drainage water began flowing through the initial 82-mile segment of the San Luis Drain between Laguna Avenue in Fresno County and the Kesterson Reservoir. The reservoir was intended to serve both as wildlife habitat and to regulate discharge until the second phase of the drain was completed (Quinn et al., 1998). However, deformities of migratory waterfowl embryos from selenium toxicosis, first observed in 1982 and 1983 in the wetlands near the reservoir led to closure of the Kesternson Reservoir as a wildlife refuge and the closure and subsequent plugging of sub-surface drainage lines from Westlands Water District (WWD) which had contributed the primary drainage inflow to the Kesterson Reservoir (SJVDP, 1990). As a result of this environmental disaster, new constraints were placed on all basin water quality control plans where selenium drainage was endemic and new water quality objectives were developed for California's Central Valley; effectively shifting the response to agricultural drainage problems from out-of-valley solutions to the in-valley disposal options proposed by the interagency San Joaquin Valley Drainage Program. The Drainage Program was charged with developing short and long-range solutions to salinity-drainage problems originating on the west-side of the San Joaquin Valley. Their final report was published in September, 1990 (SJVDP, 1990). The San Joaquin Valley Drainage Implementation Program (1999), published a series of reports in

which they assessed several management options for salinity and drainage control SJVDIP (2000). Several recommended management options are as follows:

1) Source control.

2) Drainage water reuse.

3) Evaporation ponds.

4) Land retirement.

5) Groundwater management.

6) Water treatment.

7) Discharge to the San Joaquin River.

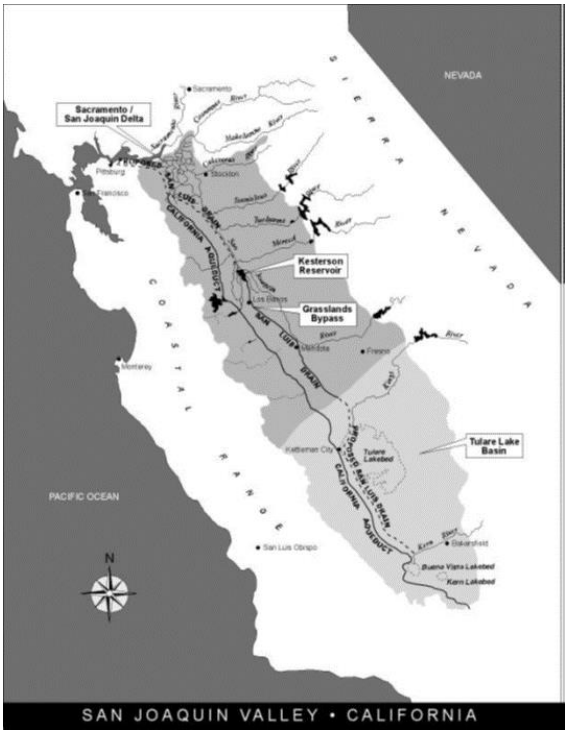

Figure 5. Map showing the completed portion of the San Luis Drain (solid line) and the proposed (uncompleted) continuation of the drain (broken line) (Letey et al., 2002).

Drainage Water Reuse

Among the options mentioned in the SJVDIP plan, drainage water reuse is considered to be the most important. And world-wide, diminishing fresh water resources, increasing population, the challenge of doubling the food production by 2050, frequent droughts, and agricultural drainage disposal problems have increased interest in water reuse technologies. Although not a long-term solution, drainage reuse is an attractive option as it: (a) reduces the volume of saline-sodic drainage water ultimately requiring the disposal or treatment, (b) provides a water supply to irrigate salt-tolerant crops; and (c) it reduces land area impacted by salinity problems. However, for sustainable reuse of saline-sodic drainage water on agricultural land in the WSJV , attention needs to be given to factors such as the selection of suitable salt-tolerant crops, avoidance of soil salinity accumulation to levels that could reduce plant growth, maintenance of soil infiltration properties, and control of concentrations of trace elements (B, Se, and Mo) in crops and forages to avoid human or livestock health impacts (Oster & Grattan, 2002).

Corwin (2012) performed a long-term study (10 years) and monitored the effects of irrigating a marginally productive experimental field plot with drainage water. The soil at the field site was extremely saline-sodic to the extent that soil leaching was difficult even with high-quality water– the physical properties of the soil had deteriorated to the point that they impaired water permeability and infiltration. The study provided evidence that drainage water reuse could help reclaim the saline-sodic soil by leaching salts from the rootzone and provide sustainable forage production. However, when irrigation with drainage water was terminated, there was evidence that the soil reclamation processes would operate in reverse and render soil conditions back to their original state (Corwin, 2012).

There are several agronomic methods for using saline drainage water for irrigation on agricultural lands. Drainage reuse strategies which include blending, cyclic re-use, and sequential re-use are discussed by Grattan et al. (2009) and Grattan et al. (2014).

Blending water. mixing saline drainage water with better quality water. The aim is to achieve a target EC of blended water suited to the salt tolerance of the irrigated crop. It is not the most desirable option as it might not always be economically feasible because of the additional costs incurred to produce a lower salinity water supply. And it does not unconditionally increase the usable water supply; for example, if the risk of potential crop damage outweighs the increase in available water supply that one might obtain.

Cyclic use. using saline drainage water and nonsaline water alternately in crop rotations that include both moderately salt-sensitive and salt-tolerant crops. This strategy allows crops of lower salt tolerance to be included in the rotation. Another approach is to use good quality non-saline water at early growth stages of the crop, and saline water at later stages. This is because the salt tolerance of many crops changes at different growth stages i.e. increases as the crop matures (Maas et al., 1999). In this system, a pre-plant leaching may be required to return the soil to a less saline condition optimum for the salt-sensitive crop in the rotation, or a crop that has lower salinity tolerance at early growth stages.

Sequential use. a system where drainage water collected from one field within a farm could be used to irrigate more salt tolerant crops in another field (see Fig. 6). The system could include more than one sequential reuse of the saline drainage water. One such system of sequential use, called integrated on-farm

drainage management (IFDM), has operated on two commercial farms in the WSJV: Red Rock Ranch in Five Points from 1996 to 2009 and Andrew's Ag Inc., in Kern County since 2002 (Suyama et al., 2007b). The main objectives of such a system are:

- Increase the productivity of tile- drained fields by irrigating with lower salinity water on most of the farm and gaining the benefits of a subsurface drainage system (increased leaching and salinity control).
- Obtain an economic benefit from the reuse of saline drainage water for the production of salt tolerance crops.
- Increase the area planted to high-value, salt-sensitive crops and reduce the volume of drainage water requiring disposal.

These three strategies discussed above are in no way mutually exclusive. All can be used in conjugation with other approaches, depending upon the objectives of the farm, type of crops grown, and the crop growth stage.

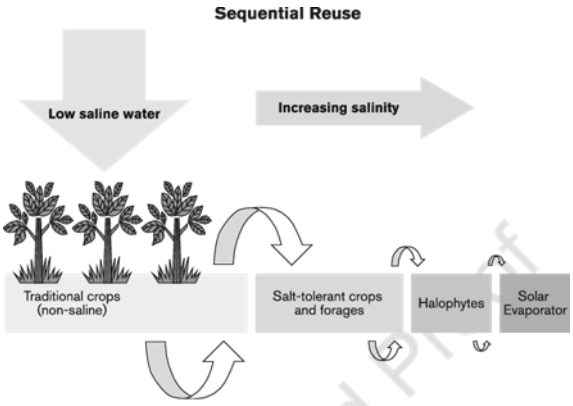

Figure 6. Sequential drainage water reuse system (Grattan et al., 2014).

Suitability of Alfalfa (*Medicago sativa)* and 'Jose' Tall-Wheatgrass (*Thinopyrum ponticum* var 'Jose') for Saline Drainage Water Irrigation

Various forage crops have been studied for their potential to be grown under saline-sodic irrigation. The suitability of forages for a drainage water reuse system depends on their ability to be grown under saline-sodic conditions and produce good quality forage for cattle Suyama et al. (2007a,) evaluated the suitability of various forages (i.e. alfalfa 'Salado/801S', 'Jose' tall wheatgrass, creeping wildrye, paspalum, Bermuda grass, alkali sacton) irrigated with drainage saline water, and concluded that Alfalfa and 'Jose' tall wheatgrass are the most suitable in terms of having high metabolized energy (ME) and dry matter production.

Studies by Benes et al. (2012), Grattan et al. (2002), Grieve et al. (2004) and Robinson et al. (2004) have shown the suitability of alfalfa and 'Jose' tall wheatgrass production under saline conditions. Alfalfa is more sensitive to salinity than 'Jose' Tall wheat grass, but it has higher yields, higher forage quality and it is more profitable. Improved varieties of alfalfa can be grown with slight or no reduction in yield at soil salinity as high as 7ds/m EC_e (Benes et al., 2014; Chahal, 2013; Suyama et al., 2007b), which is much higher than the previously established Maas-Hoffman salinity tolerance limit of 2.5 dS/m EC_e. A recent study by Cornacchione & Suarez (2015) evaluated different cultivars of alfalfa and suggested that irrigation water resulting in soil EC_e values up to 6 ds/m could be used throughout the production cycle without any significant yield loss. The study by Suyama et al. (2007a) indicates that 'Jose' tall wheatgrass has a very high level of salinity tolerance; with five years of saline drainage water application and soil salinities reaching 18 dS/m EC_e, its dry matter yield (hay production) was lower

than in earlier years, but the forage was still producing 6-7 Mt/ha (metric ton/ hectare).

Leaching to Control Root-Zone Salinity

Control of root zone salinity is a critical component of sustainable forage production using saline irrigation water. A common practice for managing root-zone salinity is the application of water such that there is a net downward movement of salt and water through the root zone. This common practice is referred to as ‘leaching.' The volume of leaching water required is dependent on the salt tolerance of the crops being irrigated and the salinity of the irrigation water. The concept of Leaching Requirement (LR) was defined by the USDA (1954) as the fraction of water infiltrating the soil that must move beyond the root zone to prevent soil salinity from exceeding a specified threshold value at which yield reduction typically occurs–- for the latter, the Maas Hoffman salinity tolerance threshold is typically used. Leaching requirement is based on the concept of Leaching fraction (LF), which is defined as the fraction of infiltrating water that moves beyond the root zone and provides an indicator of the degree of salt leaching. As the LF increases, the concentration of salts remaining in the root zone (EC_e,) decreases. It is expressed as:

$$LF = D_d/D_a = EC_a/EC_d \quad \ldots\ldots\ldots\ldots\ldots\ldots 1$$

Where,

D_d is depth of drainage water

D_a is depth of infiltrating applied water

EC_a is the EC of applied water

EC_d is the EC of drainage water.

Measuring D_d directly is impractical in agricultural fields, hence LF is frequently calculated from root-zone soil salinity data. Another approach is to use water-balance:

LF =100 x (1-ET/AW)…….2

Where,

AW = applied water (assumes no surface runoff)

ET = evapotranspiration

LF = Leaching fraction

The LR is defined as the lowest value of LF that could be allowed without EC_d becoming excessive for optimal plant growth. The LR is obtained when the maximum permissible value of EC_d (EC_d*) is inserted into eq. (1):

$LR = EC_a/EC_d$*……..*3*

Rhoades (1974) introduced an expression for approximating the appropriate values of EC_d*:

$ECd* = 5ECe* - ECa$ ……4

Where EC_e* (ds/m) is the average EC of the saturation paste extract for a given crop appropriate to the tolerable degree of yield depression.

Substituting eq. (4) into eq. (3), we get the traditional LR model, which is often used by agriculturists:

LR = EC_a/(5EC_e*-EC_a)……5

Soil salinity near the top of the root zone reflects the salinity of the applied irrigation water. At low leaching fractions, soil salinity at the bottom of the root zone may be much higher than that at the top. As the leaching fraction increases, soil salinity at the bottom of the root zone decreases and at very high leaching fractions can converge to the EC of applied irrigation water.

Types of Leaching

Hanson et al. (2006) describe two types of leaching.

Maintenance leaching. Maintenance leaching assumes that the level of soil salinity is not excessive, and only small changes in soil salinity occur over time. As the name suggests, the objective of this is to apply sufficient water so that salts do not accumulate to a level damaging for crop growth (proactive approach). This approach is not feasible when irrigation water is scarce.

Reclamation leaching. Soils with excessive salinity levels can be reclaimed by applying sufficient water to the soil to leach the salts below the root zone. Periodic, heavier applications of water are done to reclaim soil. Amendments are frequently used for successful reclamation as reduction depends on the soil's infiltration rate. Reclamation leaching methods include:

- Continuous Ponding: ponding water until desired salinity level has reached.
- Intermittent Ponding: Water is applied intermittently in small amounts, thus requiring less water than continuous ponding. These wetting and drying cycles efficiently remove salt from the finer pores of the soil. It is recommended in regions with low evaporation conditions, as high evaporation rates can result in the migration of salts to the soil surface between irrigation applications. The disadvantage of this strategy is the relatively long time required to complete the wetting and drying cycles.
- Sprinkling: sprinkler irrigation can be used for more efficient water application as compared to intermittent ponding. The average application rate of water depends on the nozzle size, pressure, and sprinkler spacing (Hanson et al., 2006).

Computer Models

There has been considerable progress in recent years in estimating leaching requirements. Initial guidelines for managing saline irrigation waters were based on steady state analysis; but with increased knowledge of the physical-chemical-biological soil interactions and the development of high-speed computers, transient-state models that take into account these dynamic interactions are being developed (Letey & Feng, 2007). Besides soil salinity, there are many other variables that play a role in impacting crop yield. Simulation models can help to estimate the outcome produced by the combined effect of a set of variables, which is hard to do experimentally in the field. Although, the Maas and Hoffman coefficients traditionally used for LR guidelines have shown to be somewhat reliable for determining which crops can be grown with irrigation water of known salinity, studies show that the traditional steady-state modeling approach using the Mass-Hoffman algorithms results in an overestimation of the LR (Shani et al., 2004). Irrigation based on a higher LR than necessary, not only wastes water, but it can leach nitrate below the root zone.

The amount of applied water needed to satisfy the crop's water requirement can be estimated from water and salt balances within the crop root zone. The major flows of water into the root zone are irrigation, rainfall, and upward capillary flow from groundwater. Water moves out of the root zone by evaporation, transpiration, and drainage. Under steady-state conditions, the change in the amount of water and salt stored in the root zone is zero. If the total water inflow is less than evaporation plus transpiration, water is extracted from soil storage, and drainage is reduced with time. In the absence of a net downward flux of water and salt below the root zone, salt will accumulate, transpiration will be reduced and crop growth and yield will be suppressed, (Hoffman, 2010).

Steady state models assume that the irrigation water infiltrates at a constant rate, irrespective of the irrigation frequency, and that evapotranspiration is constant over the growing season; moreover, it assumes that the salt concentration of the soil solution is constant at all times. Mathematically, a steady-state flow analysis does not include a time variable by definition, as opposed to a transient flow analysis (Letey et al., 2011). Steady-state assumptions may be valid in some circumstances, e.g. where transient fluxes return soil salinity to its initial conditions at the end of each irrigation season. However in general, steady-state analysis is conservative, overpredicting the negative consequences of saline water irrigation, and it recommends a higher leaching requirement than that recommended when using transient-state models. The use of traditional steady-state models for estimating LR needs to be evaluated for each agricultural system to which it is applied (Corwin et al., 2007; Letey & Feng, 2007; Letey et al., 2011).

There are several factors that need to be considered in the evaluation of model performance such as the use of an appropriate water uptake function, the effect of reduced transpiration and plant growth on leaching, uptake of water uptake from non-stressed portions of the crop root zone, salt-precipitation or dissolution processes, and the impact of preferential flow in the crop root zone which impacts infiltration assumptions.

Soil salinity is dynamic in nature and differs spatially and temporally in its distribution. The general trend is that it increases with depth in the root zone. It is crucial for the model to account for the water extraction pattern by the roots. The traditional model in eq.(4) is a steady state model used by Ayers & Westcot (1985) that assumes a 40-30-20-10 soil water extraction pattern by the roots. This means that plants take up water in the proportion 40, 30, 20, and 10% of the total crop ET

requirement from first through the fourth quarter of the root zone profile (Fig. 7). They calculated a linear average soil-water salinity of the entire root zone for each LF using the salinity of each quartile-fraction of the root zone. The soil-water salinity in the root zone calculated by a linear average depends on this assumed water-uptake distribution. However, Hoffman and Van Genuchten (1983) determined the water-uptake weighted salinity by solving the continuity equation for one-dimensional vertical flow of water through the soil and used an exponential soil water uptake function. The equation is as follows:

$$C/C_a = 1/L + [\delta/(Z\ x\ L)]\ x\ ln\ [L + (1 - L)\ x\ exp(-z/\delta)] \quad \ldots\ldots\ldots\ldots 6$$

Where, C is the salt concentration of the saturated paste extract, C_a is the salt concentration of the applied water, L is the leaching fraction, Z is the depth of the crop root zone, and δ is an empirical constant set to 0.2xZ.

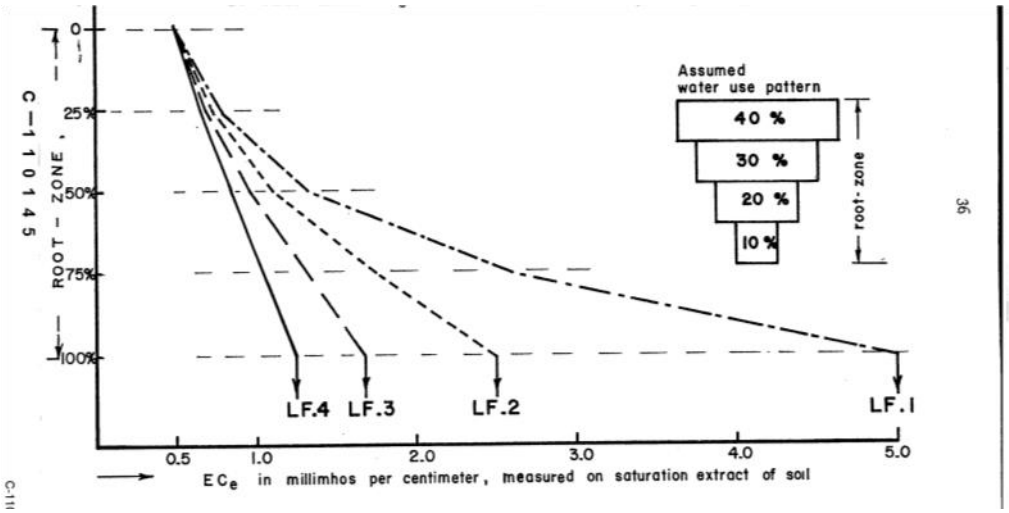

Figure 7. Salinity profile expected to develop after long-term use of water of EC_w = 1.0 mmhos/cm at various leaching fractions (LF) (Ayers & Westcot 1985).

This model resulted in relatively lower concentration factors (which indicate the average increase in soil-water concentration relative to irrigation water salinity) as compared to Ayers & Westcot (1985), especially at the lower

leaching fractions (Letey & Feng, 2007). Neither of these assumptions, however, account for the fact that plant roots tend to extract water from the non-stressed regions of the root zone when under salinity stress. Water is first extracted from the upper portions of the root zone and roots then advances downwards as the water becomes limited in the upper root-zone (Gardner, 1983).

Another steady-state assumption is that the water content and salt concentration remain constant over the simulation period (typically 1 year). According to Hoffman (2010), all steady-state and transient models are based upon the mass balance of water and salt Hence, for a unit surface area of a soil profile over a given time interval, the difference between inflow depths of irrigation (D_i) and effective precipitation (P^e) and outflows of crop evapotranspiration (ET_c) and drainage (D_d) must equal changes in soil water storage (ΔD_s).

For steady state conditions:

$$\Delta D_s = D_i + P_e - ET_c - D_d = 0$$

Since the amount of salt leaving the soil by evapotranspiration and that applied in precipitation are negligible, the change in mass of salt stored per unit area within the root zone (ΔM_s) for steady-state is given by

$$\Delta M_s = (C_i \times D_i) - (C_d \times D_d) = 0$$

Where Ci is the salt concentration in the irrigation water, and Cd is the salt concentration in the drain water. Under steady-state conditions, ΔD_s and ΔM_s are zero Hoffman (2010).

The required plant leaching fraction can be impacted by process feedbacks, as plants change the root zone salinity during the transpiration process. An increase in the relative yield of bell peppers was observed when an irrigation application was made that exceeded the potential ET (ET_p). Under deficit

irrigation, salts accumulated in the root zone and reduced transpiration, which led to an increased leaching fraction requirement (Ben-Gal et al., 2008). However, if the salinity stress is great enough to substantially reduce ET, there can be greater root zone leaching than expected for a given irrigation water volume. Deficit irrigation is not accounted for by most steady-state models, nor is the effect of reduced transpiration due to salinity. Moreover, Salt precipitation or dissolution can affect the soil-water concentration, especially in arid regions. Failure to account for the salt precipitation can result in the overestimation of the LR.

Other factors not often considered by the steady state approach include irrigation non-uniformity, variance in seasonal rainfall, and crop irrigation frequency.

Corwin et al. (2007) have compared the Leaching Requirement (LR) results from the traditional LR model originally developed by USDA-ARS, U.S. Salinity Laboratory USDA (1954) and modified by Rhoades (1974), the water production model (WPF) by Letey et al. (1985), the WATSUIT model Rhoades & Merrill (1976), TETrans Corwin & Waggoner (1990) and the UNSATCHEM Šimůnek & Suarez (1994) model. The traditional LR, WPF, and WATSUIT are steady-state models while TETrans and UNSATCHEM are transient models.

The traditional LR model is a steady-state model that assumes uniform water applications and does not adjust for salt precipitation or dissolution, nor account for variability of irrigation applications or frequency, neglects upward capillary flow, water chemical composition, and salt export in surface runoff.

The steady state WATSUIT model addresses some of these deficiencies by considering the composition of irrigation water and precipitation-dissolution reactions. Failure to account for precipitation, however, typically leads to an overestimate of the LR. A lower LF contributes to an increase in soil-water

concentration and it increases the probability for salt-precipitation (Letey & Feng, 2007).

The steady state production function (WPF) model of Letey et al. (1985) accounts for the increased leaching from the root zone when salt buildup causes a reduction in ET by plants. However, this model doesn't account for salt precipitation or dissolution, nor does it account for the effects of irrigation frequency or upward capillary water flows from the shallow water table. The WPF model assumes a uniform water distribution.

The transient TETrans model accounts for preferential flow or bypasses, a phenomenon typical of cracking clay soils. All or a part of infiltrating water passes through a portion or all of the soil profile via large pores without displacing water present in the finer pores, and thus reduces the leaching efficiency (Corwin et al., 2007).

The transient UNSATCHEM model Šimůnek & Suarez (1994) takes into account salt effects on plant growth and evapotranspiration, osmotic and matric effects on plant water uptake, and precipitation and dissolution reactions. However, the model doesn't take into account potential preferential flow and it does not adjust for the potential ET reduction in response to water stress, nor does it account for the increased water uptake by roots from the nonstressed portions of the root-zone (Letey & Feng, 2007).

Letey and Feng (2007) discussed another transient-state model called ENVIRO-GRO by Pang and Letey (1998) that takes into account almost all the factors discussed above, except it does not account for salt precipitation or dissolution reactions in the crop root zone.

CSUID-II Model

The CSUID model is a three-dimensional groundwater flow and salinity model that considers irrigation timing and sub drainage configurations for individual crop requirements. The model was developed in the late 1980's and used for compare drainage technologies to reduce the concentration of salts in drainage discharge (Alzraiee et al., 2013). The model predicts multiple crop stresses such as water deficit, water excess, and salinity while allowing for the spatial and temporal variability of three-dimensional soil parameters that include hydraulic conductivity, dispersivity, porosity, specific yield and storativity. By tracking the crop root zone over time - CSUID allows assessment of salinity impacts to crop yield at various crop growth stages and during periods of greater salt sensitivity. As previously noted - the model has been configured to serve as a potential decision support tool for further refining upstream San Joaquin River (SJR) salinity objectives. The Central Valley Salinity Coalition recently utilized the Hoffman model to develop proposed EC limits for water diverted for irrigation for a reach of the San Joaquin River between Crows Landing and Vernalis that would be protective of 95% of crops grown in the lower SJR basin approximately 95% of the time (Quinn et al., 2016). The new graphical user interface allows the inter-comparison of transient Colorado State University Irrigation Drainage model (CSUID) and the Hoffman, steady-state model to overcome the previously discussed limitations of the steady-state Hoffman model.

Use of EM -38 (Electromagnetic Induction) for Salinity Measurements

One of the first steps to make recommendations about leaching requirement is to know the current state of the salinity profile in the field. Soil salinity is a dynamic soil property which varies spatially, as well as temporally. In order to

provide leaching requirement guidelines, it is imperative to delineate the spatial distribution of salts in the field in all three dimensions (areally and in profile). The information on the salt distribution in the soil profile can be used to infer the net movement of salts in different parts of a field, and hence can be helpful in assessing the efficiency of the current irrigation and drainage system.

A fast, reliable and easily mobilized method of mapping soil salinity is necessary to assess field soil salinity. Electromagnetic induction (EMI) has been widely used by soil scientists to better understand the spatial variability of soils and soil properties at field and landscape scales. As explained by Doolittle and Brevik (2014), there have been recent improvements in instrumentation and its integration with other technologies like global-positioning systems (GPS), data processing software, and surface mapping programs, have fostered the increasing use of EMI for geospatial measurements of soil properties. The EMI sensors transmit a primary electromagnetic field which induces electrical currents in the soil, these currents then generate a secondary electromagnetic field which are read by the sensor's receiver. Under conditions known as “operating under low induction numbers”, the secondary field is proportional to the ground current and is used to calculate the “apparent” or “bulk” electrical conductivity (EC_a) for the volume of soil profile measured. Apparent electrical conductivity measurements have also been used as a surrogate to map soil moisture content (Brevik et al., 2006), soil texture (Kelley et al., 2017), and clay content (Weller et al., 2007).

Another technique that has been employed for measuring EC_a is electrical resistivity (ER), which involves measurement of the resistance to current flow across four electrodes inserted in a straight line on the soil surface at a specified distance between the electrodes. However, EMI has a primary advantage over ER as it does not require physical contact with the soil (Corwin & Lesch, 2003). The

most commonly used EMI conductivity meters in agriculture are the EM31, EM38, EM38-DD and EM38-MK2 from Geonics Limited and the Dualem1 and Dualem 2 from Dualem Inc. (Corwin & Lesch, 2003; Doolittle & Brevik, 2014). The EM38 instrument is the most widely used in agriculture because its depth of measurement roughly corresponds to the root zone of most crops (1 to 1.5 meters). The EM38-MK2 by Geonics Limited, Canada, is their most recent model. It operates at a frequency of 14.6 kHz and has one transmitter coil and two receiver coils at a distance of 1.0 m and 0.5 m respectively from the transmitter coil. This geometry of coils results in simultaneous measurements at a depth of 1.5 m and 0.75 m when operated in vertical dipole orientation, and measurements at depths 0.75 and 0.38 in horizontal dipole orientation. This meter provides simultaneous measurements of ground conductivity (Quad-Phase) and magnetic susceptibility (In-Phase).

EC_a measurements using the EM38 are suitable for characterizing the spatial variability of salinity as it facilitates a very reliable, quick, and mechanized technique for collecting salinity data as compared to the more traditional soil sampling methodology using a hand auger. Geospatial EC_a measurements are also influenced by several soil physical and chemical properties notably soil salinity, clay content, water content, bulk density, organic matter, and cation exchange capacity– hence the EC_a readings are used as a surrogate for the general spatial variability of those soil properties that are spatially correlated with EC_a (Corwin & Lesch, 2013). Under conditions of high salinity (EC_a > 2dS/m), salinity usually is the dominant property influencing the EC_a measurements (Corwin & Scudiero, 2016). Measurement of EC_a is quite complex because it responds to all factors affecting the bulk soil conductance. There are three pathways of conductance that contribute to EC_a measurement: (1) a solid-liquid pathway via exchangeable

cations associated with clay minerals, (2) a liquid phase pathway via salts contained in the soil water occupying the large pores and (3) a solid pathway via soil particles that are in direct contact and continuous contact with one another (Corwin & Lesch, 2003) as shown in Figure 8. Pathway 2, the soil solution, is of primary interest when measuring soil salinity using the EMI approach.

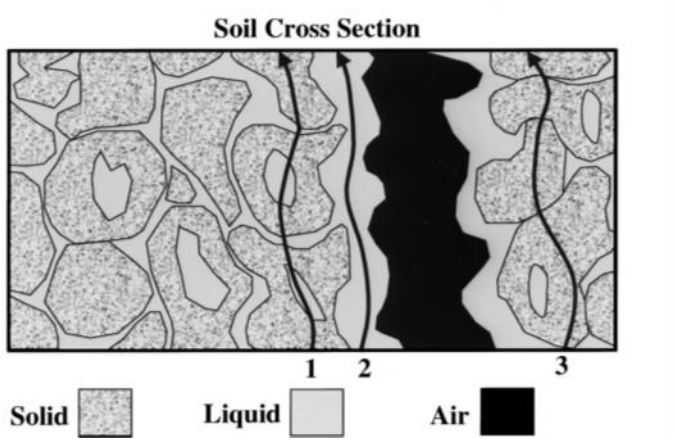

Figure 8. Pathways of electrical conductance (Corwin & Lesch, 2003).

It is important to note that any type of EM instrument utilized to measure soil conductivity and not soil salinity can be influenced by other soil properties, especially at EC_a <1-2 dS/m (Corwin & Scudiero, 2016). The leaching requirement guidelines and the Maas and Hoffman salinity tables used EC_e as a measure of soil salinity– which is suggested as a valid approach in the published literature. EC_e is the conventional soil salinity metric because it is measured by bringing the water content of the soil to saturation for all types of soil. The measured electrical conductivity of the soil (EC_a), must therefore be correlated with field validated ECe values.

After the EM-38 survey is complete, a statistical analysis of the EC_a data is performed using an appropriate statistical sampling design to establish the soil

sampling site locations. For this, either design-based or model-based sampling schemes are employed (Corwin & Lesch, 2013; Corwin et al. 2010); however, the model-generated sampling design, or more specifically a "response surface" sampling design', has an advantage in that a minimal number of soil samples are required to characterize the soil variability. The purpose of this design is to select a minimum number of sampling sites that are representative of the entire surveyed area and optimize the parameter selection for the regression model to be used to convert EC_a data into EC_e (Lesch et al., 1995b). The requirement is satisfied by the spatial sampling approach used in the Estimated Salinity Assessment Program (ESAP) software developed at the U.S. salinity laboratory by Lesch et al. (2000). This is a software package developed specifically for the collection of salinity data using the EM technology. This software allows the selection of 6 to 20 sites per field, depending on the error variance estimated during the EC_a survey.

After collection of the soil samples from the EM-38 survey sites, chosen by the software to evenly sample across the entire survey area, the samples are analyzed for soil properties such as the saturation percentage (SP), gravimetric water content, pH, and EC. The EC_a data collected during the EM-38 survey is subsequently converted to EC_e for the entire surveyed area using an EC_a/EC_e data conversion equation. The techniques utilized for the conversion of ECa data into EC_e data are classified into two types: 1) deterministic and 2) Stochastic. Deterministic and Stochastic procedures can both be applied for estimating (EC_e) from EM-38 ECa survey data (Lesch et al., 2000; Sharma et al., 2008).

The deterministic approach estimates EC_e using either theoretical or empirical models based on EC_a values. These models are 'static', and soil data collection is not needed. However, this approach does require knowledge of additional soil properties such as soil water content, bulk density, SP, and

temperature. One such model known as DPPC (dual pathway parallel conductance) model that was developed by Rhoades et al. (1989) and is shown to be applicable in a wide range of agricultural situations (Corwin & Lesch, 2003).

Stochastic estimates of EC_e are generally more accurate and include statistical modeling techniques such as spatial regression or geostatistics. Using this approach, models are 'dynamic' and soil sample collection is required (Corwin & Lesch, 2003). A small number of samples (usually 12) are collected at selected survey locations to develop an appropriate stochastic-prediction model to predict EC_e for each sample depth increment. The model established then is used to predict soil salinity (EC_e) at all the remaining non-sampled locations where EC_a data was collected. Such an approach was developed by Lesch et al. (1995a, 1995b) and named the Multiple linear regression (MLR). Both approaches discussed above (i.e. DPPC and MLR) are incorporated into the software package ESAP by Lesch et al. (2000). This software package contains three interactive and linked programs that work in an integrated fashion:

- ESAP- RSSD (Response surface sampling design): used to generate optimal soil sampling designs for stochastic calibration models.
- ESAP- Calibrate: used to convert conductivity data (EC_a) to soil salinity (EC_e) using either stochastic or deterministic calibration approaches.
- ESAP- SaltMapper: used to generate 1-D transect and 2-D raster maps of raw conductivity, estimated soil salinity, and/or estimated secondary soil physical properties.

For data acquisition, the EM38 instrument is often mounted on platforms or towed behind all-terrain vehicles (ATV). The EM38 is usually placed in a nonconductive PVC carrier-sled attached to the vehicle to avoid any erroneous

measurement since the EM sensors are sensitive to any metal within at least 3 m. A GPS receiver is mounted onto the vehicle for geo-referencing of the sampled data. The EM38 and GPS are synchronized by the software through the computer's serial data ports. The EC_a measurements are usually collected along rows (transects) spaced 25-40 m apart, which is dependent on the objective of study, time, and labor availability (Sharma et al., 2008).

The protocols for conducting a field scale EC_a survey campaign were provided by Corwin and Lesch (2005b) and Corwin and Lesch (2013). The basic elements of a field scale EC_a survey include: (i) site description and EC_a survey design; (ii) EC_a data collection with mobile GPS-based equipment; (iii) soil sampling design; (iv) soil core sampling; (v) laboratory analysis; (vi) calibration of EC_a to EC_e; (vii) spatial statistical analysis; (viii) GIS database development and graphic display. All these steps are discussed in detail in the following methods section.

MATERIALS AND METHODS

Study Site

The SJRIP (San Joaquin River Improvement Project) facility is located between the Delta Mendota Canal and Central California Irrigation District's Main Canal, and between Russell Avenue and Fairfax Avenue in Fresno County. SJRIP is a saline drainage water reuse facility that is a part of the Grassland Bypass Project – a multiagency initiative that allowed interim use of the federal San Luis Drain while drainage entities developed technologies to reduce selenium export to the San Joaquin River. By 2012, this project had reduced the drainage volume discharge to the River by 82% and Se loads by 94%, compared to discharge in 1995 (Linneman et al., 2014). The current SJRIP facility covers approximately 6,000 acres. It is operated by Panoche Water District, the lead entity responsible for meeting Regional Board load limits for salt, boron, and selenium discharge into the San Joaquin River. The SJRIP provides drainage service to 100,000 acre Grassland Drainage Area (GDA) located south of Los Banos, between the San Joaquin River and Interstate 5. The majority of fields within the GDA are installed with tile drains to protect crops from water-logging and soils from accumulating salt through upward capillarity. Implementation of the Grasslands Bypass Project in 1996 allowed agricultural subsurface drainage flows within the GDA to be collectively diverted into a 28 mile reach of the San Luis Drain and eliminate subsurface drainage contamination of approximately 100 miles of wetland conveyance channels within the Grasslands Ecological Area (GEA) Letey et al. (2002; Quinn et al. (1998). The Central Valley Regional Water Quality Control Board set selenium water quality objectives of 5 ppb for the River and for Mud and Salt Sloughs; the schedule for Mud Slough compliance is linked to the selenium load reduction schedule for the Grassland Bypass project.

Several salt tolerant crops have been cultivated over the past 20 years within SJRIP and irrigated with subsurface drainage and (on some alfalfa fields) blended groundwater – the most successful crops have been 'Jose' tall wheatgrass and alfalfa hay - which now dominate the 1,700 acres underlain by tile drainage within the 6,000-acre dedicated facility. The total acreage planted to 'Jose' Tall Wheatgrass (TWG) and Alfalfa (ALF) at the SJRIP facility is approximately 3,750 and 950 acres, respectively.

Most of the salt-tolerant crop acreage is located on 4,095 acres situated east of Russell Avenue, near the city of Firebaugh, in Fresno County, California, referred to as the SJRIP 1 (see Fig. 9). An additional 1,861 acres located west of Russel avenue acquired in 2008 were planted with 1,478 acres of salt-tolerant crops. These 1,861 acres are referred to as SJRIP 2 (see Fig. 9).

Selected Fields

Four fields (two ALF, two TWG) were selected for the study. Fields were chosen based on the availability of historical data on irrigation water quality and forage production. As shown in Fig. 9, fields 13-2 and 13-6 are alfalfa fields, and 13-1 and 10-6 are 'Jose' tall wheatgrass fields. Fields and 13-1 and 13-2 have subsurface drains installed, whereas 10-6 and 13-6 have no subsurface drainage system.

Irrigation Data

The four forage fields were installed with *In-Situ* electrical conductivity (EC) sondes to provide frequent, real-time measurement of the salinity of applied irrigation water (Fig. 10). A limited number of grab samples were also collected for salinity assessment and were sent to 'Bryte' lab for complete analysis of chemical constituents.

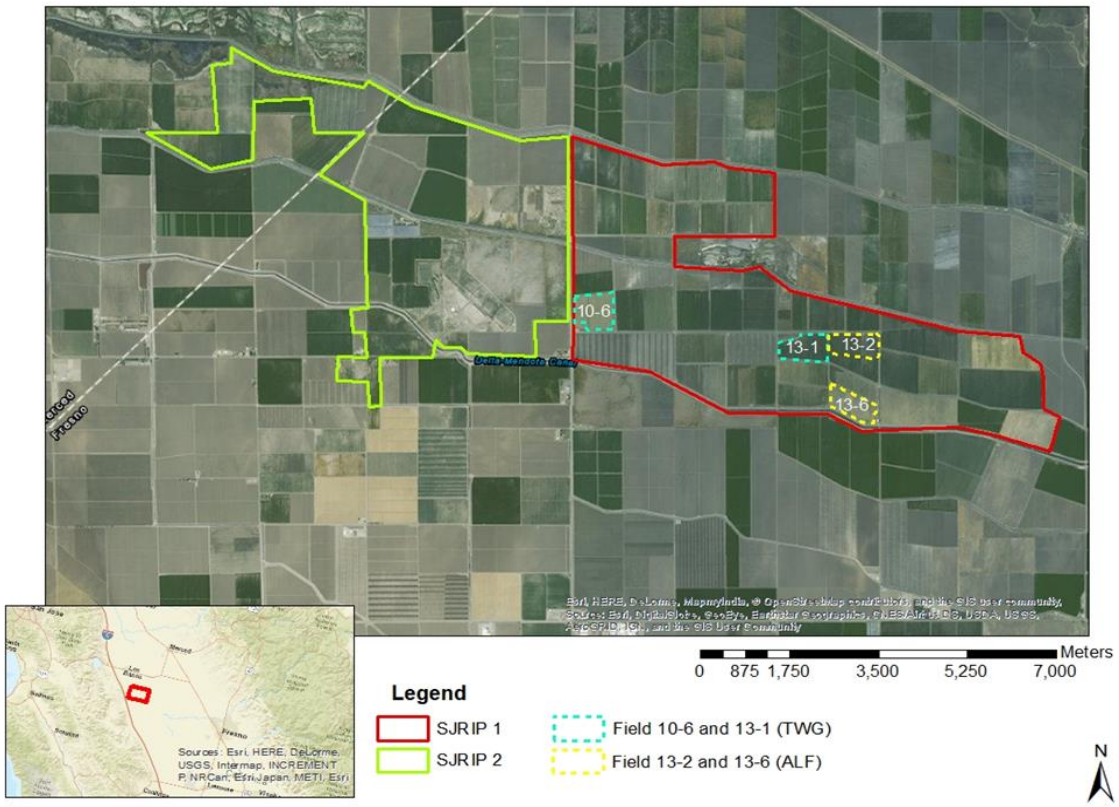

Figure 9. Map showing the location of the San Joaquin River Improvement Project (SJRIP) and the fields selected for the study.

Figure 10. EC sonde installation at one of the study field.

Components of the EM-38 Survey

The EM38-MK2 unit by Geonics Limited, Canada was used for salinity data acquisition. It operates on a 9V battery. The EM-38 and the GPS unit (Trimble) were connected to the serial ports of a portable field data logging device (Allegro-CX). Custom software for the Geonics EM38 'EM38MK2' was installed on the AllegroCX to facilitate data logging. The EM-38 was mounted on a non-conductive PVC sled and dragged behind an ATV during the salinity survey (Fig. 11). The measurement units for the EC_a readings produced by the EM-38 are "mS/m."

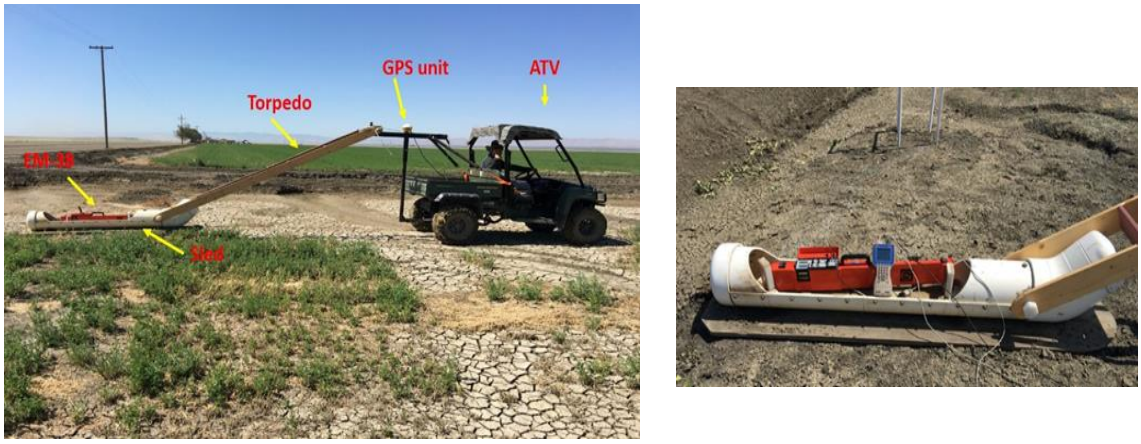

Figure 11. Components of an EM-38 soil salinity survey (left), and EM38-MK2 mounted to the sled (right) with nylon bolts. Also shown is the AllegroCX and Trimble GPS survey instrument.

Salinity Surveys

Salinity surveys were performed during the spring and fall seasons of 2016 and 2017 in the four fields selected for the study. Before beginning the survey, the EM38 was calibrated in air, mounted a distance of approximately 1.5m above ground using a stand made of PVC pipe. The battery was tested by turning on the instrument and making sure that the screen displayed a number above 720 when the knob was switched to battery mode. The instrument was kept outside for about

10-15 minutes after turning the power on for it to stabilize in the outside temperature. Any metallic objects like keys and mobile phones were kept away during both calibration and deployment because of the instrument's sensitivity to metallic objects. The calibration procedure is described in the EM38-MK2 operation manual and follows the protocol listed below:

- With the instrument in air at an elevation 1.5 meters above the ground and in the horizontal dipole mode of operation (see Fig. 12, the Q/P and I/P dial readings are set to zero.

Figure 12. EM-38 placed in horizontal dipole orientation during calibration.

- Next, with the instrument still elevated above ground - the Q/P zero control is adjusted so that an arbitrary value (i.e H=10 mS/m) appears on display, for the Q/P reading. Rotate the EM38-MK2 instrument to the vertical dipole mode position and note the reading (hypothetically V=16 mS/m). Subtract the horizontal dipole reading from the vertical (V-H=6 mS/m).
- While still in the horizontal dipole mode, rotate the Q/P zero control until the display reads the value calculated in step 2. In this example, it would be 6 mS/m. Now when you rotate the EM38 to the vertical dipole mode, the reading should be 12 mS/m.

With the EM-38 at least 1.5 meters above ground or higher, the Q/P reading or conductivity should always satisfy the following equation:

$$V = 2H$$

Where V = vertical dipole mode reading

H = horizontal dipole mode reading

Salinity surveys were conducted for each field using the ATV to drive along transects marked with flags placed about 30 meters apart. Speed of travel varied from 5-6 miles/hour, the average distance between the two consecutive sites is given in Table 1. EM38 was operated in the vertical orientation at a 1m coil separation mode, such that it was collecting simultaneous EC_a readings at 0.75m and 1.5m. These readings are referred as EM_v and EM_h respectively.

Table 1. Soil survey information for years 2016 and 2017.

Field	**Date**		**Number of transects**		**No. of survey sites**		**Avg. distance between sites (meters)**	
Year-2016	Spring	Fall	Spring	Fall	Spring	Fall	Spring	Fall
10-6 (TWG)	5/26/2016	10/17/2016	21	23	5785	5101	1.9	2.3
13-1 (TWG)	5/11/2016	10/19/2016	18	24	3812	3488	1.5	2.4
13-2 (ALF)	6/13/2016	9/20/2016	19	20	3515	3625	1.8	1.8
13-6 (ALF)	6/3/2016	9/29/2016	24	26	4283	4038	1.8	2.1
Year-2017								
10-6 (TWG)	4/24/2017	10/2/2017	21	22	4366	4346	2.5	2.6
13-1 (TWG)	4/17/2017	9/26/2017	28	27	4533	3399	2.1	2.6
13-2 (ALF)	5/22/2017	9/19/2017	28	28	3816	3076	2.3	2.8
13-6 (ALF)	4/27/2017	9/22/2017	24	24	2900	2815	2.7	2.8

Surveys were conducted 3-5 five days after an irrigation was completed on each field, and when the moisture content of the soil was close to the field capacity. This is important as the conductivity pathways for EC_a measurements can be broken when the moisture content is low. Performing a survey in such conditions can lead to erroneous readings. For each field, a strip of between 20-30 meters was left from all sides where EC_a readings were not taken to avoid any edge effects. The edges might not be representative of the entire field and can lead to a sampling design which is not desirable.

Soil Sampling (Ground-Truth Measurements)

After completing the EM38 motorized soil survey, the ESAP-RSSD program was used to establish soil sampling site locations, which follow a statistical sampling design that samples uniformly across the sample frequency distribution. Samples were collected on the same day immediately after the soil survey was completed, or the next morning to ensure the field conditions were the same or close to when the soil survey was performed. Twelve sample locations were selected across the field, identified by the ESAP program based on the range and variability of the EC_a data collected. Any dry or loose soil (if present at the soil surface) was removed since it is not reflected in EC_a measurements because of low moisture conditions. Four soil samples were collected at each of these sites at 30 cm depth increments from 0-120 cm with a hand auger. In all, 48 samples were collected from each field for lab analysis. The ESAP-RSSD program attempts to select sites that are distributed across the field. A computed number called the "Opt Criteria" provides a measure of uniformity or clustering of the sampling design. Although this calculation varies according to the situation, for a

square/rectangular field, the guidelines below could be followed to evaluate the uniformity of the sampling design (Lesch et al., 2000).

Opt Cri Value	Uniformity
< 1.15	excellent uniformity
1.15 - 1.30	reasonable uniformity
1.30 - 1.50	moderate clustering
1.50 - 1.75	serious clustering
> 1.75	excessive clustering (unacceptable design)

While selecting a given sampling design, the sampling design with lower Opt-Cri values were preferentially selected and the design factor adjusted if the number was initially high.

Soil Sample Analysis

The soil samples collected were labeled and stored in zip-lock bags. Samples were brought to lab and one portion (50-70 g) was dried in an oven at 105^{o}C for 3-4 days for gravimetric soil moisture measurements. The other portion was air dried in an oven at 55^{o}C until dried. The air-dried soil samples were ground using a mechanical pulverizer so as to pass through a 2mm sieve. Saturated soil pastes were prepared with deionized water using 200g of air dried soil and were allowed to stand overnight prior to vacuum filtration. The saturation percentage (SP) was measured for all samples.

Soil salinity (EC_e) was measured from the paste extract using an EC meter (accumet^{TM} Basic AB30 Conductivity meter, Fisher scienctific, Leicestershire, England). The pH of the soil solution extracts was also measured using a pH/conductivity meter.

ECa to ECe Calibration Equation

The ESAP-Calibrate program was used to convert EC_a data to EC_e data using spatially referenced multiple linear regression models. The program converts gravimetric water content measurements to volumetric water content measurements, and estimates the % moisture relative to FC (Field Capability). Correlation analysis between properties of the collected soil profile data was also performed. The DPPC correlation analysis was performed where a set of soil conductivity readings (referred as Calc EC_a) were estimated based on measured salinity (EC_e), SP, and water content values using Rhoades's equation (Rhoades et al., 1989). This analysis provides a theoretical value of EC_a readings at each sampling point and serves as a quality control check. Correlations between calculated EC_a, measured EC_a, EC_e, and other soil variables collected were also performed. Finally, a spatially referenced regression model was generated to predict the logarithm of salinity levels ($lnEC_e$) at four sampled depths for each site within the surveyed area. Details of the MLR results are provided in Appendix A.

Spatial Maps (Interpolation)

Maps depicting the spatial distribution of salts within each field were developed using ESRI's ArcMap 10.3.1. Maps were created for each sampled depth as well as for the average salinity of entire soil profile using satellite imagery as base-maps for better interpretation and assessment. The Inverse Distance Weighing (IDW) technique was used for interpolation of data using the Spatial analyst toolbox in ArcMap. A fixed radius setting of 40 meters was used with a minimum of 25 sample points. The output cell size was 5 meters.

Forage Samples and Analysis

$1m^2$ forage tissue samples were collected from each field before harvest from April to July of 2017. Twelve forage tissue samples were collected from each field at the same sites where the soil samples were collected (as guided by ESAP-RSSD) and a handheld GPS device. Field samples were taken to lab where the fresh weight of the biomass was taken. Samples were rinsed with deionized water to remove any surface salt and dust before further analysis.

To determine the dry matter percentage, the samples were dried for 2-3 days in a forced air oven at 60 ^{o}C to convert fresh yield to dry weight basis. The dried samples were then ground in a mechanical grinder to pass a 40-mesh screen for subsequent analysis of potassium and sodium in the shoots.

Atomic absorption spectroscopy was used for K+ analysis and atomic emission spectroscopy was used for the determination of Na+ in the alfalfa shoot tissue. For the extractions, an aliquot of ~0.5 grams of dried and ground shoot tissue were weighed and mixed with 30 ml of a 2% acetic acid. This resulted in a dilution fraction of 50 to 60. The extracts were filtered through #1 filter paper to remove any particulates.

For sodium analysis, an aliquot of extract of 0.5 ml was used for both ‘ALF’ and ‘TWG’ samples, and the resulting dilution fraction was 1200. For potassium, the volume of extract used was 0.3 ml and 0.5 ml and the dilution fraction were 2000 and 1200 respectively for ‘ALF’ and ‘TWG’ samples. The analysis was made using an Agilent 240AA Atomic Absorption and Emission Spectrophotometer at the Graduate Laboratory at California State University, Fresno. Correlation analysis were performed using statistical software ‘R’.

RESULTS AND DISCUSSION

Irrigation Water

Two to three grab samples of irrigation water were taken during the 2016 and 2017 growing seasons and sent to the Department of Water Resources' Bryte Laboratory for complete chemical analysis. In general, the irrigation waters for the forage fields were alkaline, averaging 7.7-8.0, and relatively high in bicarbonate (72-150 mg/L averages for the four fields). The salinity was more sulfate-dominated as compared to chloride and as salinity increased, the SAR and boron concentrations also increased (Tables 2 and 3). The TWG fields were irrigated with higher salinity water (3.9 – 5.1 dS/m) (Table 2) as compared to the ALF fields (2.9 dS/m average for 13-6 and only 0.8 dS/m for 13-2) (Table 3), although these ranges represent data from a very limited number of samples. EC sonde data reported below provide data from continuous monitoring and provide a more complete representation of the salinity applied to the forage fields.

Data from the EC sondes installed in the irrigation water ditches are reported as mean daily averages for the irrigation water salinity (EC_w) applied to each field from 7/1/2016 to 10/25/2017 (Figs. 13 to 16) although for the alfalfa fields data are more limited in 2016 as compared to 2017. The average daily EC as per the EC sonde measurements was 5.6, 4.8, 2.0, and 3.7 dS/m for fields 10-6 (TWG), 13-1 (TWG), 13-2 (ALF), and 13-6 (ALF) respectively.

It could be observed that Field 13-2 (ALF) was continuously receiving high quality irrigation water ($EC \leq 1$dS/m) in 2017 although from August to November 2016, irrigation water salinity was frequently in the 3 - 4 dS/m range. Field 13-6 (ALF) received irrigation water at or above 3 dS/m in 2017 and in August 2016, the EC_w was in the 3-5 dS/m range. Data from the continuous monitoring also

Table 2: Chemical composition of the irrigation water samples for TWG fields.

Field 10-6 (TWG)								
Sampling Date	**ECw (dS/m)**	**pH**	**Boron (mg/L)**	**Cl (mg/l)**	**SO4 (mg/L)**	**SAR**	**HCO3 (mg/L)**	**CO3 (mg/L)**
8/10/2016	4.5	8.3	3.72	603	1270	1.19	145	3
9/20/2016	6.9	8.1	15.2	1286	1870	12.6	124	2
4/12/2017	5.7	7.9	9.60	712	1700	9.51	177	1
5/19/2017	5.2	7.8	12.5	490	998	10.4	155	<1
9/13/2017	3.3	7.8	5.30	380	981	7.84	113	<1
Average	**5.1**	**8.0**	**9.26**	**694.2**	**1364**	**8.31**	**143**	
Field 13-1 (TWG)								
8/12/2016	3.2	7.8	2.22	378	954	5.04	137	1
9/12/2016	0.4	7.2	3.49	528	1351	4.57	170	1
4/12/2017	9.2	8.1	14.4	1086	2160	12.4	191	2
6/20/2017	2.9	7.8	2.90	530	1267	4.15	161	1
9/13/2017	3.6	7.6	3.30	480	1200	4.90	150	<1
Average	**3.9**	**7.7**	**5.26**	**600**	**1387**	**6.20**	**162**	

Table 3: Chemical composition of the irrigation water samples for ALF fields.

Field 13-2 (ALF)								
Sampling Date	**ECw (dS/m)**	**pH**	**Boron (mg/L)**	**Cl (mg/l)**	**SO4 (mg/L)**	**SAR**	**HCO3 (mg/L)**	**CO3 (mg/L)**
8/10/2016	1.0	8.4	0.94	110	222.6	4.20	76	2
9/8/2016	0.7	7.9	0.73	116	153.3	3.46	85	1
9/13/2017	0.6	7.2	0.60	35.0	115.0	2.40	55	<1
Average	**0.8**	**7.8**	**0.76**	**87.2**	**163.7**	**3.35**	**72**	
Field 13-6 (ALF)								
8/15/2016	3.9	8.2	1.08	554	1185	2.80	160	3
9/14/2016	0.4	7.7	2.58	478	1182	3.95	151	1
4/19/2017	3.4	7.8	2.80	423	1170	4.00	146	<1
5/19/2017	3.0	7.8	3.00	497	1371	4.35	142	<1
9/13/2017	3.7	7.8	2.50	480	1200	4.10	152	<1
Average	**2.9**	**7.9**	**2.39**	**487**	**1222**	**3.86**	**150**	

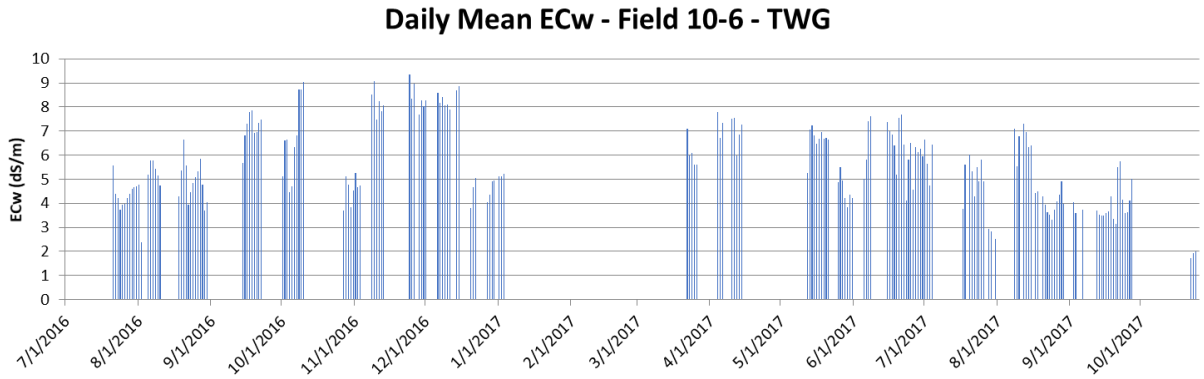

Figure 13. Mean daily EC_w applied to Field 10-6 as measured by EC sonde.

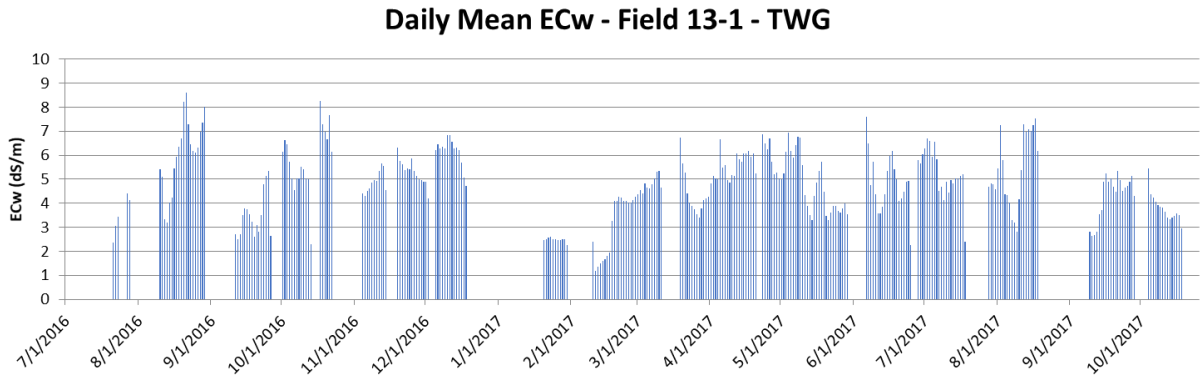

Figure 14. Mean daily EC_w applied to Field 13-1 as measured by EC sonde.

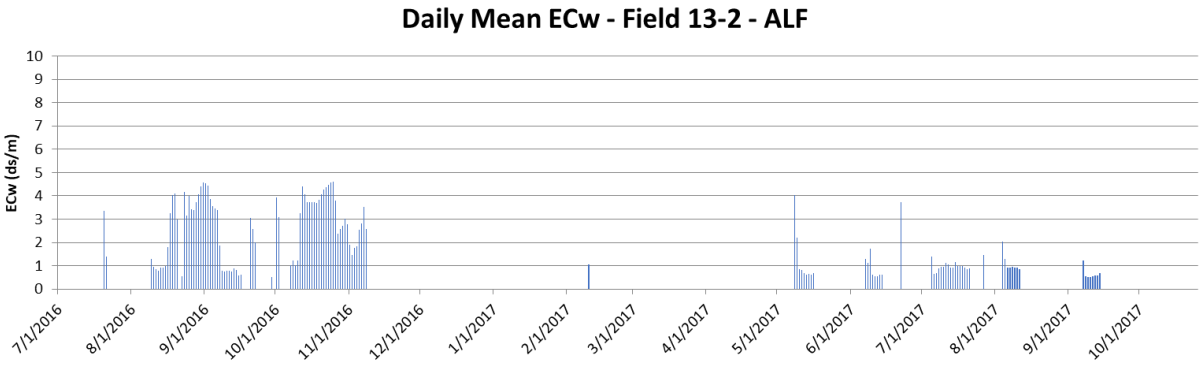

Figure 15. Mean daily EC_w applied to Field 13-2 as measured by EC sonde

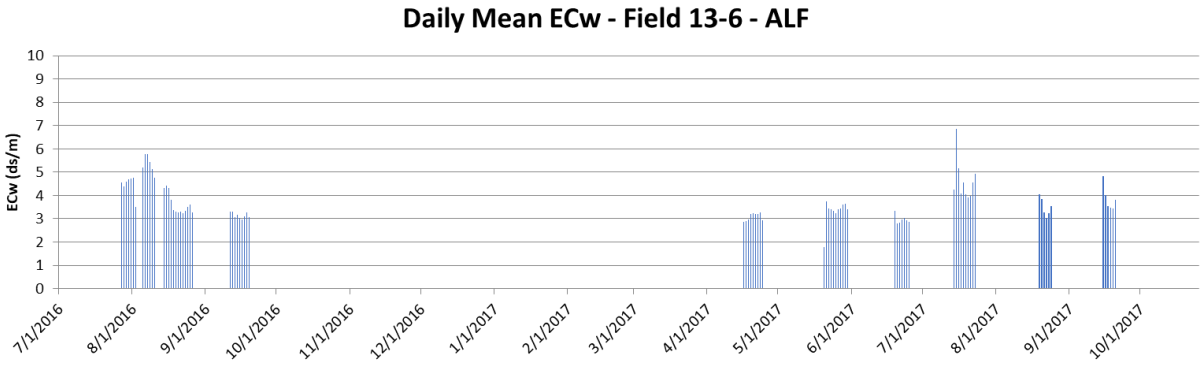

Figure 16. Mean daily EC_w applied to Field 13-6 as measured by EC sonde.

revealed that the alfalfa fields, in particular 13-2, were irrigated with lower salinity irrigation water as compared to the tall wheatgrass fields.

Soil Survey Data

The average, SD, and the range of the EM_v and EM_h data collected during the EM38 survey for each field is given in Table 4. Relying on the EC_a data is not enough as it is influenced by various other soil properties and is only used as a surrogate for the assessment of soil properties that have a strong correlation with EC_a. However, EC_a data do provide an idea of the relative distribution of salts in the field, if salinity is the dominant soil property influencing EC_a. Correlation between EM_v and EM_h data is also shown in the Table 4. High correlations were observed indicating there were no moisture or textural irregularities in the soil profile. A relatively lower correlation for Field 13-2 during Fall 2017 survey could be explained by the slight moisture variability in the field during the survey.

More complete chemical analysis was conducted on the saturation paste extracts from the surface soil samples (0-30 cm) taken for ground-truthing in Fall 2017. Soils in the TWG fields had Sodium Adsorption Ratio (SAR) and boron concentrations, roughly twice those found in the ALF fields (Table 5). The SAR of 20-22 in the TWG fields would suggest significant reductions in water infiltration

Table 4. Apparent electrical conductivity data EC_a (dS/m) collected during EM38 surveys.

Spring (2016)									
Field	**EM_v**	**SD**	**Min**	**Max**	**EM_h**	**SD**	**Min**	**Max**	**EM_v vs. EM_h correlation**
10-6	2.91	1.11	0.78	5.41	2.54	1.11	0.52	5.15	0.9864
13-1	4.67	0.5	3.3	6.38	3.59	0.54	2.25	5.53	0.9309
13-2	4.74	0.47	2.76	5.88	2.94	0.42	1.28	4.24	0.9571
13-6	2.58	0.5	1.5	3.92	1.79	0.38	0.94	3.09	0.9878
Fall (2016)									
10-6	3.16	1.03	0.73	5.29	2.74	1.07	0.55	5.28	0.9828
13-1	4.79	0.65	2.07	6.93	3.71	0.55	1.53	5.89	0.9589
13-2	3.45	0.48	1.77	4.58	2.42	0.4	1.15	3.5	0.9872
13-6	2.92	0.44	1.66	4.27	2.03	0.35	0.98	3.31	0.9684
Spring (2017)									
10-6	2.58	0.93	0.72	4.51	2.00	0.86	0.4	3.97	0.9849
13-1	4.26	0.49	2.46	5.78	3.28	0.39	1.89	4.63	0.9469
13-2	3.44	0.4	2.06	4.71	2.54	0.37	1.36	3.78	0.9804
13-6	2.86	0.46	1.75	4.06	2.20	0.36	1.28	3.12	0.991
Fall (2017)									
10-6	3.19	1.15	0.7	5.51	2.72	1.16	0.46	5.23	0.9788
13-1	5.30	0.53	3.47	6.89	4.21	0.43	2.69	5.54	0.8554
13-2	3.91	0.42	2.38	5.17	3.01	0.36	1.75	4.18	0.9881
13-6	3.46	0.51	2.14	4.72	2.79	0.43	1.65	3.93	0.9826

into the soil. This was not observed in the field, possibly due to the fibrous root system of the forage which help to improve infiltration. Likewise, the boron concentrations in the TWG fields (19 – 22 mg/L) would be detrimental to the growth of most crops demonstrating the high level of salt and boron tolerance reported earlier for '*Jose*' tall wheatgrass growing under irrigation with saline drainage water from the WSJV (Suyama et al. 2007a).

Table 5. Sodium Adsorption Ratio (SAR), major cations (Na, Ca, Mg), anions (Cl, SO_4) and B concentrations for ground-truthing samples (0-30 cm depth) taken in Fall 2017

	Field 10-6		Field 13-1		Field 13-2		Field 13-6	
	Mean	Range	Mean	Range	Mean	Range	Mean	Range
SAR	22.1	8.7 - 38.1	20.8	15.3-30.0	10.7	4.9- 15.5	7.6	4.9 - 11.5
B (mg/L)	21.9	4.1 - 38.5	18.9	12.7-26.7	11.4	5.4 - 19.1	4.0	2.1 - 7.0
Ca (meq/L)	23.9	7.1-35.6	25.4	23.3-26.5	25.5	23.4 - 31.2	29.1	23.4 - 33.2
Mg (meq/L)	30.1	4.4-63.9	31.3	25.1 - 38.2	14.6	13.0 - 19.3	16.4	11.6 - 20.5
Na (meq/L)	121.5	20.9 - 268.8	111.3	75.9 - 166.6	48.2	21.2 - 68.2	36.5	20.6 - 58.5
Cl (mg/L)	2244.6	232 - 5200	1831.2	1030 - 2712	246.1	100-420	905.4	290 - 1410
SO_4^{2} (mg/L)	5106	945 - 10800	5142	4130 - 6498	3505.70	2500-4521	2444.67	1890 - 3050

Table 6 shows the saturation percentage (SP), an indirect measure of soil texture, volumetric water content, and the volumetric water content relative to the field capacity of the soil. Field 10-6 had the largest variability in soil texture, ranging from loam to clay. Other fields had a clay to clay loam soil texture with 'TWG' fields having the highest SP (clay content). The EM-38 soil surveys were performed when the average water content was >70% of the field capacity as shown in Table 6 (Corwin & Lesch, 2013).

Table 6: Saturation percentage (SP), volumetric water content (Vol), and water content relative to field capacity (%H2o/FC) for each season by field

	Spring 2016			Fall 2016			Spring 2017			Fall 2017		
10-6 (TWG)												
Soil	Mean	SD	Range	Mean	SD	Range	Mean	SD	Range	Mean	SD	Range
SP	55.2	14.8	31.4-81.5	58.8	16.0	32.1-88.5	57.5	18.4	25.2-84.8	53.8	16.3	30.9-91.2
Vol	0.36	0.055	0.25-0.50	0.34	0.057	0.23-0.44	0.34	0.055	0.21-0.42	0.32	0.057	0.20-0.42
%H2o/FC	100	19.6	77.4-163	90.6	13.9	52.7-131	92.8	20.3	58.4-153	92.0	19.1	62.7-156
13-1 (TWG)												
SP	80.1	2.84	75.4-88.8	86.1	4.50	75.2-96.3	80.6	3.60	74.1-91.3	83.6	3.77	75.5-92.6
Vol	0.46	0.035	0.31-0.51	0.42	0.032	0.35-0.50	0.45	0.031	0.39-0.51	0.42	0.036	0.25-0.49
%H2o/FC	95.3	7.11	67.5-107	84.2	6.26	66.4-100	93.1	6.85	80.3-107	86.1	7.26	49.8-99.4
13-2 (TWG)												
SP	74.7	5.27	59.7-83.2	78.6	8.41	54.2-108	80.7	9.04	60.4-103.2	84.6	7.44	70.9-113.9
Vol	0.41	0.031	0.35-0.54	0.38	0.038	0.28-0.46	0.39	0.037	0.25-0.46	0.40	0.031	0.33-0.49
%H2o/FC	89.1	9.37	72.1-136	81.7	8.81	63.4-109	82.5	10.2	52.6-109	81.1	7.43	62.6-102
13-6 (TWG)												
SP	67.0	6.89	52.8-76.8	71.9	7.48	53.5-87.8	72.8	7.70	55.1-84.2	72.5	8.51	52.6-85.5
Vol	0.38	0.034	0.29-0.44	0.38	0.035	0.28-0.47	0.41	0.027	0.35-0.47	0.41	0.025	0.37-0.46
%H2o/FC	88.2	11.8	70.7-121	85.4	11.1	64.0-127	91.6	6.78	75.5-106	92.6	8.93	77.8-122

Results from the quality check of the EC_a data collected are shown in Table 7 as DPPC correlations. These are the correlations between log of 'CalcEC_a' and the z1[1] signal (EM data) averaged for the entire sampled soil profile (Lesch et al., 2000). More details on the DPPC correlations results can be found in Appendix B. Poor correlations were observed for field 13-1 during the fall season of both years.

Table 7. DPPC model correlations

	Spring 2016	**Fall 2016**	**Spring 2017**	**Fall 2017**
10-6 (TWG)	0.977	0.966	0.899	0.897
13-1 (TWG)	0.868	0.216	0.878	0.536
13-2 (ALF)	0.905	0.788	0.949	0.812
13-6 (ALF)	0.79	0.844	0.963	0.917

After the quality check, a model was selected that produced the best predictions of (log) salinity levels at each surveyed point. The MLR models that were selected, in each case, are shown in the Table 8.

Where, b0, b1, b2, b3, and b4 are the regression parameters.

z1 and z2[2] are the transformed and decorrelated EM signal readings. (i.e. EM_v and EM_h).

x and y[3] are the centered and scaled location coordinates.

---

[1] z1here is the average of the ECv and ECh conductivity readings.

[2] Instead of raw conductivity readings i.e. EM_v and EM_h, z1 and z2 are used respectively (also called Principal component scores)

[3] Similarly, instead of raw location coordinates, x and y are used which are centered and scaled. Lesch et al. (1995b)

Table 8. Multiple linear regression models used for converting EC_a data to EC_e with the model r-square values to show goodness of fit

Season	Field	MLR Model used	R-square (averaged over 0-120 cm)
Spring 2016	10-6 (TWG)	ln(ECe) = b0 + b1(z1) + b2(z2)	0.9104**
	13-1 (TWG)	ln(ECe) = b0 + b1(z1) + b2(y)	0.7842**
	13-2 (ALF)	ln(ECe) = b0 + b1(z1)	0.8367**
	13-6 (ALF)	ln(ECe) = b0 + b1(z1)	0.5504**
Fall 2016	10-6 (TWG)	ln(ECe) = b0 + b1(z1) + b2(z1^2) + b3(x)	0.9475**
	13-1 (TWG)	ln(ECe) = b0 + b1(z1) + b2(z2) + b3(z1^2) + b4(x)	0.8265**
	13-2 (ALF)	ln(ECe) = b0 + b1(z1)	0.4357*
	13-6 (ALF)	ln(ECe) = b0 + b1(z1) + b2(z2)	0.8459**
Spring 2017	10-6 (TWG)	ln(ECe) = b0 + b1(z1)	0.7934**
	13-1 (TWG)	ln(ECe) = b0 + b1(z1) + b2(z2)	0.8465**
	13-2 (ALF)	ln(ECe) = b0 + b1(z1) + b2(z2) + b3(y)	0.9561**
	13-6 (ALF)	ln(ECe) = b0 + b1(z1) + b2(z2)	0.9597**
Fall 2017	10-6 (TWG)	ln(ECe) = b0 + b1(z1) + b2(z2)	0.8309**
	13-1 (TWG)	ln(ECe) = b0 + b1(z1) + b2(z2)	0.5070*
	13-2 (ALF)	ln(ECe) = b0 + b1(z1) + b2(y)	0.6092*
	13-6 (ALF)	ln(ECe) = b0 + b1(z1) + b2(x) + b3(y)	0.9287**

*Significant at $P \leq 0.05$
**Significant at $P \leq 0.01$

Soil salinity (EC_e) data for all fields, sampling times and depths (0-120 cm in 30 cm increments) are shown in Table 9. These data are the converted EC_e data for all surveyed points where EC_a was measured by the EM-38. Similar data for actual soil samples taken at the 12 ground-truthing locations selected by the ESAP software during each survey can be found in Appendix C.

Table 9. Average soil salinity EC_e(dS/m), standard deviation and range for each depth for all surveyed points in each field

	Spring 2016		**Fall 2016**		**Spring 2017**		**Fall 2017**	
10-6 (TWG)								
Depth (cm)	**Mean**	**Range**	**Mean**	**Range**	**Mean**	**Range**	**Mean**	**Range**
0-30	10.6	2.47-23.3	15.5	3.28-34.0	11.8	4.12-19.0	14.6	3.25-38.2
30-60	13.9	3.17-27.3	17	1.69-32.4	14.8	5.10-23.9	16.5	5.83-33.4
60-90	12.2	3.09-23.3	18.1	1.44-28.1	15.6	5.56-25.0	16.4	5.99-28.8
90-120	12.7	2.97-26.0	16.7	1.09-27.0	15.2	5.69-23.8	14.8	4.37-27.5
[0-120]	**12.5**	**2.47-27.3**	**17**	**1.09-34.0**	**14.4**	**4.12-25.0**	**15.7**	**3.25-38.2**
13-1 (TWG)								
0-30	13.0	10.3-17.3	12.6	6.83-40.7	12	6.07-17.7	13.4	9.53-16.6
30-60	19.6	13.2-33.3	17.0	9.13-31.0	16.3	7.19-25.1	19.6	14.2-25.4
60-90	20.8	15.1-31.4	17.5	11.4-45.5	18.5	9.30-27.1	20.3	14.9-26.0
90-120	23.2	18.6-29.8	19.2	8.21-47.9	18.6	9.59-26.4	21.0	16.1-25.0
[0-120]	**19.3**	**10.3-33.3**	**16.6**	**6.83-47.9**	**16.4**	**6.07-27.1**	**18.6**	**9.53-26.0**
13-2 (ALF)								
0-30	9.56	3.34-17.1	8.00	4.74-10.2	7.01	2.33-13.4	7.02	3.57-10.4
30-60	14.0	6.67-21.2	12.0	7.41-15.1	11.5	3.84-22.0	13.7	10.1-16.0
60-90	16.5	10.6-21.4	14.9	11.1-17.2	14.1	6.45-22.5	16.2	13.6-17.8
90-120	17.2	8.55-25.4	15.2	13.58-16.1	15.2	7.56-23.3	15.8	12.2-19.6
[0-120]	**14.4**	**3.34-25.4**	**12.6**	**4.74-17.2**	**12**	**2.33-23.3**	**13.3**	**3.57-19.6**
13-6 (ALF)								
0-30	5.72	3.02-9.52	7.2	4.32-10.9	5.06	1.80-14.6	6.87	4.47-9.86
30-60	8.94	5.03-14.18	10.3	6.33-15.5	9.87	3.30-27.0	10.6	6.02-17.4
60-90	10.8	7.57-14.33	12.1	8.46-15.6	12.0	5.82-22.8	12.2	6.52-18.3
90-120	10.25	6.74-14.44	11.0	6.46-16.4	10.8	6.60-17.4	11.8	7.14-16.2
[0-120]	**8.97**	**3.02-14.44**	**10.2**	**4.32-16.4**	**9.49**	**1.80-27.0**	**10.4**	**4.47-18.3**

TWG field 13-1 was the most saline field averaging 16.4 – 19.3 dS/m EC_e for the 0-120 cm soil depth in 2016 and 2017, but reaching 20 – 23 dS/m EC_e in the lower portion of the profile. This field was drained and there was evidence of leaching given that in all four sampling periods, soil salinity was lowest in the 0-30 cm soil depth and highest in the 90-120 depth. TWG field 10-6 was less saline averaging 12.5 – 17.0 dS/m ECe for the 0 - 120 cm soil depth in 2016 and 2017 and salinity was much more uniform with depth which is consistent with the lack of a subsurface drainage system in this field.

The ALF fields (13-2 and 13-6) had lower soil salinity than the TWG fields which is consistent with the application of less saline water to alfalfa fields as compared to tall wheatgrass fields. Soil salinity in the 0-120 cm soil depth averaged 12 to 14.4 dS/m EC_e for field 13-2 and 9.0 – 10.4 dS/m ECe for field 13-6 which was irrigated with the least saline water. In Field 13-2 which is drained, soil salinity was lowest near the surface (0-30 cm depth) and increased with each depth increment. Field 13-6 is not drained, but soil salinity was lowest in surface 30 cm and increased in the lower soil depths (60 – 120 cm) which indicated some degree of leaching. In the ALF fields there was little or no increase in soil salinity from the spring to the fall and in field 13-2 in 2016, soil salinities were lower in the fall as compared to the spring. This could be explained by a lack of rainfall in the winter of 2016 such that irrigation in the summer helped to leach some of the salts below the 120 cm soil depth.

The salt distribution in the field 10-6 was highly variable as compared to the other fields (see Fig. 17). It could also be observed that most of the salts were accumulating mostly at the 2nd and 3rd foot depth in the soil profile indicating the lack of adequate drainage, which was expected as this field had no tile drainage system installed.

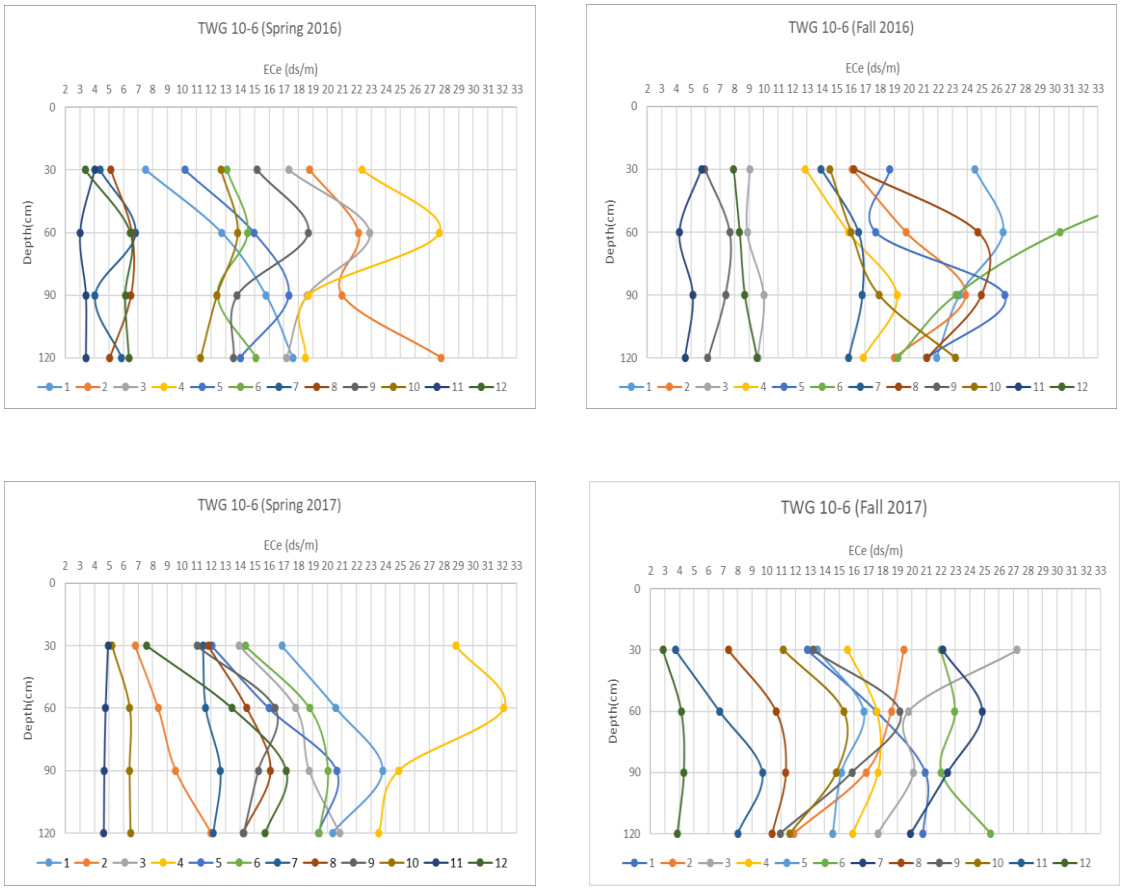

Figure 17. Salinity distribution in the soil profile at the 12 sampling locations in Field 10-6 for Spring (left) and Fall (right) surveys conducted in 2016 (upper) and 2017 (lower).

Spatial maps showing the salinity distribution for the field 10-6 are shown in Figures 18 and 19 for year 2016 and 2017, respectively. Green and yellow areas represent lower salinity and orange and white areas represent higher salinity. It was observed that the western part of field 10-6 had relatively lower EC_e values (<8 dS/m) than in the eastern part throughout the study period. This could be attributed to the soil textural variability of the field, as the western part was comprised of lighter texture soil (lower SP values). The maps show an increase in salinity during the fall season and accumulation of most salt in 2nd (30-60cm) and 3rd (60-90cm) foot depths in both seasons.

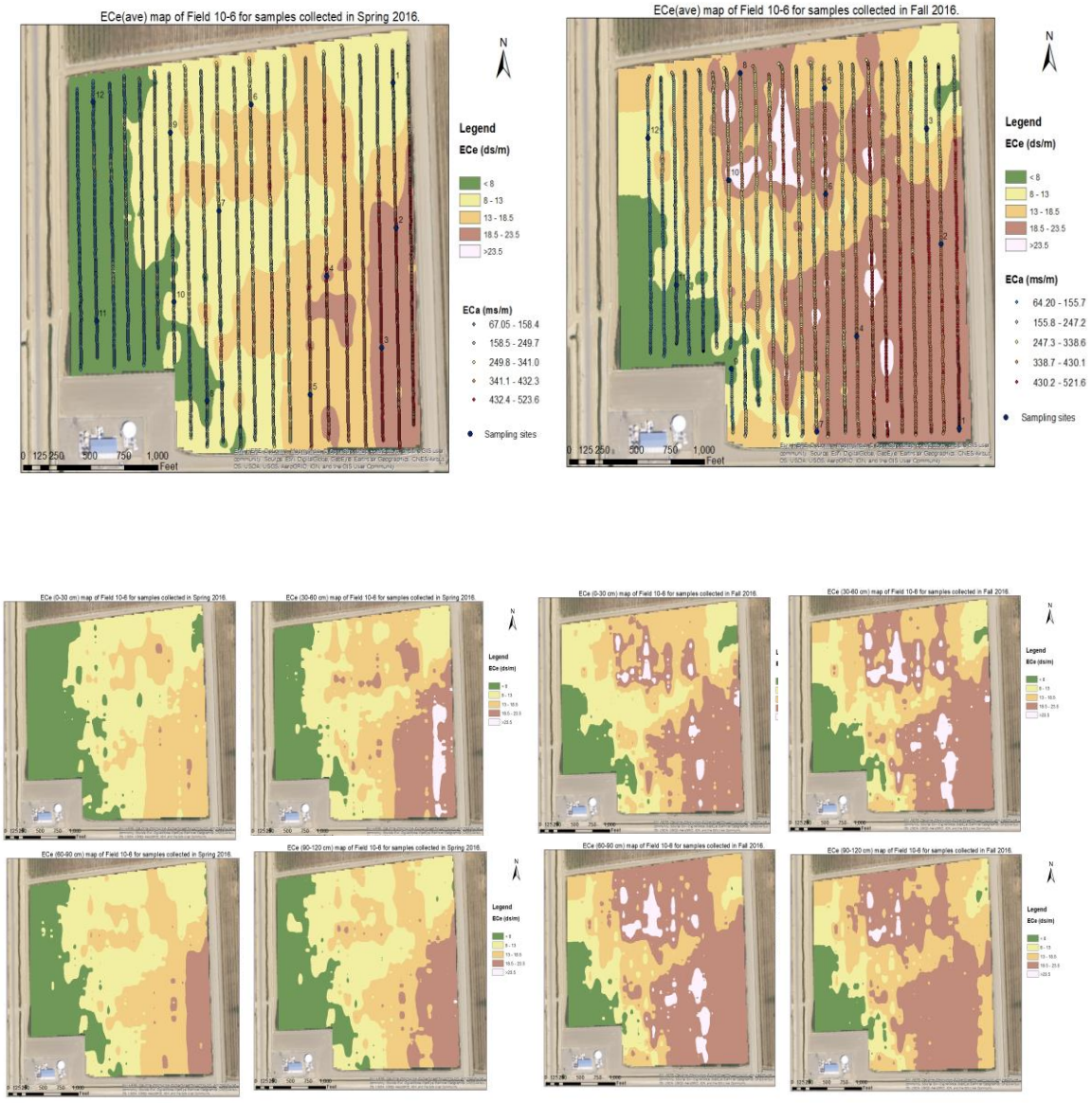

Figure 18. Spatial distribution of average salinity (0 – 120 cm) (top) and for each depth (bottom) in Field 10-6 for Spring (left) and Fall (right) 2016.

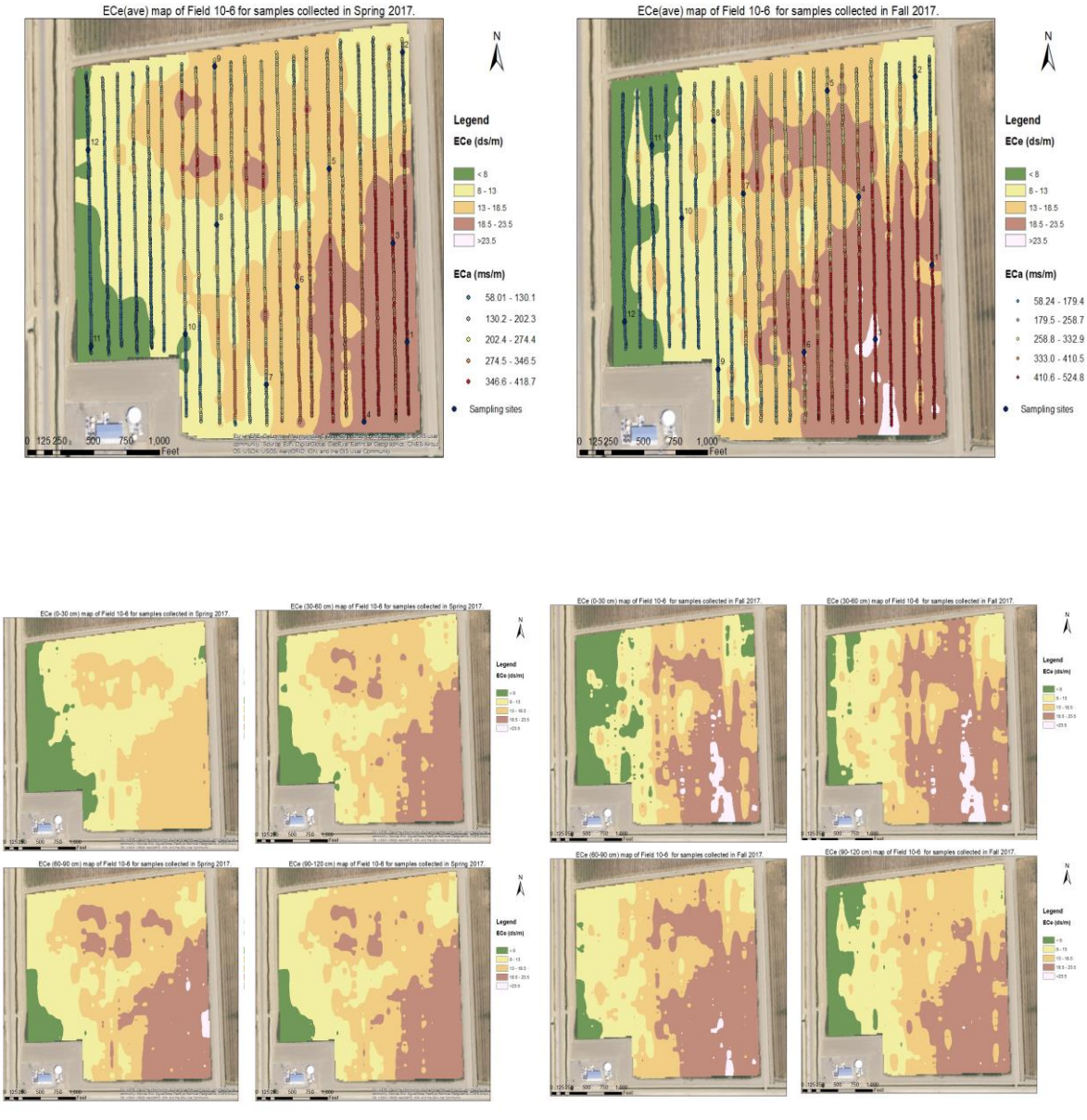

Figure 19. Spatial distribution of average salinity (0-120 cm) (top) and for each depth (bottom) in Field 10-6 for Spring (left) and Fall (right) 2017.

Also shown in all of the spatial maps are the transects/rows where the EC_a (mS/m) measurements were taken in the field during EM38 surveys, and the blue points represent the soil sampling sites. EC_a measurements overlaid on these maps are the averages of the EM_v and EM_h data.

The salinity profile for the drained field 13-1 (Fig. 20) shows evidence of improved drainage as indicated by higher salinity values at the bottom of the soil profile. Figs. 21 and 22 are the spatial maps showing the spatial distribution of the salts in Field 13-1 for 2016 and 2017, respectively. It should be noted that only a part of the field was surveyed in spring 2016 (see Fig. 21) due to high water content in the western part of the field. In fall 2016, poor estimation of EC_e from EC_a was observed (lower DPPC correlations), as pointed out earlier. Poor EC_e estimations are particularly discernable in the south-east corner of the field where the EC_a readings were lower, but the map delineated this area as being of high EC_e (see Fig. 21). Thus, there was a mismatch between the EC_a and EC_e data for this field. Also, worth noting is the higher accumulation of the salts at the bottom of the soil profile, and we can see the parts of the field where most accumulation occurred.

Field 13-2 (ALF) continually received good quality irrigation water, as a result of which, a well leached salinity profile was developed over time. This effect is most peculiar for fall 2017 where a uniformly leached surface layer of the soil profile could be observed (Fig. 23). Since, this was a drained field, most salt accumulation was observed at the bottom of the soil profile as a result of better drainage. Spatial maps for years 2016 and 2017 are shown in Fig. 24 and 25, respectively. Only a portion of the field was surveyed in year 2016 because of the high water content of the field at the time of survey.

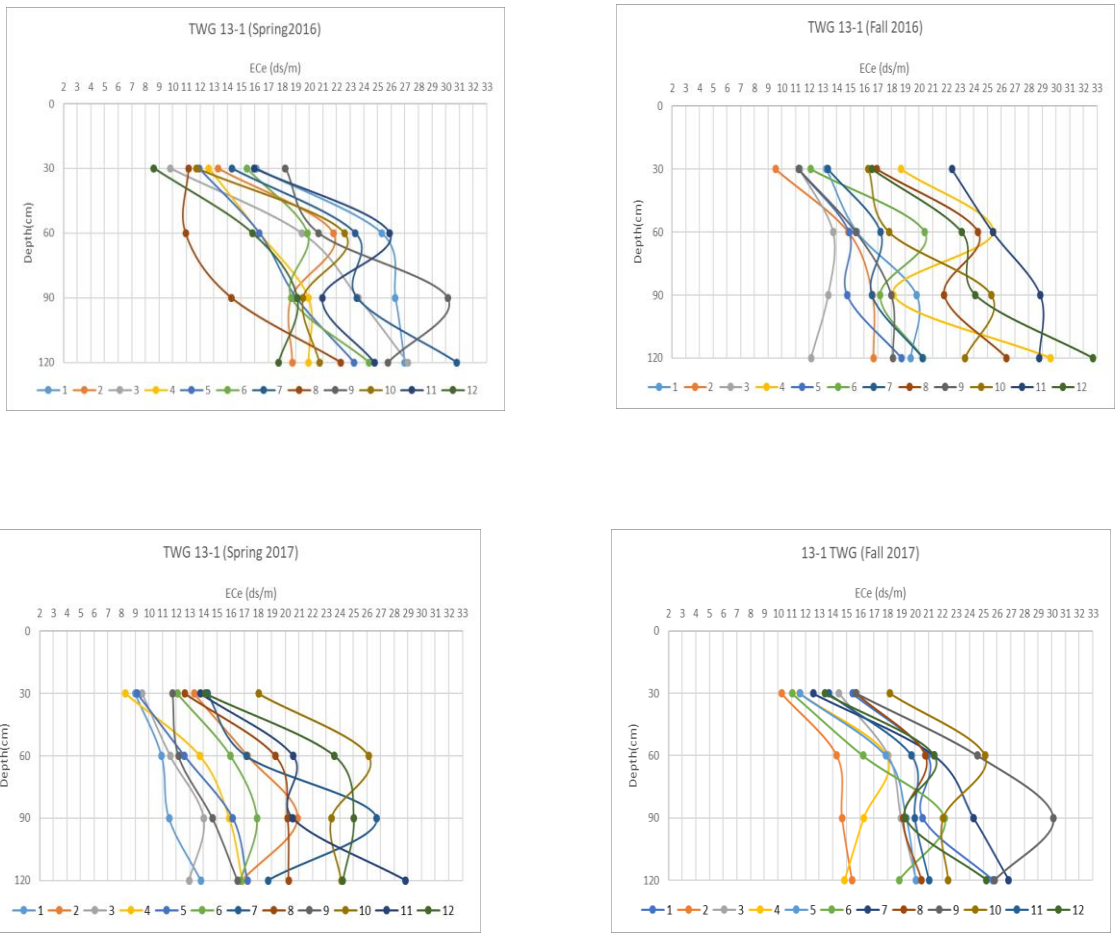

Figure 20. Salinity distribution in the soil profile at the 12 sampling locations in Field 13-1 for Spring (left) and Fall (right) surveys conducted in 2016 (upper) and 2017 (lower).

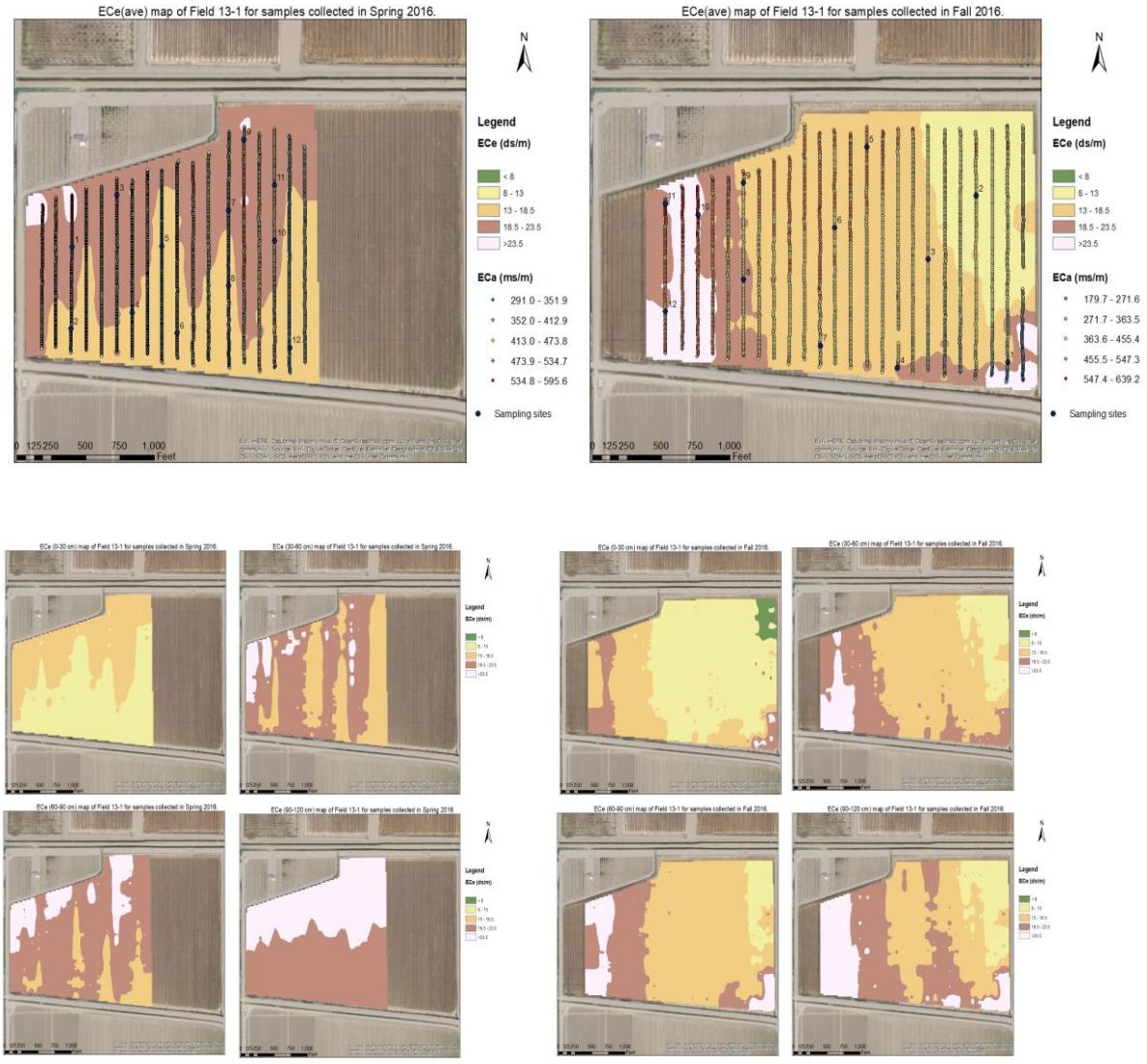

Figure 21. Spatial distribution of average salinity (0-120 cm) (top) and for each depth (bottom) in Field 13-1 for Spring (left) and Fall (right) 2016.

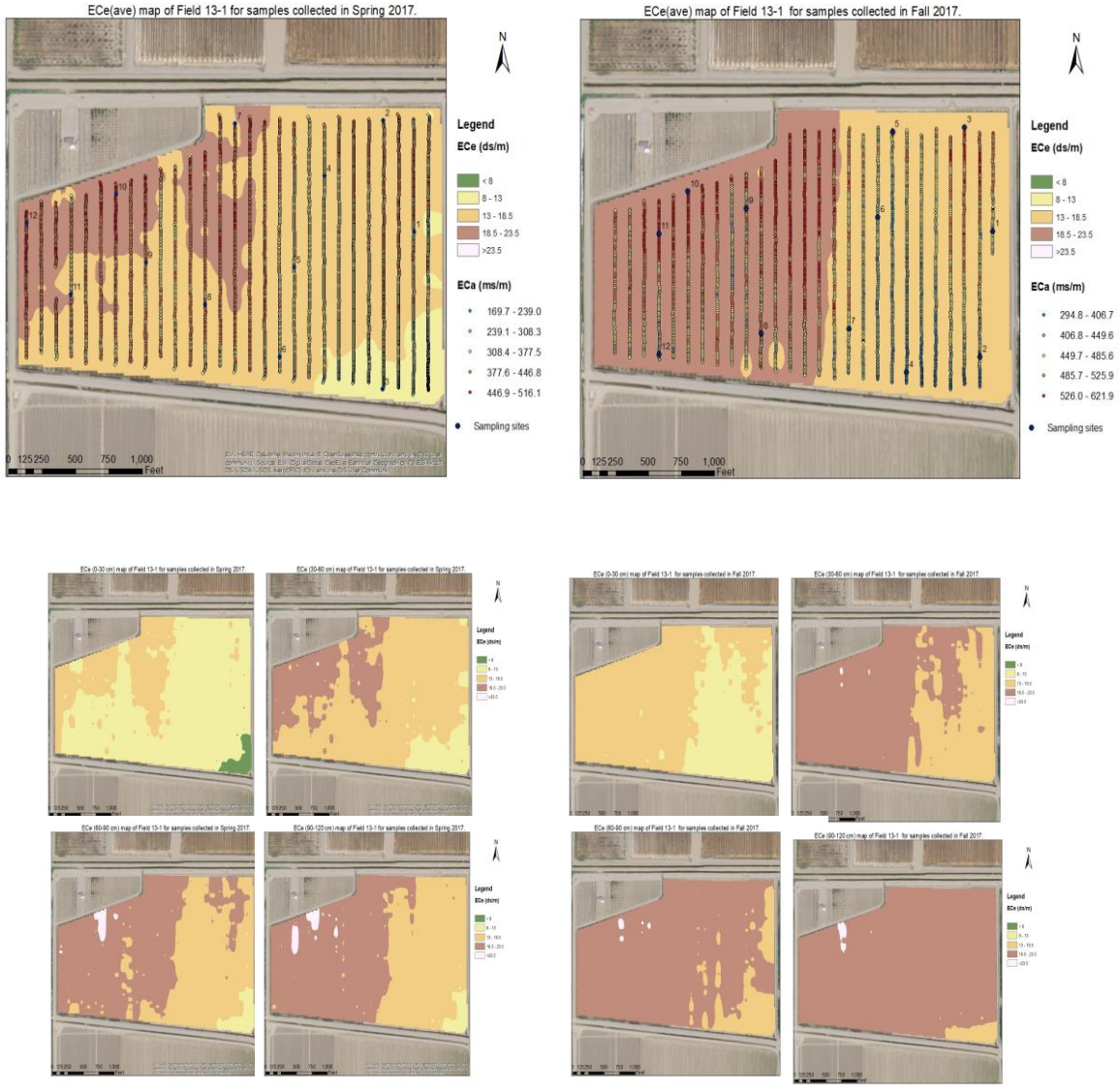

Figure 22. Spatial distribution of average salinity (0 – 120 cm) (top) and for each depth (bottom) in Field 13-1 for Spring (left) and Fall (right) 2017.

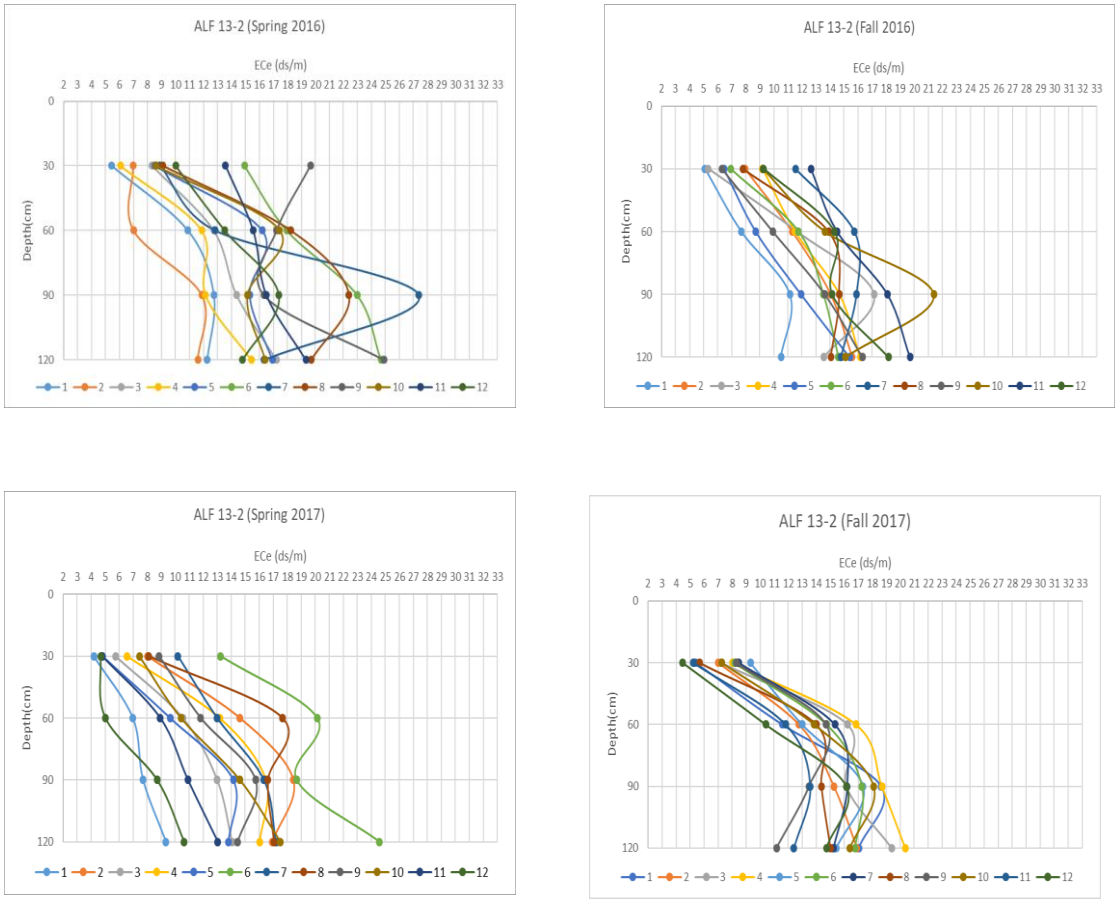

Figure 23. Salinity distribution in the soil profile at the 12 sampling locations in field 13-2 for Spring (left) and Fall (right) surveys conducted in 2016 (upper) and 2017 (lower).

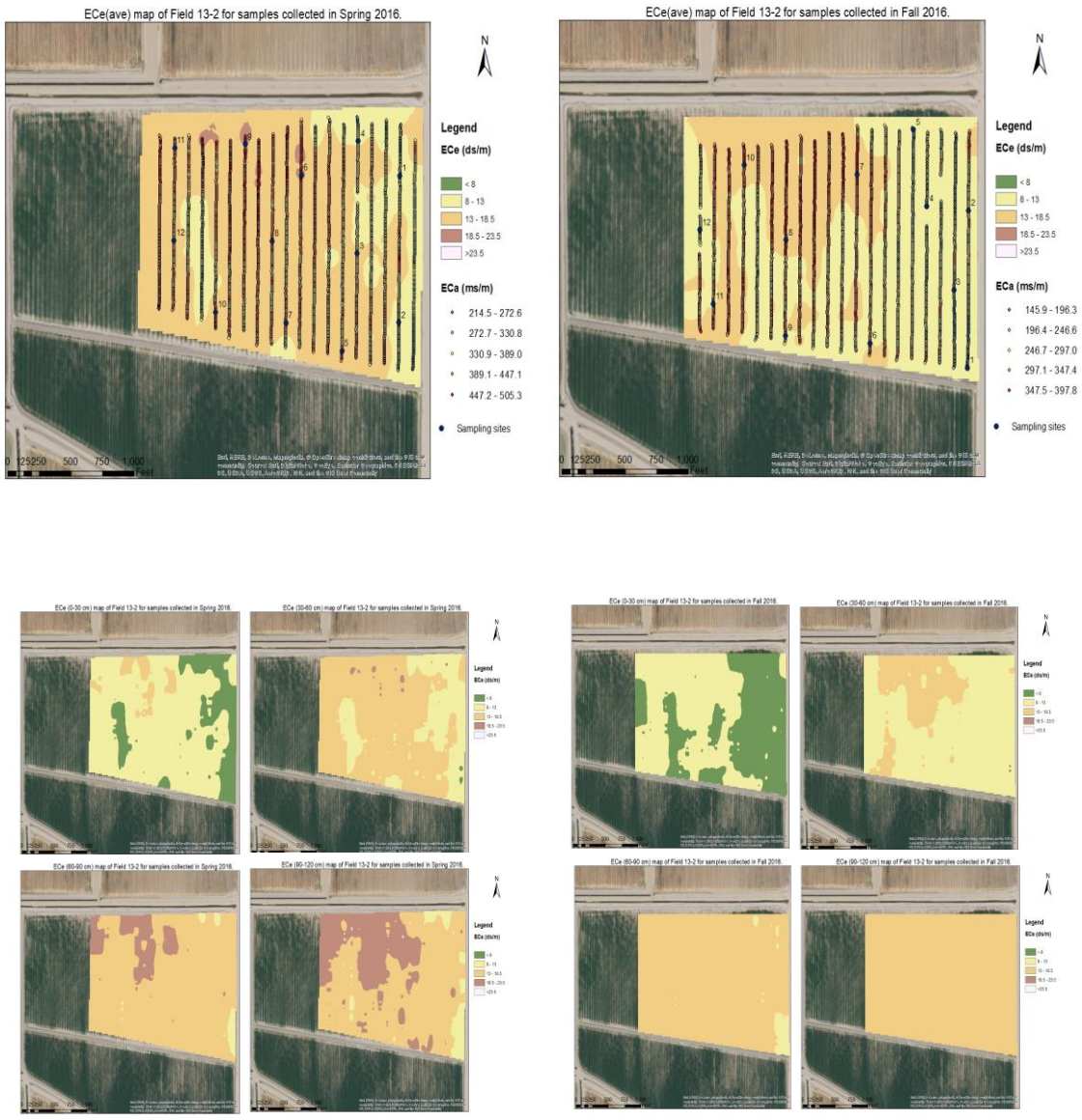

Figure 24. Spatial distribution of average salinity (0 – 120 cm) (top) and for each depth (bottom) in Field 13-2 for Spring (left) and Fall (right) 2016.

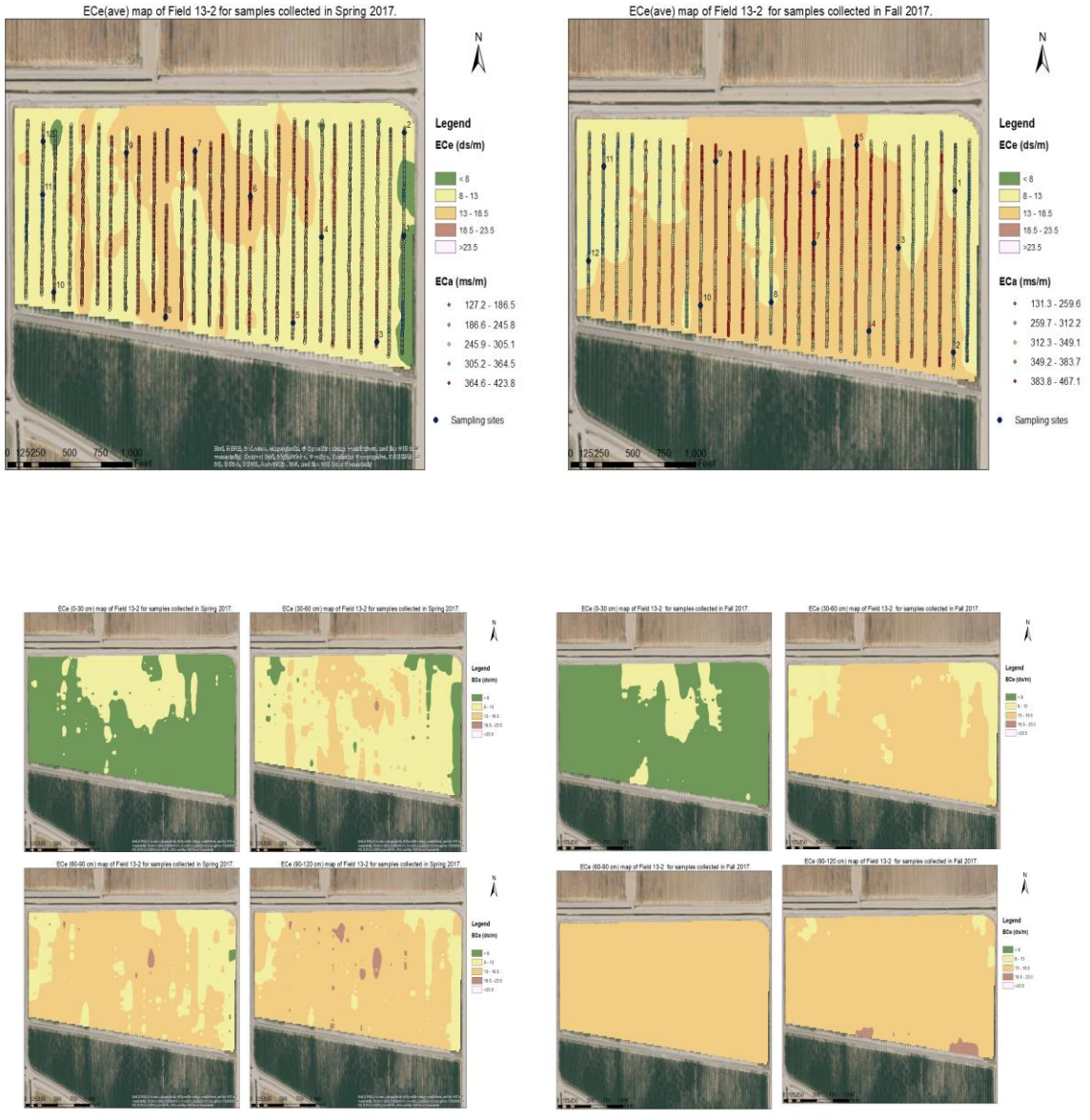

Figure 25. Spatial distribution of average salinity (0 – 120 cm) (top) and for each depth (bottom) in Field 13-2 for Spring (left) and Fall (right) 2017.

Similarly, the salinity profile for Field 13-6 for each season is shown in Figure 26. Most of the salt accumulation occurred at the 2nd and 3rd layers of soil profile, similar to the other undrained field 10-6. This field had the lowest salinity levels compared to the other fields. Spatial distribution of the salt within the field is shown in Fig. 27 and 28 for years 2016 and 2108, respectively.

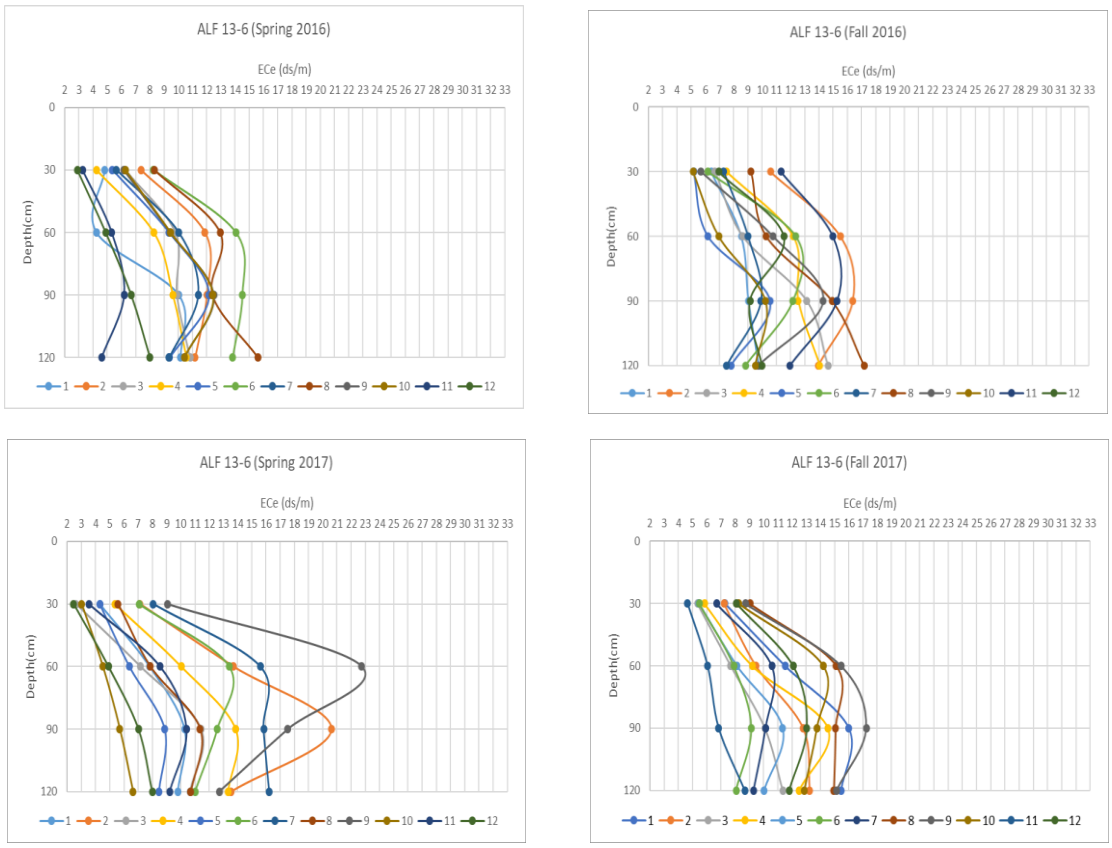

Figure 26. Salinity distribution in the soil profile at the 12 sampling locations in field 13-6 for Spring (left) and Fall (right) surveys conducted in 2016 (upper) and 2017 (lower).

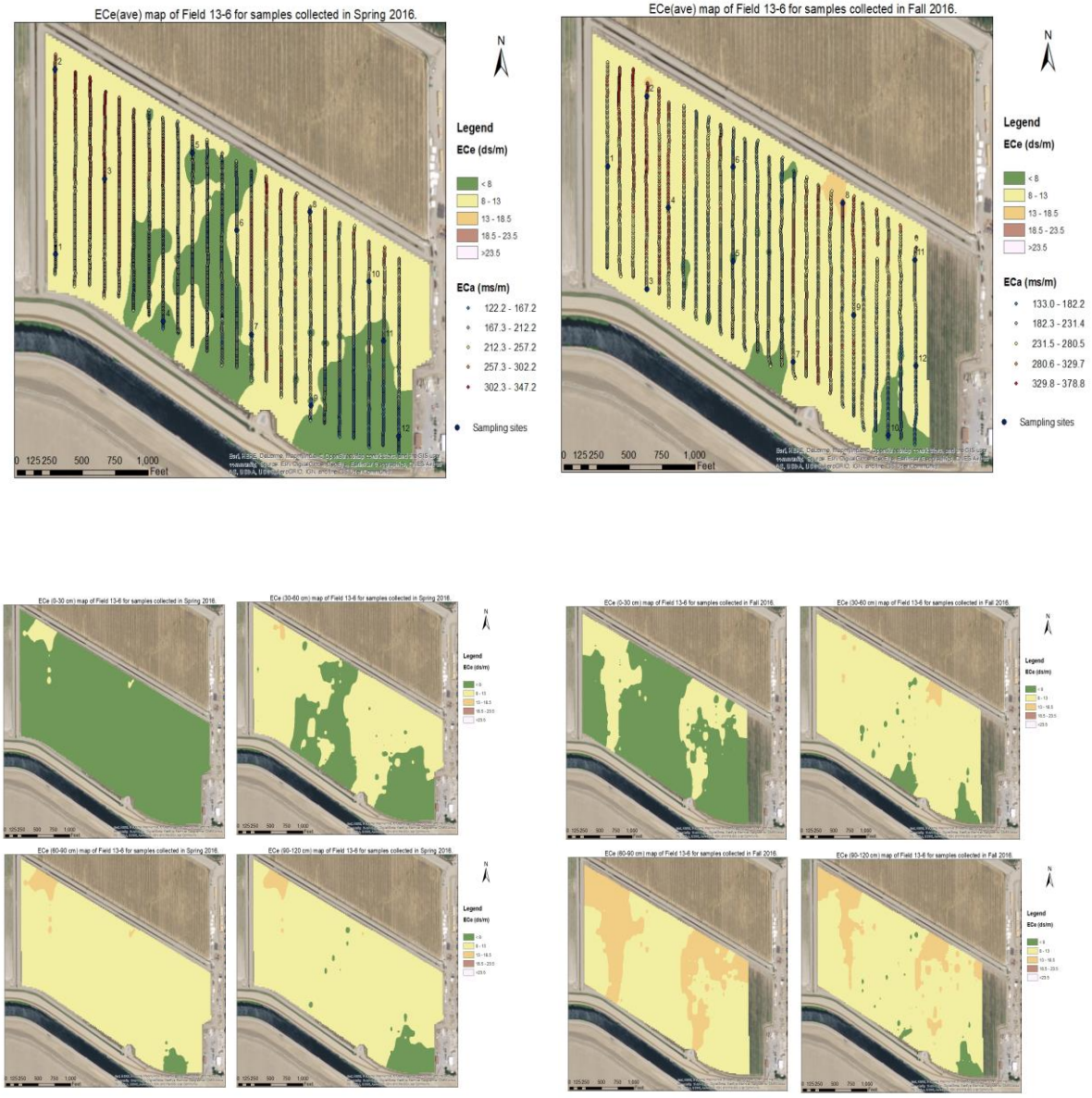

Figure 27. Spatial distribution of average salinity (0 – 120 cm) (top) and for each depth (bottom) in field 13-6 for Spring (left) and Fall (right) 2016.

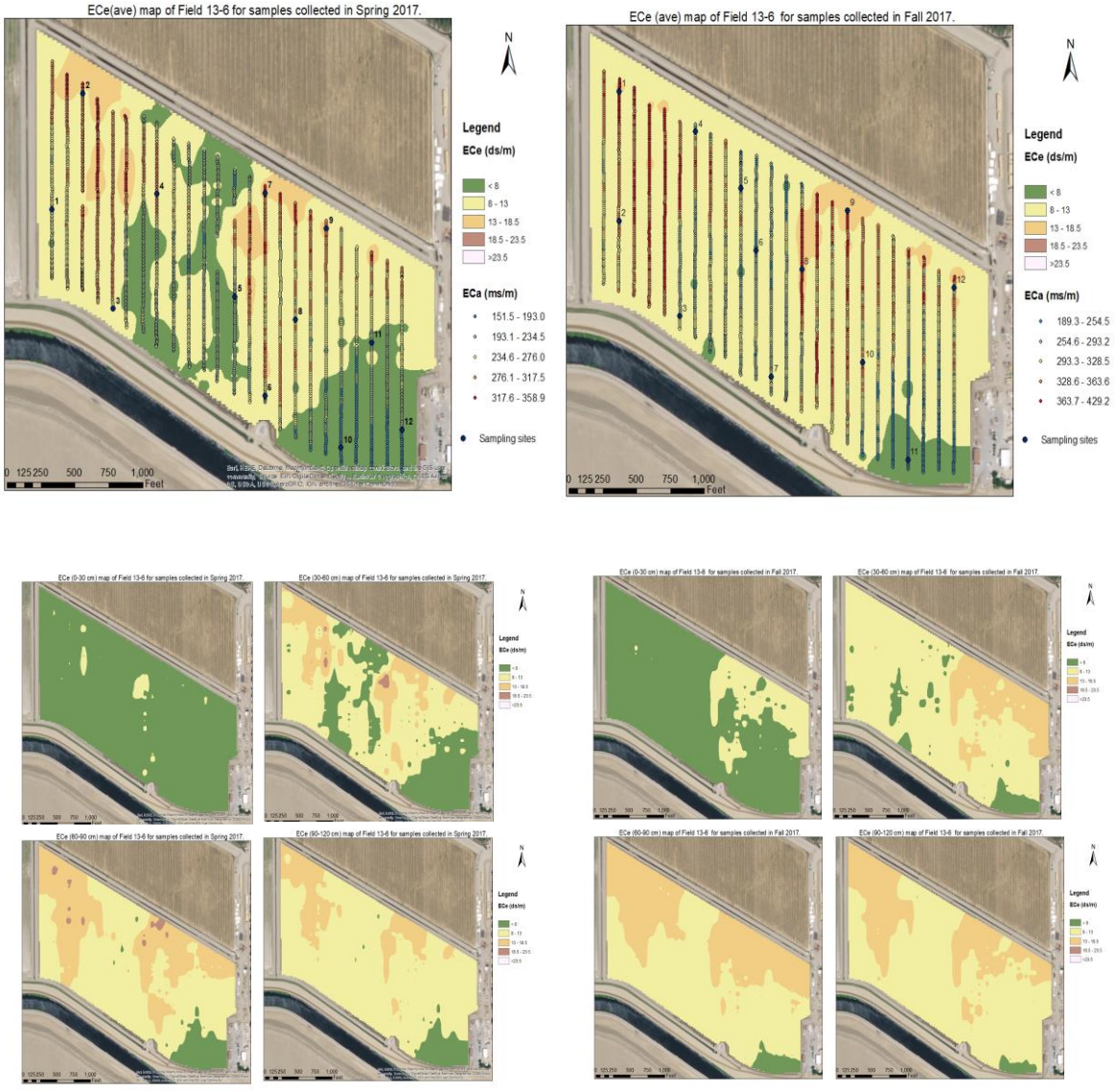

Figure 28. Spatial distribution of average salinity (0 – 120 cm) (top) and for each depth (bottom) in field 13-6 for Spring (left) and Fall (right) 2017.

Forage Analysis

The results for the forage tissue sample analysis are shown in Table 10. This table provide information about the date when the forage tissue samples were collected, mean, standard deviation (SD) and range of the forage dry weight, Na%, and K%.

Table 10. Forage dry weight, Na %, and K% for forage samples collected from 12 ESAP guided locations for Spring 2017.

Field	Date	Average Forage Dry wt. (g)	SD	Min	Max	Na % (avg)	SD	Min	Max	K % (avg)	SD	Min	Max
10-6 (TWG)	4/24/2017	269.4	173.3	103.0	617.2	0.62	0.07	0.52	0.73	1.11	0.36	0.77	2.17
	7/6/2017	91.0	42.0	26.5	147.3	0.73	0.17	0.52	1.01	1.01	0.17	0.8	1.31
13-1 (TWG)	4/17/2017	184.7	74.9	87.3	342.8	0.73	0.07	0.64	0.84	1.22	0.15	1.02	1.57
	5/22/2017	347.3	108.9	243.7	567.2	0.72	0.11	0.55	0.92	0.97	0.16	0.68	1.00
13-2 (ALF)	5/31/2017	139.7	59.0	70.5	266.6	0.52	0.11	0.37	0.7	2.5	0.27	1.96	2.84
	6/30/2017	123.3	56.7	47.8	214.9	0.46	0.12	0.24	0.61	2.2	0.12	2.01	2.43
13-6 (ALF)	6/9/2017	89.8	34.8	19.0	158.2	0.43	0.08	0.29	0.53	2.18	0.27	1.88	2.71
	7/6/2017	74.5	43.5	12.0	175.8	0.46	0.17	0.21	0.82	2.04	0.21	1.8	2.46

The results from the correlations between Na% and forage dry weight, and soil salinity (EC_e) and forage dry weight for each field are shown in Figures 29 to 32. The correlation coefficient (R) and the P-value are also provided in the figures. Stronger correlations were observed for ALF fields as compared to the TWG fields. For TWG fields, the only significant correlation was observed between EC_e and forage dry weight for field 10-6 (P-value < 0.05). However, correlations were significant for ALF fields except for the field 13-6, where the correlation between Na% and forage dry weight was not significant (P-value >0.05). More information about the correlation analysis is given in Appendix D.

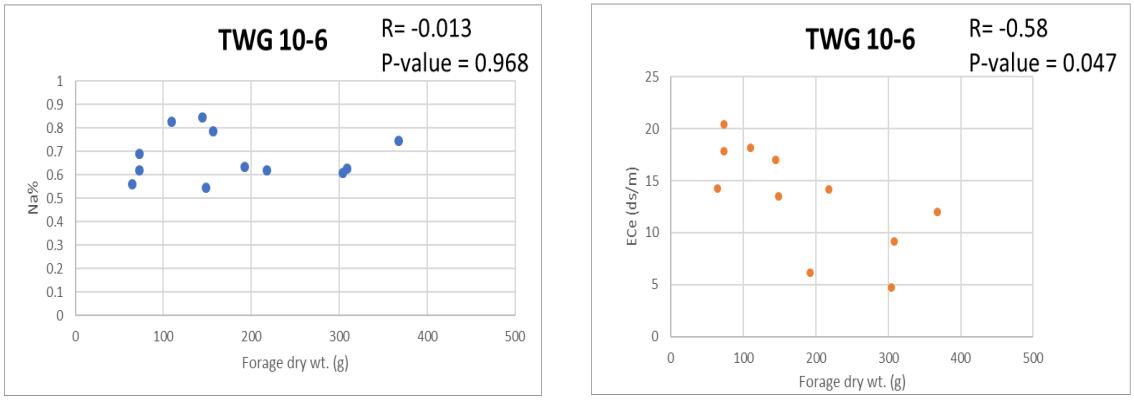

Figure 29. Correlation between Na% and forage dry weight (left), and soil salinity (EC_e) and forage dry weight (right) for field 10-6.

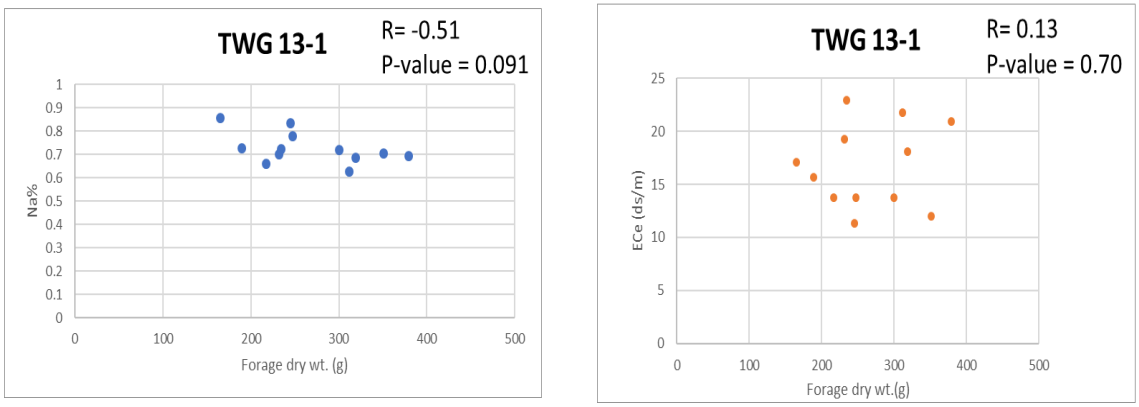

Figure 30. Correlation between Na% and forage dry weight (left), and soil salinity (EC_e) and forage dry weight (right) for field 13-1.

This could be explained by the high sensitivity of ALF to salinity than TWG (Suyama et al., 2007a). Na% was correlated with the forage dry weight because it affects the plant growth when accumulated to toxic levels (Maas et al., 1999). From the correlations, it can be concluded that a combined effect of osmotic stress (salinity) and Na ion toxicity could be causing yield declines in ALF fields whereas for TWG, salinity is the major factor affecting the forage yield.

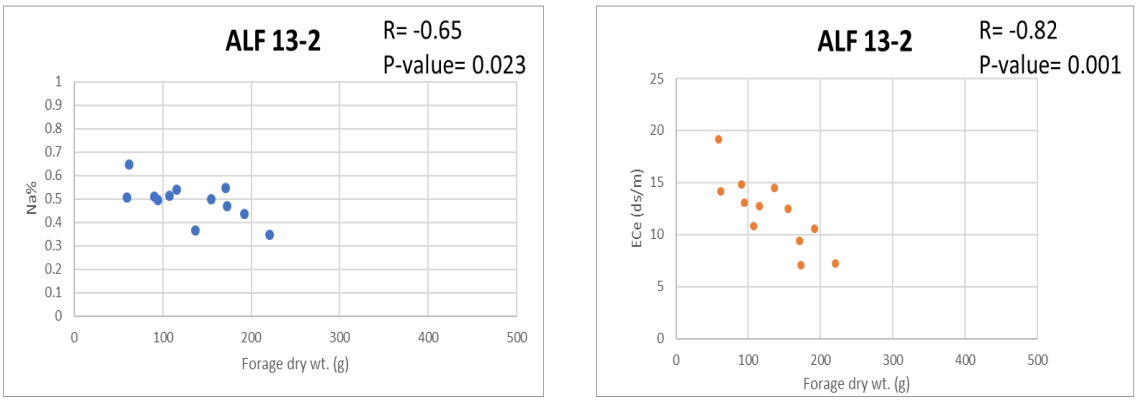

Figure 31. Correlation between Na% and forage dry weight (left), and soil salinity (EC_e) and forage dry weight (right) for field 13-2.

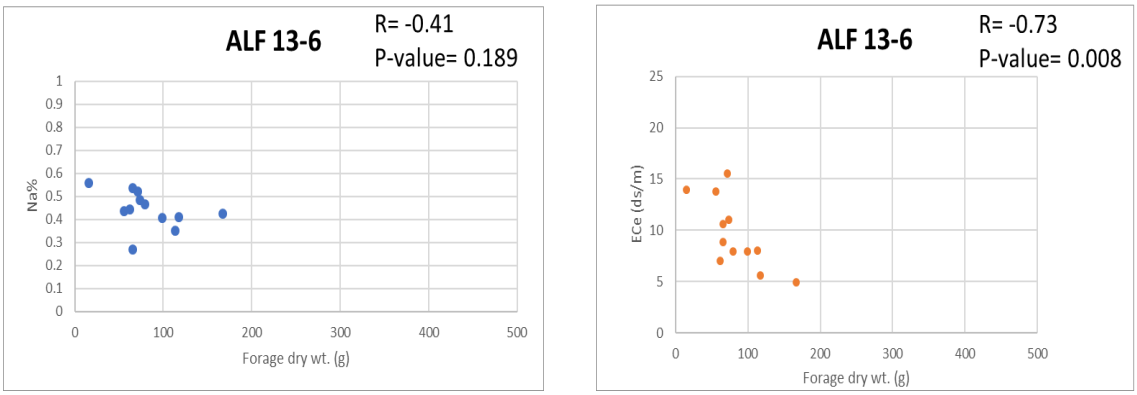

Figure 32. Correlation between Na% and forage dry weight (left), and soil salinity (EC_e) and forage dry weight (right) for field 13-6.

CONCLUSION

Four fields planted with Jose Tall wheatgrass (TWG) and Alfalfa (ALF) were surveyed with an EM38 instrument to determine the spatial and temporal variability of salinity. TWG fields were irrigated with higher salinity water compared to the ALF fields. Field 13-2 (ALF) received relatively good quality irrigation water throughout the study period. Tile drained fields 13-1 (TWG) and 13-2 (ALF) had improved leaching as most salt accumulation was found at the lower soil profile. In contrast, the 2nd and 3rd layers of the soil profile were the sites of most salt accumulation in the other two fields. Field 10-6 had the largest variability in spatial salt distribution which could be attributed to the variability in soil texture. Field 13-2 showed improvement in salt leaching with time as Fall 2017 had uniformly leached surface soil layer, which was the result of good quality irrigation water applications. Generally, for all fields except field 13-2, there was an increase in salinity level in the fall season compared to the spring season, which was expected because of the leaching of salts due to winter rains. Salinity levels didn't decrease much in the year 2017, which was expected because of the heavy rains of 2016. More years of data will be required to see the change in salinity patterns over the years. This should be taken into consideration for the CSUID model simulations.

Poor salinity (EC_e) estimations were observed during Fall season of both years for fields 13-1 (TWG) and 13-2 (ALF), as suggested by poor DPPC correlations or poor R-squares for the regression model used to convert EC_a data to EC_e. Confounding results in these fields could be explained because of the high clay content (based on higher SP values) of these fields, which might be influencing the EC_a readings (Corwin & Lesch, 2013). Nonetheless, the model R-

square was significant in all cases for estimation of average salinity of the rootzone (0-120cm).

Since the 1-D version of the model was used for the simulations, average rootzone salinity conditions can be successfully used for the calibration of the model. Preliminary simulations were run using the survey data from spring 2016 as calibration datasets and the results are reported in the interim final report to the funding source (CA Department of Water Resources). It was acknowledged that more years of data will be needed to develop a reliable calibration of the CSUID model.

Spatial maps delineating the areas of high and low salinity in the SJRIP fields could be very useful in guiding their irrigation management practices. These maps have been shared and discussed with PWD in two data meetings and in a poster. The other significance of this study is that the data could be used as a ground-truthing dataset for soil salinity assessment using remote sensing techniques. High resolution ground-truthing data is often hard to obtain for such studies. Moreover, the 12 sampling locations established in each field could potentially serve as monitoring sites. Although keeping in mind that the purpose of the sampling design is to optimize the parameter selection for the regression model for accurate salinity (EC_e) estimation, and is not intended to be used for directly estimating the salinity statistics (Lesch et al. 1995a, 1995b). But, since the selected sites depicts the full range of variability present throughout the surveyed area, these sites could also be used as representative sites to monitor changes in salinity levels in these fields over time, if seasonal or yearly EM38 surveys are no longer feasible.

The use of EM38 soil surveys or remote sensing/aerial imagery could be feasible for reuse facilities using saline water for irrigation to monitor soil salinity

increase over time and take proactive steps to protect against the declining crop yields. Strategic reclamation may be required to return soil salinity to acceptable levels, but this should be undertaken when nitrogen levels are low in the soil profile to prevent nitrate leaching to groundwater. At present the forage fields are not fertilized, but rather maintained on nitrogen present in the incoming subsurface drainage water, but the pistachio fields in the SJRIP do receive nitrogen fertilizer. The eventual goal is to use the CSUID model as a decision support tool to allow water districts reusing saline waters to apply appropriate, but not excessive leaching fractions in order to maintain the long term sustainability of forage, or other crop, production using saline waters.

In the case of the SJRIP, successful operation of the reuse facility is critical to allow the 100,000 acre Grasslands Drainage Area to continue to utilize subsurface drainage systems for salinity and water table control and to meet the strict water quality objectives imposed on them in the Grasslands Bypass Agreement. Panoche Drainage District is required to go to zero discharge to the San Joaquin River by 2020 and is expanding SJRIP acreage (primarily 'Jose' tall wheatgrass plantings) to meet this mandate. Appropriate soil and irrigation management will be key to maintain the forage productivity (and revenue generation for the SJRIP). The availability of decision support tools such as the CSUID model and the EM38 or other remote sensing tools for soil salinity mapping– along with skilled technical support– will increase the likelihood of successful and sustainable operation of the SJRIP over the long term.

FUTURE WORK

The EM38 soil surveys are providing valuable data for the calibration of the computer model and are important to define the spatial variability of soil salinity within the selected fields. However, EM38 surveys require significant expertise time and effort and are unlikely to be continued by the District alone given resource limitations of current water district personnel. Future collaborations with universities and project funding may allow the continuation of the EM38 mapping program. In the interim the installation of representative cluster wells within each of the experimental fields may allow the District to track salinity trends at two intervals within the soil profile with currently available resources and monitoring equipment. These wells will help to assess the adequacy of current salt leaching practices as well as providing data for further calibration of the CSUID model. By developing a proxy relationship between each well and the average salinity at shallow (5-8 ft) and deep (14-17 ft) depths, the well EC data can be useful in showing trends in field salinization.

The one dimensional (1-D) CSUID model uses the average irrigation application and EC to keep track of crop root zone leaching and ambient salinity and assumes homogenous conditions in each soil layer within the soil profile of each field. If a field is tile drained – the 1-D assumption implies that drainage yield is similarly evenly distributed. Although results of the surveys show that the assumption of field homogeneity is invalid at present there is insufficient field data to support the development and calibration of a 3-D model. Moreover, running simulations in 3-D would increase model run times substantially and impair the use of the model as a decision support system – which relies on having the ability to evaluate multiple scenarios in quick succession. The long-term aim is to have a credible, reliable and easy to use decision support tool than can guide future

irrigation water quality management practices at SJRIP, i.e. customizing the blend of subsurface drainage water and treatment plant product water to allow sustainable forage production in both alfalfa and Jose tall wheatgrass fields.

REFERENCES

REFERENCES

Allbed, A., & Kumar, L. (2013). Soil salinity mapping and monitoring in arid and semi-arid regions using remote sensing technology: a review. *Advances in remote sensing, 2013*.

Alzraiee, A. H., Gates, T. K., & Garcia, L. A. (2013). Modeling Subsurface Heterogeneity of Irrigated and Drained Fields. II: Multivariate Stochastic Analysis of Root-Zone Hydrosalinity and Crop Yield. *Journal of Irrigation and Drainage Engineering, 139*(10), 809-820. doi:10.1061/(asce)ir.1943-4774.0000587

Assouline, S., Russo, D., Silber, A., & Or, D. (2015). Balancing water scarcity and quality for sustainable irrigated agriculture. *Water Resources Research, 51*(5), 3419-3436.

Ayers, R. S., & Westcot, D. W. (1985). *Water quality for agriculture* (Vol. 29): Food and Agriculture Organization of the United Nations Rome.

Backlund, V. L., & Hoppes, R. R. (1984). Status of soil salinity in California. *California Agriculture, 38*(10), 8-9.

Ben-Gal, A., Ityel, E., Dudley, L., Cohen, S., Yermiyahu, U., Presnov, E., Shani, U. (2008). Effect of irrigation water salinity on transpiration and on leaching requirements: A case study for bell peppers. *Agricultural Water Management, 95*(5), 587-597.

Ben-Gal, A., & Shani, U. (2002). Yield, transpiration and growth of tomatoes under combined excess boron and salinity stress. *Plant and soil, 247*(2), 211-221.

Benes, S. (2013). Salinity and Drainage Management in the Western San Joaquin Valley—Where are we Today? *KEEPING CALIFORNIA AGRICULTURE PROACTIVE AND INNOVATIVE*, 141.

Benes, S., Adhikari, D., Grattan, S., & Snyder, R. (2012). Evapotranspiration potential of forages irrigated with saline-sodic drainage water. *Agricultural Water Management, 105*, 1-7.

Benes, S., Aragüés, R., Austin, R., & Grattan, S. (1996a). Brief pre-and post-irrigation sprinkling with fresh water reduces foliar salt uptake in maize and barley sprinkler irrigated with saline water. *Plant and soil, 180*(1), 87-95.

Benes, S., Aragüés, R., Grattan, S., & Austin, R. (1996b). Foliar and root absorption of Na+ and Cl− in maize and barley: Implications for salt tolerance screening and the use of saline sprinkler irrigation. Plant and soil, 180(1), 75-86.

Benes, S.E., Putnam, D.H., Chahal, I., Grattan, S.R., Bushoven J. (2014*). What is the Ability of Alfalfa to Sustain Saline Conditions?* Proceedings of the California Alfalfa, Grain and Forage Symposium. Long Beach, CA. Dec. 10-12, 2014. http://alfalfa.ucdavis.edu/+symposium/2014/index.aspx

Brady, N., & Weil, R. (2008). Soils of dry regions: alkalinity, salinity, and sodicity. *The Nature and Properties of Soils, 14th ed. Pearson. Upper Saddle River, NJ*, 401-442.

Brevik, E. C., Fenton, T. E., & Lazari, A. (2006). Soil electrical conductivity as a function of soil water content and implications for soil mapping. *Precision Agriculture, 7*(6), 393-404.

Chahal, I. (2013). Comparison of salt tolerant alfalfa (medicago sativa) genotypes: Seed germination, emergence, and dry matter yield and mineral composition of mature plants. (Master of Science), California State University, Fresno.

Cornacchione, M. V., & Suarez, D. L. (2015). Emergence, forage production, and ion relations of alfalfa in response to saline waters. *Crop science*, *55*(1), 444-457.

Corwin, D., & Lesch, S. (2003). Application of soil electrical conductivity to precision agriculture. *Agronomy Journal, 95*(3), 455-471.

Corwin, D., & Lesch, S. (2005a). Apparent soil electrical conductivity measurements in agriculture. *Computers and electronics in agriculture, 46*(1), 11-43.

Corwin, D., & Lesch, S. (2005b). Characterizing soil spatial variability with apparent soil electrical conductivity: I. Survey protocols. *Computers and electronics in agriculture, 46*(1), 103-133.

Corwin, D., & Waggoner, B. (1990). TETRANS: solute transport modeling software user's guide. *IBM compatible version, 1*.

Corwin, D. L. (2012). Field-scale monitoring of the long-term impact and sustainability of drainage water reuse on the west side of California's San Joaquin Valley. *Journal of Environmental Monitoring, 14*(6), 1576-1596.

Corwin, D. L., & Lesch, S. M. (2013). Protocols and guidelines for field-scale measurement of soil salinity distribution with ECa-directed soil sampling. *Journal of Environmental and Engineering Geophysics, 18*(1), 1-25.

Corwin, D. L., Lesch, S. M., Segal, E., Skaggs, T. H., & Bradford, S. A. (2010). Comparison of sampling strategies for characterizing spatial variability with apparent soil electrical conductivity directed soil sampling. *Journal of Environmental & Engineering Geophysics, 15*(3), 147-162.

Corwin, D. L., Rhoades, J. D., & Šimůnek, J. (2007). Leaching requirement for soil salinity control: Steady-state versus transient models. *Agricultural Water Management, 90*(3), 165-180. doi:10.1016/j.agwat.2007.02.007

Corwin, D. L., & Scudiero, E. (2016). Field-Scale Apparent Soil Electrical Conductivity. *Methods of Soil Analysis, 1*(1).

Doolittle, J. A., & Brevik, E. C. (2014). The use of electromagnetic induction techniques in soils studies. *Geoderma, 223-225*, 33-45. doi:10.1016/j.geoderma.2014.01.027

FAO, I. (2015). Status of the World's Soil Resources (SWSR)–Main Report. *Food and Agriculture Organization of the United Nations and Intergovernmental Technical Panel on Soils, Rome, Italy*, 650.

Frenkel, H., Goertzen, J., & Rhoades, J. (1978). Effects of clay type and content, exchangeable sodium percentage, and electrolyte concentration on clay dispersion and soil hydraulic conductivity. *Soil Science Society of America Journal, 42*(1), 32-39.

Gardner, W. (1983). Soil properties and efficient water use: an overview. *Limitations to efficient water use in crop production*, 45-64.

Grattan, S., & From, C. (2006). Irrigation Water Composition and Salinization. *Agricultural Salinity and Drainage*, 5-6.

Grattan, S., Grieve, C., Poss, J., Robinson, P., Suarez, D., & Benes, S. (2002). *Reuse of saline-sodic drainage water for irrigation in California: Evaluation of potential forages.* Paper presented at the Proceedings of the 17th World Congress on Soil Salinity, Bangkok, Thailand.

Grattan, S. R., Oster, J. D., Benes, S., & Kaffka, S. (2009). Use of saline drainage waters for irrigation *Agricultural salinity assessment and management* (pp. 433-449).

Grattan, S. R., Oster, J. D., Letey, J., & Kaffka, S. R. (2014). Drainage Water Reuse: Concepts, Practices and Potential Crops *Salinity and Drainage in San Joaquin Valley, California* (pp. 277-302): Springer.

Gregory, P. J., & George, T. S. (2011). Feeding nine billion: the challenge to sustainable crop production. *Journal of experimental botany, 62*(15), 5233-5239.

Grieve, C., Poss, J., Grattan, S., Suarez, D., Benes, S., & Robinson, P. (2004). Evaluation of salt-tolerant forages for sequential water reuse systems: II. Plant–ion relations. *Agricultural Water Management, 70*(2), 121-135.

Hanson, B., Grattan, S. R., & Fulton, A. (2006). *Agricultural salinity and drainage*: University of California Irrigation Program University of California, Davis.

Hilgard, E. (1889). Irrigation and alkali in India. *Coll Agric Univ Calif Berkeley Bull, 86*.

Hilgard, E. (1893). The physical and industrial geography of California. *The Geographical Journal, 1*(6), 536-539.

Hoffman, G. J. (2010). Salt Tolerance of Crops in the Southern Sacramento-San Joaquin Delta. *Report for the California Environmental Protection Agency. Available at www. swrcb. ca. gov/waterrights/water_issues/programs/bay_delta/bay_delta_plan/water_quality_control_planning/d ocs/final_study_report. pdf*.

Hoffman, G. J., & Van Genuchten, M. T. (1983). Soil properties and efficient water use: water management for salinity control. *Limitations to efficient water use in crop production*(limitationstoef), 73-85.

Howitt, R., Kaplan, J., Larson, D., MacEwan, D., Medellín-Azuara, J., Horner, G., & Lee, N. (2009). The economic impacts of Central Valley salinity. *University of California Davis, Final Report to the State Water Resources Control Board Contract*, 05-417.

Jacobsen, T., & Adams, R. M. (1958). Salt and silt in ancient Mesopotamian agriculture. *Science, 128*(3334), 1251-1258.

Kelley, J., Higgins, C. W., Pahlow, M., & Noller, J. (2017). Mapping Soil Texture by Electromagnetic Induction: A Case for Regional Data Coordination. *Soil Science Society of America Journal, 81*(4), 923-931.

Laird, J., Jr., E. G. B., & Cowin, M. (2015). San Joaquin Valley Drainage Monitoring Program 2011 - 2012.

Läuchli, A., & Grattan, S. R. (2007). Plant Growth And Development Under Salinity Stress. In M. Jenks, P. Hasegawa, & S. M. Jain (Eds.), *Advances in Molecular Breeding Toward Drought and Salt Tolerant Crops* (pp. 1-32): Springer Netherlands.

Lesch, S., Rhoades, J., & Corwin, D. (2000). ESAP-95 Version 2.01 R: User manual and tutorial guide. *Research Rpt, 146*.

Lesch, S. M., Strauss, D. J., & Rhoades, J. D. (1995a). Spatial prediction of soil salinity using electromagnetic induction techniques 1. Statistical prediction models: A comparison of multiple linear regression and cokriging. *Water Resources Research, 31*(2), 373-386.

Lesch, S. M., Strauss, D. J., & Rhoades, J. D. (1995b). Spatial prediction of soil salinity using electromagnetic induction techniques: 2. An efficient spatial sampling algorithm suitable for multiple linear regression model identification and estimation. *Water Resources Research, 31*(2), 387-398.

Letey, J. (1986). *An agricultural dilemma: Drainage water and toxics disposal in the San Joaquin Valley*: Division of Agriculture and Natural Resources, University of California.

Letey, J. (2000). Soil salinity poses challenges for sustainable agriculture and wildlife. *California Agriculture, 54*(2), 43-48.

Letey, J., Dinar, A., & Knapp, K. C. (1985). Crop-water production function model for saline irrigation waters. *Soil Science Society of America Journal, 49*(4), 1005-1009.

Letey, J., & Feng, G. (2007). Dynamic versus steady-state approaches to evaluate irrigation management of saline waters. *Agricultural Water Management, 91*(1), 1-10.

Letey, J., Hoffman, G. J., Hopmans, J. W., Grattan, S. R., Suarez, D., Corwin, D. L., . . . Amrhein, C. (2011). Evaluation of soil salinity leaching requirement guidelines. *Agricultural Water Management, 98*(4), 502-506. doi:http://dx.doi.org/10.1016/j.agwat.2010.08.009

Letey, J., Williams, C. F., & Alemi, M. (2002). Salinity, drainage and selenium problems in the Western San Joaquin Valley of California. *Irrigation and Drainage Systems, 16*(4), 253-259. doi:10.1023/A:1024812826664

Linneman, C., Falaschi, A., Oster, J.D., Kaffka, S., Benes, S.E. (2014). Drainage reuse by Grassland Area farmers: the road to zero discharge. Proceedings of the "Groundwater Issues and Water Management—Strategies Addressing the Challenges of Sustainability" meeting. U.S. Committee on Irrigation and Drainage (US-CID), Sacramento, CA, Mar. 4-7, 2014.

Lobell, D., Lesch, S., Corwin, D., Ulmer, M., Anderson, K., Potts, D., . . . Baltes, M. (2010). Regional-scale assessment of soil salinity in the Red River Valley using multi-year MODIS EVI and NDVI. *Journal of Environmental Quality, 39*(1), 35-41.

Lobell, D. B., Ortiz-Monasterio, J. I., Gurrola, F. C., & Valenzuela, L. (2007). Identification of saline soils with multiyear remote sensing of crop yields. *Soil Science Society of America Journal, 71*(3), 777-783.

Maas, E. V., Grattan, S., Skaggs, R., & Schilfgaarde, J. v. (1999). Crop yields as affected by salinity. *Agricultural drainage.*, 55-108.

Maas, E. V., & Hoffman, G. (1977). Crop salt tolerance\-current assessment. *Journal of the irrigation and drainage division, 103*(2), 115-134.

McNeal, B., Layfield, D., Norvell, W., & Rhoades, J. (1968). Factors influencing hydraulic conductivity of soils in the presence of mixed-salt solutions. *Soil Science Society of America Journal, 32*(2), 187-190.

Munns, R. (2005). Genes and salt tolerance: bringing them together. *New Phytol, 167*(3), 645-663. doi:10.1111/j.1469-8137.2005.01487.x

Munns, R., & Tester, M. (2008). Mechanisms of salinity tolerance. *Annu Rev Plant Biol, 59*, 651-681. doi:10.1146/annurev.arplant.59.032607.092911

Oster, J. (1994). Irrigation with poor quality water. *Agricultural Water Management, 25*(3), 271-297.

Oster, J., & Grattan, S. (2002). Drainage water reuse. *Irrigation and Drainage Systems, 16*(4), 297-310.

Oster, J., Sposito, G., & Smith, C. (2016). Accounting for potassium and magnesium in irrigation water quality assessment. *California Agriculture, 70*(2), 71-76.

Pang, X., & Letey, J. (1998). Development and evaluation of ENVIRO-GRO, an integrated water, salinity, and nitrogen model. *Soil Science Society of America Journal, 62*(5), 1418-1427.

Quinn, N., McGahan, J., & Delamore, M. (1998). Innovative strategies reduce selenium in Grasslands drainage. *California Agriculture, 52*(5), 12-18.

Quinn, N. W. T., Alzraiee, A. H., Mathiot, C., & Longley, K. E. (2016). *Developing water quality objectives for diversions to agriculture from the San Joaquin River using steady-state (Hoffman) and transient (CSUID) models*. Paper presented at the California Water and Environmental Modeling Forum Annual Meeting, 2016. Modeling Extremes: Drought to Flood and In-Between's., At Folsom, California, Volume: 1.

Rhoades, J. (1974). Drainage for salinity control. *Drainage for agriculture*(drainageforagri), 433-461.

Rhoades, J., & Chanduvi, F. (1999). *Soil salinity assessment: Methods and interpretation of electrical conductivity measurements* (Vol. 57): Food & Agriculture Org.

Rhoades, J., Manteghi, N., Shouse, P., & Alves, W. (1989). Soil electrical conductivity and soil salinity: New formulations and calibrations. *Soil Science Society of America Journal, 53*(2), 433-439.

Rhoades, J., & Merrill, S. (1976). Assessing the suitability of water for irrigation: theoretical and empirical approaches *Prognosis of Salinity and Alkalinity. Soils Bulletin 31* (pp. 69-109): FAO, Rome.

Roberts, L. (2011). 9 Billion?: American Association for the Advancement of Science.

Robinson, P. H., Grattan, S. R., Getachew, G., Grieve, C. M., Poss, J. A., Suarez, D. L., & Benes, S. E. (2004). Biomass accumulation and potential nutritive value of some forages irrigated with saline-sodic drainage water. *Animal Feed Science and Technology, 111*(1–4), 175-189. doi:http://dx.doi.org/10.1016/S0377-8401(03)00213-X

San Joaquin Valley Drainage Program. 1990. A Management Plan for Agricultural Subsurface Drainage and Related Problems on the Westside San Joaquin Valley. Sacramento, California.

Schoups, G., Hopmans, J. W., Young, C. A., Vrugt, J. A., Wallender, W. W., Tanji, K. K., & Panday, S. (2005). Sustainability of irrigated agriculture in the San Joaquin Valley, California. *Proceedings of the National Academy of Sciences, 102*(43), 15352-15356.

Scudiero, E., Corwin, D., Anderson, R., Yemoto, K., Clary, W., Wang, Z., & Skaggs, T. (2017). Remote sensing is a viable tool for mapping soil salinity in agricultural lands. *California Agriculture*, 1-8.

Scudiero, E., Skaggs, T. H., & Corwin, D. L. (2015). Regional-scale soil salinity assessment using Landsat ETM+ canopy reflectance. *Remote Sensing of Environment, 169*, 335-343.

Shainberg, I., & Letey, J. (1984). *Response of soils to sodic and saline conditions*: University of California, Division of Agriculture and Natural Resources.

Sharma, F. C., Goorahoo, D., Zoldoske, D., & Adhikari, D. (2008). Mapping Soil Salinity Using Ground-Based Electromagnetic induction technique *Remote sensing of soil salinization: Impact on land management* (pp. 199-233): CRC Press.

Šimůnek, J., & Suarez, D. L. (1994). Two- dimensional transport model for variably saturated porous media with major ion chemistry. *Water Resources Research, 30*(4), 1115-1133.

Suarez, D. L., & Jurinak, J. (2012). The chemistry of salt-affected soils and waters. *ASCE Manual and Reports on Engineering Practice*(71), 57-88.

Suarez, D. L., Wood, J. D., & Lesch, S. M. (2006). Effect of SAR on water infiltration under a sequential rain–irrigation management system. *Agricultural Water Management, 86*(1), 150-164.

Suarez, D. L., Wood, J. D., & Lesch, S. M. (2008). Infiltration into cropped soils: effect of rain and sodium adsorption ratio–impacted irrigation water. *Journal of Environmental Quality, 37*(5_Supplement), S-169-S-179.

Suyama, H., Benes, S. E., Robinson, P. H., Getachew, G., Grattan, S. R., & Grieve, C. M. (2007a). Biomass yield and nutritional quality of forage species under long-term irrigation with saline-sodic drainage water: Field evaluation. *Animal Feed Science and Technology, 135*(3–4), 329-345. doi:http://dx.doi.org/10.1016/j.anifeedsci.2006.08.010

Suyama, H., Benes, S. E., Robinson, P. H., Grattan, S. R., Grieve, C. M., & Getachew, G. (2007b). Forage yield and quality under irrigation with saline-sodic drainage water: Greenhouse evaluation. *Agricultural Water Management, 88*(1–3), 159-172. doi:http://dx.doi.org/10.1016/j.agwat.2006.10.011

Tanji, K. K., & Wallender, W. W. (2012). Agricultural salinity assessment and management *ASCE manual and reports on engineering practice ; no. 71* (Vol. 2nd ed. / prepared by the Water Quality Technical Committee of the Irrigation and Drainage Council of the Environmental and Water Resources Institute of the American Society of Civil Engineers ; edited by Wesley W. Wallender and Kenneth K. Tanji): Reston, Va. : American Society of Civil Engineers, 2012.

Tilman, D., Balzer, C., Hill, J., & Befort, B. L. (2011). Global food demand and the sustainable intensification of agriculture. *Proceedings of the National Academy of Sciences, 108*(50), 20260-20264.

USDA. (1954). *Diagnosis and improvement of saline and alkali soils. Agriculture Handbook, 60.* .

Weber, E., Grattan, S., Hanson, B., Vivaldi, G., Meyer, R., Prichard, T., & Schwankl, L. (2014). Recycled water causes no salinity or toxicity issues in Napa vineyards. *California Agriculture, 68*(3), 59-67.

Weller, U., Zipprich, M., Sommer, M., Castell, W. Z., & Wehrhan, M. (2007). Mapping clay content across boundaries at the landscape scale with electromagnetic induction. *Soil Science Society of America Journal, 71*(6), 1740-1747

APPENDICES

APPENDIX A: MLR ANALYSIS AND STATISTICS

Field 10-6 (Spring 2016)

MLR Model Form:
ln(ECe) = b0 + b1(z1) + b2(z2)

Basic Regression Summary Statistics

Depth	R-square	Root MSE	Est.%CV
30.00	0.8512	0.2824	28.81
60.00	0.9269	0.1970	19.89
90.00	0.8348	0.2835	28.93
120.00	0.8831	0.2399	24.34
bulk	0.9104	0.2069	20.91

AOV Table and Parameter Estimates for depth: 30.00

Source	DF	SS	MS	F value	Prob >F
Model	2	4.1053	2.0526	25.75	0.0002
Error	9	0.7175	0.0797		
C-Total	11	4.8228			

model R-square = 0.8512
root MSE = 0.2824
estimated CV = 28.8078

press score = 1.101

Parameter	Estimate	Standard Error	t value para=0	Prob >|t|
intercept	2.2694	0.0818	27.74	0.0001
z1	0.4392	0.0641	6.85	0.0001
z2	-0.0838	0.0563	-1.49	0.1707

AOV Table and Parameter Estimates for depth: 60.00

Source	DF	SS	MS	F value	Prob >F
Model	2	4.4321	2.2161	57.10	0.0001
Error	9	0.3493	0.0388		
C-Total	11	4.7814			

model R-square = 0.9269
root MSE = 0.1970
estimated CV = 19.8931

press score = 0.543

Parameter	Estimate	Standard Error	t value para=0	Prob >|t|

intercept	2.5273	0.0571	44.28	0.0001
z1	0.4742	0.0447	10.60	0.0001
z2	-0.0143	0.0393	-0.36	0.7237

AOV Table and Parameter Estimates for depth: 90.00

Source	DF	SS	MS	F value	Prob >F
Model	2	3.6548	1.8274	22.74	0.0003
Error	9	0.7232	0.0804		
C-Total	11	4.3780			

model R-square =	0.8348
root MSE =	0.2835
estimated CV =	28.9270
press score =	1.062

Parameter	Estimate	Standard Error	t value para=0	Prob >|t|
intercept	2.4165	0.0821	29.43	0.0001
z1	0.4341	0.0644	6.74	0.0001
z2	0.0402	0.0565	0.71	0.4950

AOV Table and Parameter Estimates for depth: 120.00

Source	DF	SS	MS	F value	Prob >F
Model	2	3.9129	1.9565	33.99	0.0001
Error	9	0.5180	0.0576		
C-Total	11	4.4309			

model R-square =	0.8831
root MSE =	0.2399
estimated CV =	24.3399
press score =	0.948

Parameter	Estimate	Standard Error	t value para=0	Prob >|t|
intercept	2.4464	0.0695	35.20	0.0001
z1	0.4475	0.0545	8.21	0.0001
z2	0.0711	0.0478	1.49	0.1711

AOV Table and Parameter Estimates for bulk average model

Source	DF	SS	MS	F value	Prob >F

Model	2	3.9147	1.9573	45.72	0.0001
Error	9	0.3853	0.0428		
C-Total	11	4.3000			

model R-square = 0.9104
root MSE = 0.2069
estimated CV = 20.9136

press score = 0.556

Parameter	Estimate	Standard Error	t value para=0	Prob >|t|
intercept	2.4303	0.0599	40.54	0.0001
z1	0.4482	0.0470	9.54	0.0001
z2	0.0093	0.0412	0.23	0.8262

Field 10-6 (Fall 2016)

MLR Model Form:
ln(ECe) = b0 + b1(z1) + b2(z1^2) + b3(x)

Basic Regression Summary Statistics

Depth	R-square	Root MSE	Est.%CV
30.00	0.8602	0.2523	25.64
60.00	0.9271	0.1868	18.85
90.00	0.9115	0.1940	19.58
120.00	0.9433	0.1517	15.26
bulk	0.9475	0.1488	14.96

AOV Table and Parameter Estimates for depth: 30.00

Source	DF	SS	MS	F value	Prob >F
Model	3	3.1322	1.0441	16.40	0.0009
Error	8	0.5092	0.0637		
C-Total	11	3.6414			

model R-square = 0.8602
root MSE = 0.2523
estimated CV = 25.6361

press score = 1.076

Parameter	Estimate	Standard Error	t value para=0	Prob >|t|
intercept	2.9475	0.2040	14.45	0.0001
z1	0.5447	0.1011	5.39	0.0007
z1^2	0.0156	0.0536	0.29	0.7782
x	-0.5837	0.3424	-1.70	0.1266

AOV Table and Parameter Estimates for depth: 60.00

Source	DF	SS	MS	F value	Prob >F
Model	3	3.5543	1.1848	33.94	0.0001
Error	8	0.2793	0.0349		
C-Total	11	3.8336			

model R-square =	0.9271
root MSE =	0.1868
estimated CV =	18.8485

press score = 0.546

Parameter	Estimate	Standard Error	t value para=0	Prob >|t|
intercept	3.0997	0.1511	20.52	0.0001
z1	0.5089	0.0749	6.80	0.0001
z1^2	-0.0586	0.0397	-1.47	0.1785
x	-0.5590	0.2536	-2.20	0.0586

AOV Table and Parameter Estimates for depth: 90.00

Source	DF	SS	MS	F value	Prob >F
Model	3	3.1011	1.0337	27.47	0.0001
Error	8	0.3011	0.0376		
C-Total	11	3.4022			

model R-square =	0.9115
root MSE =	0.1940
estimated CV =	19.5840

press score = 0.723

Parameter	Estimate	Standard Error	t value para=0	Prob >|t|
intercept	3.1160	0.1569	19.87	0.0001
z1	0.4018	0.0777	5.17	0.0009
z1^2	-0.1027	0.0412	-2.49	0.0375
x	-0.3596	0.2633	-1.37	0.2092

AOV Table and Parameter Estimates for depth: 120.00

Source	DF	SS	MS	F value	Prob >F
Model	3	3.0609	1.0203	44.34	0.0001
Error	8	0.1841	0.0230		
C-Total	11	3.2449			

```
  model R-square =        0.9433
  root MSE =              0.1517
  estimated CV =         15.2564

  press score =           0.481

                                  Standard     t value
  Parameter        Estimate         Error      para=0    Prob >|t|

  intercept          3.1598        0.1226       25.76       0.0001
  z1                 0.3961        0.0608        6.52       0.0002
  z1^2              -0.1292        0.0322       -4.01       0.0039
  x                 -0.5457        0.2059       -2.65       0.0292


AOV Table and Parameter Estimates for bulk average model

  Source       DF         SS              MS       F value    Prob >F

  Model         3     3.2004          1.0668         48.17     0.0001
  Error         8     0.1772          0.0221
  C-Total      11     3.3776

  model R-square =        0.9475
  root MSE =              0.1488
  estimated CV =         14.9648

  press score =           0.301

                                  Standard     t value
  Parameter        Estimate         Error      para=0    Prob >|t|

  intercept          3.1043        0.1203       25.80       0.0001
  z1                 0.4731        0.0596        7.94       0.0001
  z1^2              -0.0671        0.0316       -2.12       0.0667
  x                 -0.5390        0.2020       -2.67       0.0284
```

Field 10-6 (Spring 2017)

```
MLR Model Form:
ln(ECe)  =  b0 + b1(z1)

Basic Regression Summary Statistics

    Depth      R-square      Root MSE       Est.%CV
    30.00        0.8130        0.2296         23.26
    60.00        0.7586        0.2726         27.78
    90.00        0.7349        0.2829         28.87
   120.00        0.7541        0.2557         26.00
     bulk        0.7934        0.2391         24.25
```

AOV Table and Parameter Estimates for depth: 30.00

Source	DF	SS	MS	F value	Prob >F
Model	1	2.2918	2.2918	43.48	0.0001
Error	10	0.5271	0.0527		
C-Total	11	2.8189			

model R-square =	0.8130
root MSE =	0.2296
estimated CV =	23.2643
press score =	0.782

Parameter	Estimate	Standard Error	t value para=0	Prob >|t|
intercept	2.4148	0.0666	36.27	0.0001
z1	0.3385	0.0513	6.59	0.0001

AOV Table and Parameter Estimates for depth: 60.00

Source	DF	SS	MS	F value	Prob >F
Model	1	2.3355	2.3355	31.43	0.0002
Error	10	0.7432	0.0743		
C-Total	11	3.0787			

model R-square =	0.7586
root MSE =	0.2726
estimated CV =	27.7754
press score =	1.093

Parameter	Estimate	Standard Error	t value para=0	Prob >|t|
intercept	2.6376	0.0790	33.37	0.0001
z1	0.3417	0.0609	5.61	0.0002

AOV Table and Parameter Estimates for depth: 90.00

Source	DF	SS	MS	F value	Prob >F
Model	1	2.2184	2.2184	27.72	0.0004
Error	10	0.8004	0.0800		
C-Total	11	3.0188			

model R-square =	0.7349
root MSE =	0.2829
estimated CV =	28.8670

press score = 1.257

Parameter	Estimate	Standard Error	t value para=0	Prob >|t|
intercept	2.6977	0.0820	32.88	0.0001
z1	0.3330	0.0633	5.26	0.0004

AOV Table and Parameter Estimates for depth: 120.00

Source	DF	SS	MS	F value	Prob >F
Model	1	2.0057	2.0057	30.67	0.0002
Error	10	0.6539	0.0654		
C-Total	11	2.6596			

model R-square = 0.7541
root MSE = 0.2557
estimated CV = 25.9951

press score = 1.065

Parameter	Estimate	Standard Error	t value para=0	Prob >|t|
intercept	2.6718	0.0741	36.03	0.0001
z1	0.3166	0.0572	5.54	0.0002

AOV Table and Parameter Estimates for bulk average model

Source	DF	SS	MS	F value	Prob >F
Model	1	2.1943	2.1943	38.39	0.0001
Error	10	0.5716	0.0572		
C-Total	11	2.7659			

model R-square = 0.7934
root MSE = 0.2391
estimated CV = 24.2530

press score = 0.866

Parameter	Estimate	Standard Error	t value para=0	Prob >|t|
intercept	2.6173	0.0693	37.75	0.0001
z1	0.3312	0.0534	6.20	0.0001

Field 10-6 (Fall 2017)

MLR Model Form:
ln(ECe) = b0 + b1(z1) + b2(z2)

Basic Regression Summary Statistics

Depth	R-square	Root MSE	Est.%CV
30.00	0.8431	0.3068	31.41
60.00	0.7389	0.2996	30.64
90.00	0.7483	0.2578	26.21
120.00	0.8681	0.2028	20.49
bulk	0.8309	0.2400	24.35

AOV Table and Parameter Estimates for depth: 30.00

Source	DF	SS	MS	F value	Prob >F
Model	2	4.5491	2.2746	24.17	0.0002
Error	9	0.8469	0.0941		
C-Total	11	5.3960			

model R-square = 0.8431
root MSE = 0.3068
estimated CV = 31.4113

press score = 1.583

Parameter	Estimate	Standard Error	t value para=0	Prob >|t|
intercept	2.5606	0.0900	28.44	0.0001
z1	0.4639	0.0729	6.36	0.0001
z2	-0.2274	0.0650	-3.50	0.0067

AOV Table and Parameter Estimates for depth: 60.00

Source	DF	SS	MS	F value	Prob >F
Model	2	2.2858	1.1429	12.74	0.0024
Error	9	0.8076	0.0897		
C-Total	11	3.0935			

model R-square = 0.7389
root MSE = 0.2996
estimated CV = 30.6406

press score = 1.737

Parameter	Estimate	Standard Error	t value para=0	Prob >|t|

intercept	2.7408	0.0879	31.18	0.0001
z1	0.3284	0.0712	4.61	0.0013
z2	-0.1620	0.0635	-2.55	0.0310

AOV Table and Parameter Estimates for depth: 90.00

Source	DF	SS	MS	F value	Prob >F
Model	2	1.7780	0.8890	13.38	0.0020
Error	9	0.5980	0.0664		
C-Total	11	2.3760			

model R-square =	0.7483
root MSE =	0.2578
estimated CV =	26.2111

press score = 1.364

Parameter	Estimate	Standard Error	t value para=0	Prob >|t|
intercept	2.7495	0.0756	36.35	0.0001
z1	0.3071	0.0612	5.01	0.0007
z2	-0.1000	0.0546	-1.83	0.1003

AOV Table and Parameter Estimates for depth: 120.00

Source	DF	SS	MS	F value	Prob >F
Model	2	2.4349	1.2175	29.61	0.0001
Error	9	0.3701	0.0411		
C-Total	11	2.8050			

model R-square =	0.8681
root MSE =	0.2028
estimated CV =	20.4882

press score = 0.817

Parameter	Estimate	Standard Error	t value para=0	Prob >|t|
intercept	2.6279	0.0595	44.16	0.0001
z1	0.3639	0.0482	7.55	0.0001
z2	-0.0994	0.0430	-2.31	0.0459

AOV Table and Parameter Estimates for bulk average model

Source	DF	SS	MS	F value	Prob >F

Model	2	2.5475	1.2737	22.11	0.0003
Error	9	0.5185	0.0576		
C-Total	11	3.0660			

model R-square = 0.8309
root MSE = 0.2400
estimated CV = 24.3527

press score = 1.144

Parameter	Estimate	Standard Error	t value para=0	Prob >|t|
intercept	2.6833	0.0704	38.09	0.0001
z1	0.3599	0.0570	6.31	0.0001
z2	-0.1421	0.0508	-2.79	0.0209

Field 13-1 (Spring 2016)

MLR Model Form:
ln(ECe) = b0 + b1(z1) + b2(y)

Basic Regression Summary Statistics

Depth	R-square	Root MSE	Est.%CV
30.00	0.2955	0.2040	20.62
60.00	0.6072	0.1692	17.04
90.00	0.7517	0.1060	10.63
120.00	0.5136	0.1274	12.79
bulk	0.7842	0.0828	8.29

AOV Table and Parameter Estimates for depth: 30.00

Source	DF	SS	MS	F value	Prob >F
Model	2	0.1572	0.0786	1.89	0.2067
Error	9	0.3746	0.0416		
C-Total	11	0.5318			

model R-square = 0.2955
root MSE = 0.2040
estimated CV = 20.6165

press score = 0.645

Parameter	Estimate	Standard Error	t value para=0	Prob >|t|
intercept	2.4956	0.1426	17.50	0.0001
z1	0.0714	0.0595	1.20	0.2606
y	0.1797	0.3421	0.53	0.6121

AOV Table and Parameter Estimates for depth: 60.00

Source	DF	SS	MS	F value	Prob >F
Model	2	0.3984	0.1992	6.96	0.0149
Error	9	0.2577	0.0286		
C-Total	11	0.6561			

model R-square =	0.6072
root MSE =	0.1692
estimated CV =	17.0433
press score =	0.471

Parameter	Estimate	Standard Error	t value para=0	Prob >|t|
intercept	2.9930	0.1183	25.31	0.0001
z1	0.1564	0.0493	3.17	0.0114
y	-0.0798	0.2837	-0.28	0.7848

AOV Table and Parameter Estimates for depth: 90.00

Source	DF	SS	MS	F value	Prob >F
Model	2	0.3063	0.1531	13.63	0.0019
Error	9	0.1011	0.0112		
C-Total	11	0.4074			

model R-square =	0.7517
root MSE =	0.1060
estimated CV =	10.6308
press score =	0.192

Parameter	Estimate	Standard Error	t value para=0	Prob >|t|
intercept	2.9506	0.0741	39.82	0.0001
z1	0.1040	0.0309	3.37	0.0083
y	0.2197	0.1777	1.24	0.2477

AOV Table and Parameter Estimates for depth: 120.00

Source	DF	SS	MS	F value	Prob >F
Model	2	0.1542	0.0771	4.75	0.0390
Error	9	0.1460	0.0162		
C-Total	11	0.3002			

model R-square =	0.5136

root MSE = 0.1274
estimated CV = 12.7882

press score = 0.246

Parameter	Estimate	Standard Error	t value para=0	Prob >|t|
intercept	2.9847	0.0890	33.53	0.0001
z1	0.0266	0.0371	0.71	0.4928
y	0.4269	0.2135	2.00	0.0766

AOV Table and Parameter Estimates for bulk average model

Source	DF	SS	MS	F value	Prob >F
Model	2	0.2242	0.1121	16.35	0.0010
Error	9	0.0617	0.0069		
C-Total	11	0.2859			

model R-square = 0.7842
root MSE = 0.0828
estimated CV = 8.2938

press score = 0.100

Parameter	Estimate	Standard Error	t value para=0	Prob >|t|
intercept	2.8771	0.0579	49.72	0.0001
z1	0.0862	0.0241	3.57	0.0060
y	0.2084	0.1388	1.50	0.1675

Field 13-1 (Fall 2016)

MLR Model Form:
ln(ECe) = b0 + b1(z1) + b2(z2) + b3(z1^2) + b4(x)

Basic Regression Summary Statistics

Depth	R-square	Root MSE	Est.%CV
30.00	0.7422	0.1614	16.25
60.00	0.6930	0.1608	16.19
90.00	0.7770	0.1350	13.56
120.00	0.8422	0.1399	14.06
bulk	0.8265	0.1209	12.13

AOV Table and Parameter Estimates for depth: 30.00

Source	DF	SS	MS	F value	Prob >F

Source	DF	SS	MS	F value	Prob >F
Model	4	0.5250	0.1313	5.04	0.0313
Error	7	0.1824	0.0261		
C-Total	11	0.7074			

model R-square = 0.7422
root MSE = 0.1614
estimated CV = 16.2483

press score = 0.614

Parameter	Estimate	Standard Error	t value para=0	Prob >|t|
intercept	3.0031	0.1447	20.75	0.0001
z1	-0.1418	0.0590	-2.40	0.0473
z2	-0.0936	0.0559	-1.67	0.1380
z1^2	0.0649	0.0273	2.38	0.0491
x	-1.0646	0.3009	-3.54	0.0095

AOV Table and Parameter Estimates for depth: 60.00

Source	DF	SS	MS	F value	Prob >F
Model	4	0.4088	0.1022	3.95	0.0549
Error	7	0.1811	0.0259		
C-Total	11	0.5899			

model R-square = 0.6930
root MSE = 0.1608
estimated CV = 16.1881

press score = 0.540

Parameter	Estimate	Standard Error	t value para=0	Prob >|t|
intercept	3.3967	0.1442	23.55	0.0001
z1	-0.1704	0.0588	-2.90	0.0231
z2	-0.1207	0.0557	-2.17	0.0668
z1^2	0.0153	0.0272	0.56	0.5914
x	-1.1331	0.2998	-3.78	0.0069

AOV Table and Parameter Estimates for depth: 90.00

Source	DF	SS	MS	F value	Prob >F
Model	4	0.4447	0.1112	6.10	0.0195
Error	7	0.1276	0.0182		
C-Total	11	0.5723			

model R-square = 0.7770
root MSE = 0.1350
estimated CV = 13.5629

press score = 0.424

Parameter	Estimate	Standard Error	t value para=0	Prob >|t|
intercept	3.1741	0.1211	26.22	0.0001
z1	-0.0637	0.0494	-1.29	0.2380
z2	-0.0352	0.0468	-0.75	0.4756
z1^2	0.0633	0.0228	2.77	0.0277
x	-0.7492	0.2516	-2.98	0.0206

AOV Table and Parameter Estimates for depth: 120.00

Source	DF	SS	MS	F value	Prob >F
Model	4	0.7313	0.1828	9.34	0.0062
Error	7	0.1371	0.0196		
C-Total	11	0.8684			

model R-square = 0.8422
root MSE = 0.1399
estimated CV = 14.0614

press score = 0.400

Parameter	Estimate	Standard Error	t value para=0	Prob >|t|
intercept	3.6564	0.1255	29.14	0.0001
z1	-0.1992	0.0512	-3.89	0.0059
z2	-0.1844	0.0485	-3.80	0.0067
z1^2	0.0443	0.0237	1.87	0.1035
x	-1.5022	0.2608	-5.76	0.0007

AOV Table and Parameter Estimates for bulk average model

Source	DF	SS	MS	F value	Prob >F
Model	4	0.4873	0.1218	8.34	0.0085
Error	7	0.1023	0.0146		
C-Total	11	0.5896			

model R-square = 0.8265
root MSE = 0.1209
estimated CV = 12.1335

press score = 0.281

Parameter	Estimate	Standard Error	t value para=0	Prob >|t|
intercept	3.3347	0.1084	30.76	0.0001
z1	-0.1469	0.0442	-3.32	0.0127
z2	-0.1136	0.0419	-2.71	0.0300
z1^2	0.0460	0.0205	2.25	0.0593
x	-1.1340	0.2253	-5.03	0.0015

Field 13-1 (Spring 2017)

MLR Model Form:
ln(ECe) = b0 + b1(z1) + b2(z2)

Basic Regression Summary Statistics

Depth	R-square	Root MSE	Est.%CV
30.00	0.8352	0.1051	10.54
60.00	0.7827	0.1476	14.84
90.00	0.6958	0.1553	15.63
120.00	0.8298	0.1070	10.73
bulk	0.8465	0.1025	10.28

AOV Table and Parameter Estimates for depth: 30.00

Source	DF	SS	MS	F value	Prob >F
Model	2	0.5036	0.2518	22.80	0.0003
Error	9	0.0994	0.0110		
C-Total	11	0.6030			

model R-square =	0.8352
root MSE =	0.1051
estimated CV =	10.5372
press score =	0.203

Parameter	Estimate	Standard Error	t value para=0	Prob >|t|
intercept	2.4712	0.0303	81.45	0.0001
z1	0.1499	0.0222	6.75	0.0001
z2	0.0061	0.0219	0.28	0.7858

AOV Table and Parameter Estimates for depth: 60.00

Source	DF	SS	MS	F value	Prob >F
Model	2	0.7065	0.3533	16.21	0.0010

Error	9	0.1962	0.0218
C-Total	11	0.9027	

model R-square = 0.7827
root MSE = 0.1476
estimated CV = 14.8447

press score = 0.322

Parameter	Estimate	Standard Error	t value para=0	Prob >|t|
intercept	2.7771	0.0426	65.15	0.0001
z1	0.1695	0.0312	5.43	0.0004
z2	0.0658	0.0307	2.14	0.0608

AOV Table and Parameter Estimates for depth: 90.00

Source	DF	SS	MS	F value	Prob >F
Model	2	0.4967	0.2484	10.29	0.0047
Error	9	0.2172	0.0241		
C-Total	11	0.7139			

model R-square = 0.6958
root MSE = 0.1553
estimated CV = 15.6286

press score = 0.419

Parameter	Estimate	Standard Error	t value para=0	Prob >|t|
intercept	2.9076	0.0449	64.83	0.0001
z1	0.1481	0.0328	4.51	0.0015
z2	0.0278	0.0323	0.86	0.4125

AOV Table and Parameter Estimates for depth: 120.00

Source	DF	SS	MS	F value	Prob >F
Model	2	0.5019	0.2509	21.93	0.0003
Error	9	0.1030	0.0114		
C-Total	11	0.6049			

model R-square = 0.8298
root MSE = 0.1070
estimated CV = 10.7272

press score = 0.210

Parameter	Estimate	Standard Error	t value para=0	Prob >|t|
intercept	2.9126	0.0309	94.31	0.0001
z1	0.1205	0.0226	5.33	0.0005
z2	0.0969	0.0222	4.36	0.0018

AOV Table and Parameter Estimates for bulk average model

Source	DF	SS	MS	F value	Prob >F
Model	2	0.5216	0.2608	24.82	0.0002
Error	9	0.0946	0.0105		
C-Total	11	0.6162			

model R-square =	0.8465
root MSE =	0.1025
estimated CV =	10.2789
press score =	0.175

Parameter	Estimate	Standard Error	t value para=0	Prob >|t|
intercept	2.7865	0.0296	94.14	0.0001
z1	0.1467	0.0217	6.77	0.0001
z2	0.0531	0.0213	2.49	0.0344

Field 13-1 (Fall 2017)

MLR Model Form:
ln(ECe) = b0 + b1(z1) + b2(z2)

Basic Regression Summary Statistics

Depth	R-square	Root MSE	Est.%CV
30.00	0.5476	0.1279	12.84
60.00	0.5787	0.1174	11.78
90.00	0.4163	0.1549	15.58
120.00	0.2519	0.1855	18.71
bulk	0.5070	0.1237	12.42

AOV Table and Parameter Estimates for depth: 30.00

Source	DF	SS	MS	F value	Prob >F
Model	2	0.1782	0.0891	5.45	0.0282
Error	9	0.1472	0.0164		
C-Total	11	0.3254			

model R-square =	0.5476

root MSE = 0.1279
estimated CV = 12.8416

press score = 0.262

Parameter	Estimate	Standard Error	t value para=0	Prob >|t|
intercept	2.5944	0.0370	70.20	0.0001
z1	0.0746	0.0258	2.89	0.0180
z2	0.0388	0.0266	1.46	0.1786

AOV Table and Parameter Estimates for depth: 60.00

Source	DF	SS	MS	F value	Prob >F
Model	2	0.1703	0.0852	6.18	0.0205
Error	9	0.1240	0.0138		
C-Total	11	0.2944			

model R-square = 0.5787
root MSE = 0.1174
estimated CV = 11.7794

press score = 0.220

Parameter	Estimate	Standard Error	t value para=0	Prob >|t|
intercept	2.9726	0.0339	87.64	0.0001
z1	0.0444	0.0237	1.87	0.0937
z2	0.0704	0.0244	2.88	0.0181

AOV Table and Parameter Estimates for depth: 90.00

Source	DF	SS	MS	F value	Prob >F
Model	2	0.1540	0.0770	3.21	0.0887
Error	9	0.2159	0.0240		
C-Total	11	0.3699			

model R-square = 0.4163
root MSE = 0.1549
estimated CV = 15.5832

press score = 0.404

Parameter	Estimate	Standard Error	t value para=0	Prob >|t|
intercept	3.0049	0.0448	67.13	0.0001

z1	0.0416	0.0313	1.33	0.2163
z2	0.0673	0.0322	2.09	0.0661

AOV Table and Parameter Estimates for depth: 120.00

Source	DF	SS	MS	F value	Prob >F
Model	2	0.1042	0.0521	1.52	0.2709
Error	9	0.3095	0.0344		
C-Total	11	0.4138			

model R-square =	0.2519
root MSE =	0.1855
estimated CV =	18.7060

press score = 0.596

Parameter	Estimate	Standard Error	t value para=0	Prob >|t|
intercept	3.0431	0.0536	56.79	0.0001
z1	0.0485	0.0375	1.30	0.2275
z2	0.0424	0.0386	1.10	0.2998

AOV Table and Parameter Estimates for bulk average model

Source	DF	SS	MS	F value	Prob >F
Model	2	0.1416	0.0708	4.63	0.0415
Error	9	0.1377	0.0153		
C-Total	11	0.2793			

model R-square =	0.5070
root MSE =	0.1237
estimated CV =	12.4158

press score = 0.261

Parameter	Estimate	Standard Error	t value para=0	Prob >|t|
intercept	2.9222	0.0357	81.76	0.0001
z1	0.0498	0.0250	1.99	0.0775
z2	0.0566	0.0257	2.20	0.0552

Field 13-2 (Spring 2016)

MLR Model Form:
ln(ECe) = b0 + b1(z1)

Basic Regression Summary Statistics

Depth	R-square	Root MSE	Est.%CV
30.00	0.7882	0.1788	18.02
60.00	0.7119	0.1555	15.65
90.00	0.2925	0.2324	23.55
120.00	0.8735	0.0877	8.79
bulk	0.8367	0.1015	10.17

AOV Table and Parameter Estimates for depth: 30.00

Source	DF	SS	MS	F value	Prob >F
Model	1	1.1893	1.1893	37.21	0.0001
Error	10	0.3196	0.0320		
C-Total	11	1.5089			

model R-square = 0.7882
root MSE = 0.1788
estimated CV = 18.0209

press score = 0.505

Parameter	Estimate	Standard Error	t value para=0	Prob >|t|
intercept	2.2291	0.0516	43.18	0.0001
z1	0.2470	0.0405	6.10	0.0001

AOV Table and Parameter Estimates for depth: 60.00

Source	DF	SS	MS	F value	Prob >F
Model	1	0.5977	0.5977	24.71	0.0006
Error	10	0.2419	0.0242		
C-Total	11	0.8396			

model R-square = 0.7119
root MSE = 0.1555
estimated CV = 15.6481

press score = 0.406

Parameter	Estimate	Standard Error	t value para=0	Prob >|t|
intercept	2.6223	0.0449	58.38	0.0001
z1	0.1751	0.0352	4.97	0.0006

AOV Table and Parameter Estimates for depth: 90.00

Source	DF	SS	MS	F value	Prob >F

Source	DF	SS	MS	F value	Prob >F
Model	1	0.2232	0.2232	4.13	0.0694
Error	10	0.5399	0.0540		
C-Total	11	0.7631			

model R-square = 0.2925
root MSE = 0.2324
estimated CV = 23.5531

press score = 0.716

Parameter	Estimate	Standard Error	t value para=0	Prob >|t|
intercept	2.7995	0.0671	41.72	0.0001
z1	0.1070	0.0526	2.03	0.0694

AOV Table and Parameter Estimates for depth: 120.00

Source	DF	SS	MS	F value	Prob >F
Model	1	0.5316	0.5316	69.08	0.0001
Error	10	0.0770	0.0077		
C-Total	11	0.6086			

model R-square = 0.8735
root MSE = 0.0877
estimated CV = 8.7898

press score = 0.111

Parameter	Estimate	Standard Error	t value para=0	Prob >|t|
intercept	2.8290	0.0253	111.67	0.0001
z1	0.1652	0.0199	8.31	0.0001

AOV Table and Parameter Estimates for bulk average model

Source	DF	SS	MS	F value	Prob >F
Model	1	0.5273	0.5273	51.23	0.0001
Error	10	0.1029	0.0103		
C-Total	11	0.6302			

model R-square = 0.8367
root MSE = 0.1015
estimated CV = 10.1712

press score = 0.138

Parameter	Estimate	Standard Error	t value para=0	Prob >|t|
intercept	2.6571	0.0293	90.70	0.0001
z1	0.1645	0.0230	7.16	0.0001

Field 13-2 (Fall 2016)

MLR Model Form:
ln(ECe) = b0 + b1(z1)

Basic Regression Summary Statistics

Depth	R-square	Root MSE	Est.%CV
30.00	0.3971	0.2321	23.53
60.00	0.5875	0.1463	14.71
90.00	0.3343	0.1522	15.31
120.00	0.0636	0.1580	15.90
bulk	0.4357	0.1326	13.32

AOV Table and Parameter Estimates for depth: 30.00

Source	DF	SS	MS	F value	Prob >F
Model	1	0.3549	0.3549	6.59	0.0281
Error	10	0.5389	0.0539		
C-Total	11	0.8938			

model R-square = 0.3971
root MSE = 0.2321
estimated CV = 23.5301

press score = 0.722

Parameter	Estimate	Standard Error	t value para=0	Prob >|t|
intercept	2.0718	0.0672	30.85	0.0001
z1	0.1240	0.0483	2.57	0.0281

AOV Table and Parameter Estimates for depth: 60.00

Source	DF	SS	MS	F value	Prob >F
Model	1	0.3047	0.3047	14.24	0.0036
Error	10	0.2140	0.0214		
C-Total	11	0.5187			

model R-square = 0.5875
root MSE = 0.1463
estimated CV = 14.7069

press score = 0.299

Parameter	Estimate	Standard Error	t value para=0	Prob >|t|
intercept	2.4803	0.0423	58.60	0.0001
z1	0.1149	0.0304	3.77	0.0036

AOV Table and Parameter Estimates for depth: 90.00

Source	DF	SS	MS	F value	Prob >F
Model	1	0.1164	0.1164	5.02	0.0489
Error	10	0.2318	0.0232		
C-Total	11	0.3482			

model R-square = 0.3343
root MSE = 0.1522
estimated CV = 15.3129

press score = 0.357

Parameter	Estimate	Standard Error	t value para=0	Prob >|t|
intercept	2.7018	0.0441	61.33	0.0001
z1	0.0710	0.0317	2.24	0.0489

AOV Table and Parameter Estimates for depth: 120.00

Source	DF	SS	MS	F value	Prob >F
Model	1	0.0170	0.0170	0.68	0.4289
Error	10	0.2496	0.0250		
C-Total	11	0.2666			

model R-square = 0.0636
root MSE = 0.1580
estimated CV = 15.8983

press score = 0.361

Parameter	Estimate	Standard Error	t value para=0	Prob >|t|
intercept	2.7215	0.0457	59.53	0.0001
z1	0.0271	0.0329	0.82	0.4287

AOV Table and Parameter Estimates for bulk average model

Source	DF	SS	MS	F value	Prob >F
Model	1	0.1358	0.1358	7.72	0.0195
Error	10	0.1759	0.0176		
C-Total	11	0.3117			

model R-square =	0.4357
root MSE =	0.1326
estimated CV =	13.3195

press score = 0.242

Parameter	Estimate	Standard Error	t value para=0	Prob >|t|
intercept	2.5316	0.0384	65.98	0.0001
z1	0.0767	0.0276	2.78	0.0195

Field 13-2 (Spring 2017)

MLR Model Form:
ln(ECe) = b0 + b1(z1) + b2(z2) + b3(y)

Basic Regression Summary Statistics

Depth	R-square	Root MSE	Est.%CV
30.00	0.9688	0.0737	7.38
60.00	0.9280	0.1206	12.11
90.00	0.8280	0.1392	13.99
120.00	0.8664	0.1078	10.81
bulk	0.9561	0.0723	7.24

AOV Table and Parameter Estimates for depth: 30.00

Source	DF	SS	MS	F value	Prob >F
Model	3	1.3496	0.4499	82.81	0.0001
Error	8	0.0435	0.0054		
C-Total	11	1.3931			

model R-square =	0.9688
root MSE =	0.0737
estimated CV =	7.3807

press score = 0.083

Parameter	Estimate	Standard Error	t value para=0	Prob >|t|
intercept	1.7382	0.0435	39.97	0.0001
z1	0.2386	0.0158	15.15	0.0001
z2	-0.0152	0.0163	-0.93	0.3793
y	0.6773	0.1416	4.78	0.0014

AOV Table and Parameter Estimates for depth: 60.00

Source	DF	SS	MS	F value	Prob >F
Model	3	1.5002	0.5001	34.36	0.0001
Error	8	0.1164	0.0146		
C-Total	11	1.6166			

model R-square =	0.9280
root MSE =	0.1206
estimated CV =	12.1078

press score = 0.262

Parameter	Estimate	Standard Error	t value para=0	Prob >|t|
intercept	2.4680	0.0712	34.67	0.0001
z1	0.2467	0.0258	9.57	0.0001
z2	-0.0830	0.0267	-3.11	0.0143
y	-0.2166	0.2318	-0.93	0.3773

AOV Table and Parameter Estimates for depth: 90.00

Source	DF	SS	MS	F value	Prob >F
Model	3	0.7460	0.2487	12.84	0.0020
Error	8	0.1550	0.0194		
C-Total	11	0.9009			

model R-square =	0.8280
root MSE =	0.1392
estimated CV =	13.9855

press score = 0.378

Parameter	Estimate	Standard Error	t value para=0	Prob >|t|
intercept	2.6340	0.0821	32.07	0.0001
z1	0.1719	0.0297	5.78	0.0004
z2	-0.0661	0.0308	-2.15	0.0637
y	-0.0265	0.2674	-0.10	0.9236

AOV Table and Parameter Estimates for depth: 120.00

Source	DF	SS	MS	F value	Prob >F
Model	3	0.6030	0.2010	17.29	0.0007

Error	8	0.0930	0.0116	
C-Total	11	0.6961		

model R-square = 0.8664
root MSE = 0.1078
estimated CV = 10.8145

press score = 0.215

Parameter	Estimate	Standard Error	t value para=0	Prob >|t|
intercept	2.7137	0.0636	42.65	0.0001
z1	0.1584	0.0230	6.87	0.0001
z2	-0.0482	0.0238	-2.02	0.0776
y	-0.0258	0.2072	-0.12	0.9039

AOV Table and Parameter Estimates for bulk average model

Source	DF	SS	MS	F value	Prob >F
Model	3	0.9105	0.3035	58.07	0.0001
Error	8	0.0418	0.0052		
C-Total	11	0.9523			

model R-square = 0.9561
root MSE = 0.0723
estimated CV = 7.2389

press score = 0.103

Parameter	Estimate	Standard Error	t value para=0	Prob >|t|
intercept	2.4547	0.0427	57.55	0.0001
z1	0.1950	0.0154	12.63	0.0001
z2	-0.0575	0.0160	-3.60	0.0070
y	0.0344	0.1389	0.25	0.8106

Field 13-2 (Fall 2017)

MLR Model Form:
ln(ECe) = b0 + b1(z1) + b2(y)

Basic Regression Summary Statistics

Depth	R-square	Root MSE	Est.%CV
30.00	0.8217	0.1074	10.77
60.00	0.4176	0.1218	12.22
90.00	0.2279	0.1110	11.13
120.00	0.3852	0.1453	14.60
bulk	0.6092	0.0778	7.79

AOV Table and Parameter Estimates for depth: 30.00

Source	DF	SS	MS	F value	Prob >F
Model	2	0.4782	0.2391	20.74	0.0004
Error	9	0.1038	0.0115		
C-Total	11	0.5819			

model R-square =	0.8217
root MSE =	0.1074
estimated CV =	10.7682

press score = 0.176

Parameter	Estimate	Standard Error	t value para=0	Prob >|t|
intercept	1.9444	0.0651	29.86	0.0001
z1	0.1550	0.0243	6.37	0.0001
y	-0.0277	0.2219	-0.12	0.9033

AOV Table and Parameter Estimates for depth: 60.00

Source	DF	SS	MS	F value	Prob >F
Model	2	0.0957	0.0479	3.23	0.0878
Error	9	0.1335	0.0148		
C-Total	11	0.2292			

model R-square =	0.4176
root MSE =	0.1218
estimated CV =	12.2241

press score = 0.232

Parameter	Estimate	Standard Error	t value para=0	Prob >|t|
intercept	2.6928	0.0739	36.46	0.0001
z1	0.0667	0.0276	2.42	0.0388
y	-0.2946	0.2517	-1.17	0.2718

AOV Table and Parameter Estimates for depth: 90.00

Source	DF	SS	MS	F value	Prob >F
Model	2	0.0327	0.0164	1.33	0.3124
Error	9	0.1108	0.0123		
C-Total	11	0.1435			

model R-square = 0.2279
root MSE = 0.1110
estimated CV = 11.1314

press score = 0.192

Parameter	Estimate	Standard Error	t value para=0	Prob >|t|
intercept	2.8341	0.0673	42.11	0.0001
z1	0.0383	0.0251	1.52	0.1621
y	-0.1890	0.2294	-0.82	0.4312

AOV Table and Parameter Estimates for depth: 120.00

Source	DF	SS	MS	F value	Prob >F
Model	2	0.1190	0.0595	2.82	0.1120
Error	9	0.1899	0.0211		
C-Total	11	0.3089			

model R-square = 0.3852
root MSE = 0.1453
estimated CV = 14.6032

press score = 0.291

Parameter	Estimate	Standard Error	t value para=0	Prob >|t|
intercept	2.9233	0.0881	33.18	0.0001
z1	0.0438	0.0329	1.33	0.2156
y	-0.6483	0.3002	-2.16	0.0591

AOV Table and Parameter Estimates for bulk average model

Source	DF	SS	MS	F value	Prob >F
Model	2	0.0849	0.0425	7.01	0.0146
Error	9	0.0545	0.0061		
C-Total	11	0.1394			

model R-square = 0.6092
root MSE = 0.0778
estimated CV = 7.7929

press score = 0.090

Parameter	Estimate	Standard Error	t value para=0	Prob >|t|

intercept	2.6620	0.0472	56.41	0.0001
z1	0.0613	0.0176	3.48	0.0070
y	-0.3130	0.1608	-1.95	0.0834

Field 13-6 (Spring 2016)

MLR Model Form:
ln(ECe) = b0 + b1(z1)

Basic Regression Summary Statistics

Depth	R-square	Root MSE	Est.%CV
30.00	0.7357	0.1809	18.24
60.00	0.4539	0.2987	30.55
90.00	0.3823	0.2133	21.57
120.00	0.4043	0.2431	24.68
bulk	0.5504	0.2011	20.31

AOV Table and Parameter Estimates for depth: 30.00

Source	DF	SS	MS	F value	Prob >F
Model	1	0.9109	0.9109	27.84	0.0004
Error	10	0.3272	0.0327		
C-Total	11	1.2381			

model R-square =	0.7357
root MSE =	0.1809
estimated CV =	18.2380
press score =	0.570

Parameter	Estimate	Standard Error	t value para=0	Prob >|t|
intercept	1.7199	0.0524	32.84	0.0001
z1	0.2248	0.0426	5.28	0.0004

AOV Table and Parameter Estimates for depth: 60.00

Source	DF	SS	MS	F value	Prob >F
Model	1	0.7415	0.7415	8.31	0.0163
Error	10	0.8921	0.0892		
C-Total	11	1.6337			

model R-square =	0.4539
root MSE =	0.2987
estimated CV =	30.5474
press score =	1.231

Parameter	Estimate	Standard Error	t value para=0	Prob >|t|
intercept	2.1705	0.0865	25.10	0.0001
z1	0.2028	0.0704	2.88	0.0163

AOV Table and Parameter Estimates for depth: 90.00

Source	DF	SS	MS	F value	Prob >F
Model	1	0.2815	0.2815	6.19	0.0321
Error	10	0.4549	0.0455		
C-Total	11	0.7364			

model R-square =	0.3823
root MSE =	0.2133
estimated CV =	21.5724
press score =	0.747

Parameter	Estimate	Standard Error	t value para=0	Prob >|t|
intercept	2.3659	0.0618	38.31	0.0001
z1	0.1250	0.0502	2.49	0.0321

AOV Table and Parameter Estimates for depth: 120.00

Source	DF	SS	MS	F value	Prob >F
Model	1	0.4011	0.4011	6.79	0.0263
Error	10	0.5911	0.0591		
C-Total	11	0.9922			

model R-square =	0.4043
root MSE =	0.2431
estimated CV =	24.6757
press score =	0.929

Parameter	Estimate	Standard Error	t value para=0	Prob >|t|
intercept	2.3161	0.0704	32.90	0.0001
z1	0.1492	0.0573	2.60	0.0263

AOV Table and Parameter Estimates for bulk average model

Source	DF	SS	MS	F value	Prob >F

Source	DF	SS	MS	F value	Prob >F
Model	1	0.4950	0.4950	12.24	0.0057
Error	10	0.4043	0.0404		
C-Total	11	0.8993			

model R-square = 0.5504
root MSE = 0.2011
estimated CV = 20.3122

press score = 0.649

Parameter	Estimate	Standard Error	t value para=0	Prob >|t|
intercept	2.1803	0.0582	37.45	0.0001
z1	0.1657	0.0474	3.50	0.0057

Field 13-6 (Fall 2016)

MLR Model Form:
ln(ECe) = b0 + b1(z1) + b2(z2)

Basic Regression Summary Statistics

Depth	R-square	Root MSE	Est.%CV
30.00	0.6812	0.1609	16.20
60.00	0.5141	0.2179	22.05
90.00	0.5382	0.1560	15.69
120.00	0.7152	0.1563	15.73
bulk	0.8459	0.0918	9.20

AOV Table and Parameter Estimates for depth: 30.00

Source	DF	SS	MS	F value	Prob >F
Model	2	0.4979	0.2489	9.61	0.0058
Error	9	0.2331	0.0259		
C-Total	11	0.7309			

model R-square = 0.6812
root MSE = 0.1609
estimated CV = 16.1968

press score = 0.412

Parameter	Estimate	Standard Error	t value para=0	Prob >|t|
intercept	1.9595	0.0465	42.17	0.0001
z1	0.1401	0.0388	3.61	0.0057
z2	0.0945	0.0385	2.45	0.0366

AOV Table and Parameter Estimates for depth: 60.00

Source	DF	SS	MS	F value	Prob >F
Model	2	0.4521	0.2261	4.76	0.0388
Error	9	0.4272	0.0475		
C-Total	11	0.8793			

model R-square =	0.5141
root MSE =	0.2179
estimated CV =	22.0487

press score = 0.752

Parameter	Estimate	Standard Error	t value para=0	Prob >|t|
intercept	2.3188	0.0629	36.86	0.0001
z1	0.1303	0.0525	2.48	0.0350
z2	0.0945	0.0522	1.81	0.1034

AOV Table and Parameter Estimates for depth: 90.00

Source	DF	SS	MS	F value	Prob >F
Model	2	0.2551	0.1276	5.24	0.0309
Error	9	0.2189	0.0243		
C-Total	11	0.4740			

model R-square =	0.5382
root MSE =	0.1560
estimated CV =	15.6910

press score = 0.355

Parameter	Estimate	Standard Error	t value para=0	Prob >|t|
intercept	2.4874	0.0450	55.23	0.0001
z1	0.1109	0.0376	2.95	0.0162
z2	0.0489	0.0373	1.31	0.2230

AOV Table and Parameter Estimates for depth: 120.00

Source	DF	SS	MS	F value	Prob >F
Model	2	0.5523	0.2761	11.30	0.0035
Error	9	0.2199	0.0244		
C-Total	11	0.7722			

model R-square =	0.7152
root MSE =	0.1563

```
  estimated CV =         15.7270

  press score =            0.405

                                 Standard     t value
  Parameter        Estimate         Error      para=0    Prob >|t|

  intercept          2.3828        0.0451       52.79       0.0001
  z1                 0.1528        0.0377        4.05       0.0029
  z2                 0.0915        0.0374        2.44       0.0371


AOV Table and Parameter Estimates for bulk average model

  Source       DF         SS              MS       F value   Prob >F

  Model         2     0.4166          0.2083         24.69    0.0002
  Error         9     0.0759          0.0084
  C-Total      11     0.4925

  model R-square =        0.8459
  root MSE =              0.0918
  estimated CV =          9.2036

  press score =            0.113

                                 Standard     t value
  Parameter        Estimate         Error      para=0    Prob >|t|

  intercept          2.3145        0.0265       87.27       0.0001
  z1                 0.1318        0.0221        5.95       0.0002
  z2                 0.0809        0.0220        3.68       0.0051
```

Field 13-6 (Spring 2017)

```
MLR Model Form:
ln(ECe)  =  b0 + b1(z1) + b2(z2)

Basic Regression Summary Statistics

    Depth      R-square      Root MSE       Est.%CV
    30.00       0.8898        0.1630         16.41
    60.00       0.9321        0.1391         13.98
    90.00       0.8911        0.1343         13.49
   120.00       0.9498        0.0627          6.28
     bulk       0.9597        0.0799          8.00

AOV Table and Parameter Estimates for depth: 30.00

  Source       DF         SS              MS       F value   Prob >F

  Model         2     1.9306          0.9653         36.33    0.0001
  Error         9     0.2391          0.0266
  C-Total      11     2.1697
```

model R-square = 0.8898
root MSE = 0.1630
estimated CV = 16.4086

press score = 0.452

Parameter	Estimate	Standard Error	t value para=0	Prob >|t|
intercept	1.5700	0.0471	33.35	0.0001
z1	0.2649	0.0384	6.91	0.0001
z2	-0.1871	0.0391	-4.79	0.0010

AOV Table and Parameter Estimates for depth: 60.00

Source	DF	SS	MS	F value	Prob >F
Model	2	2.3908	1.1954	61.80	0.0001
Error	9	0.1741	0.0193		
C-Total	11	2.5649			

model R-square = 0.9321
root MSE = 0.1391
estimated CV = 13.9757

press score = 0.323

Parameter	Estimate	Standard Error	t value para=0	Prob >|t|
intercept	2.2257	0.0402	55.40	0.0001
z1	0.3327	0.0327	10.16	0.0001
z2	-0.1400	0.0333	-4.20	0.0023

AOV Table and Parameter Estimates for depth: 90.00

Source	DF	SS	MS	F value	Prob >F
Model	2	1.3287	0.6644	36.83	0.0001
Error	9	0.1624	0.0180		
C-Total	11	1.4911			

model R-square = 0.8911
root MSE = 0.1343
estimated CV = 13.4917

press score = 0.337

Parameter	Estimate	Standard Error	t value para=0	Prob >|t|

intercept	2.4460	0.0388	63.05	0.0001
z1	0.2702	0.0316	8.55	0.0001
z2	-0.0166	0.0322	-0.52	0.6188

AOV Table and Parameter Estimates for depth: 120.00

Source	DF	SS	MS	F value	Prob >F
Model	2	0.6701	0.3351	85.15	0.0001
Error	9	0.0354	0.0039		
C-Total	11	0.7056			

model R-square =	0.9498
root MSE =	0.0627
estimated CV =	6.2793
press score =	0.059

Parameter	Estimate	Standard Error	t value para=0	Prob >|t|
intercept	2.3640	0.0181	130.46	0.0001
z1	0.1925	0.0148	13.04	0.0001
z2	-0.0019	0.0150	-0.13	0.9011

AOV Table and Parameter Estimates for bulk average model

Source	DF	SS	MS	F value	Prob >F
Model	2	1.3665	0.6832	107.04	0.0001
Error	9	0.0574	0.0064		
C-Total	11	1.4239			

model R-square =	0.9597
root MSE =	0.0799
estimated CV =	8.0021
press score =	0.111

Parameter	Estimate	Standard Error	t value para=0	Prob >|t|
intercept	2.2135	0.0231	95.92	0.0001
z1	0.2649	0.0188	14.09	0.0001
z2	-0.0675	0.0191	-3.52	0.0065

Field 13-6 (Fall 2017)

MLR Model Form:
ln(ECe) = b0 + b1(z1) + b2(x) + b3(y)

Basic Regression Summary Statistics

Depth	R-square	Root MSE	Est.%CV
30.00	0.8837	0.0884	8.86
60.00	0.8773	0.1217	12.22
90.00	0.9141	0.0916	9.18
120.00	0.8365	0.1050	10.53
bulk	0.9287	0.0743	7.44

AOV Table and Parameter Estimates for depth: 30.00

Source	DF	SS	MS	F value	Prob >F
Model	3	0.4746	0.1582	20.25	0.0004
Error	8	0.0625	0.0078		
C-Total	11	0.5371			

model R-square = 0.8837
root MSE = 0.0884
estimated CV = 8.8554

press score = 0.163

Parameter	Estimate	Standard Error	t value para=0	Prob >|t|
intercept	1.7671	0.1157	15.28	0.0001
z1	0.1623	0.0236	6.87	0.0001
x	0.3070	0.1096	2.80	0.0231
y	-0.0178	0.1582	-0.11	0.9131

AOV Table and Parameter Estimates for depth: 60.00

Source	DF	SS	MS	F value	Prob >F
Model	3	0.8470	0.2823	19.06	0.0005
Error	8	0.1185	0.0148		
C-Total	11	0.9655			

model R-square = 0.8773
root MSE = 0.1217
estimated CV = 12.2157

press score = 0.316

Parameter	Estimate	Standard Error	t value para=0	Prob >|t|
intercept	2.0753	0.1593	13.03	0.0001
z1	0.2094	0.0325	6.43	0.0002
x	0.4605	0.1509	3.05	0.0158
y	0.0729	0.2178	0.33	0.7465

AOV Table and Parameter Estimates for depth: 90.00

Source	DF	SS	MS	F value	Prob >F
Model	3	0.7143	0.2381	28.37	0.0001
Error	8	0.0671	0.0084		
C-Total	11	0.7815			

model R-square =	0.9141
root MSE =	0.0916
estimated CV =	9.1802

press score = 0.156

Parameter	Estimate	Standard Error	t value para=0	Prob >|t|
intercept	2.1126	0.1199	17.62	0.0001
z1	0.1432	0.0245	5.85	0.0004
x	0.2527	0.1136	2.22	0.0568
y	0.5679	0.1640	3.46	0.0085

AOV Table and Parameter Estimates for depth: 120.00

Source	DF	SS	MS	F value	Prob >F
Model	3	0.4510	0.1503	13.64	0.0016
Error	8	0.0882	0.0110		
C-Total	11	0.5392			

model R-square =	0.8365
root MSE =	0.1050
estimated CV =	10.5280

press score = 0.178

Parameter	Estimate	Standard Error	t value para=0	Prob >|t|
intercept	2.3653	0.1374	17.21	0.0001
z1	0.1445	0.0281	5.15	0.0009
x	0.0682	0.1302	0.52	0.6145
y	0.1403	0.1879	0.75	0.4765

AOV Table and Parameter Estimates for bulk average model

Source	DF	SS	MS	F value	Prob >F
Model	3	0.5748	0.1916	34.74	0.0001

Error	8	0.0441	0.0055
C-Total	11	0.6189	

model R-square =	0.9287
root MSE =	0.0743
estimated CV =	7.4363

press score = 0.104

Parameter	Estimate	Standard Error	t value para=0	Prob >|t|
intercept	2.1023	0.0972	21.63	0.0001
z1	0.1632	0.0199	8.22	0.0001
x	0.2585	0.0921	2.81	0.0230
y	0.2208	0.1329	1.66	0.1353

APPENDIX B: DPPC CORRELATION RESULTS

Field 10-6 (Spring 2016)

I. ln(Calc ECa) Correlation Structure and
ln(Calc ECa) v.s. z1-signal Correlation Structure

	depth specific ln(Calc ECa) sample depth levels				
	30.00	60.00	90.00	120.00	ave
ave ln(Calc ECa)	0.964	0.987	0.980	0.954	1.000
z1-signal data	0.955	0.970	0.941	0.933	0.977

II. Bulk ave ln(Calc ECa) v.s. bulk ave Pri/Sec Soil Variable Correlations

Column Labels:

0. ln(Calc ECa)
1. ln(ECe)
2. SP
3. Vol H2o
4. Bulk Den

	0	1	2	3	4
0	1.000	0.981	0.889	0.702	-0.889
1	0.981	1.000	0.791	0.619	-0.791
2	0.889	0.791	1.000	0.745	-1.000
3	0.702	0.619	0.745	1.000	-0.745
4	-0.889	-0.791	-1.000	-0.745	1.000

IV. ECe <-> Calc ECa Signal Deterioration: by depth

depth level	% Signal Deterioration
30.00	6.9
60.00	4.1
90.00	5.7
120.00	7.0
ave	3.7

V. Observed bulk ave & depth specific Pri/Sec Soil Variables v.s. z1-signal Correlations

Pri/Sec Soil Variable	sample depth levels 30.00	60.00	90.00	120.00	ave
ln(ECe)	0.903	0.962	0.909	0.924	0.954
SP	0.826	0.857	0.864	0.796	0.878
Vol H2o	0.828	0.734	0.483	0.256	0.721
Bulk Den	-0.826	-0.857	-0.864	-0.796	-0.878

VI. Predicted v.s. observed Bulk ave Pri/Sec Soil Variable / z1-signal Correlation Estimates

DPPC Model Correlation: 0.977

Pri/Sec Soil Variable	Calc CECa Corr	Prd ECa Corr	95% CI	Obs ECa Corr
ln(ECe)	0.981	0.958	0.933 to 0.983	0.954
SP	0.889	0.868	0.808 to 0.927	0.878
Vol H2o	0.702	0.686	0.593 to 0.778	0.721
Bulk Den	-0.889	-0.868	-0.927 to -0.808	-0.878

Field 10-6 (Fall 2016)

I. ln(Calc ECa) Correlation Structure and ln(Calc ECa) v.s. z1-signal Correlation Structure

	depth specific ln(Calc ECa) sample depth levels 30.00	60.00	90.00	120.00	ave
ave ln(Calc ECa)	0.944	0.992	0.980	0.967	1.000
z1-signal data	0.960	0.946	0.921	0.929	0.966

II. Bulk ave ln(Calc ECa) v.s. bulk ave Pri/Sec Soil Variable Correlations

Column Labels:
0. ln(Calc ECa)
1. ln(ECe)
2. SP
3. Vol H2o
4. Bulk Den

	0	1	2	3	4
0	1.000	0.950	0.688	0.775	-0.688
1	0.950	1.000	0.433	0.576	-0.433
2	0.688	0.433	1.000	0.905	-1.000
3	0.775	0.576	0.905	1.000	-0.905
4	-0.688	-0.433	-1.000	-0.905	1.000

IV. ECe <-> Calc ECa Signal Deterioration: by depth

depth level	% Signal Deterioration
30.00	7.5
60.00	9.3

90.00	13.1
120.00	12.0
ave	9.8

V. Observed bulk ave & depth specific Pri/Sec Soil Variables v.s. z1-signal Correlations

Pri/Sec Soil Variable	sample depth levels 30.00	60.00	90.00	120.00	ave
ln(ECe)	0.899	0.926	0.902	0.874	0.929
SP	0.641	0.632	0.523	0.695	0.649
Vol H2o	0.698	0.695	0.786	0.654	0.786
Bulk Den	-0.641	-0.632	-0.523	-0.695	-0.649

VI. Predicted v.s. observed Bulk ave Pri/Sec Soil Variable / z1-signal Correlation Estimates

DPPC Model Correlation: 0.966

Pri/Sec Soil Variable	Calc CECa Corr	Prd ECa Corr	95% CI	Obs ECa Corr
ln(ECe)	0.950	0.918	0.870 to 0.966	0.929
SP	0.688	0.665	0.553 to 0.777	0.649
Vol H2o	0.775	0.749	0.651 to 0.846	0.786
Bulk Den	-0.688	-0.665	-0.777 to -0.553	-0.649

Field 10-6 (Spring 2017)

I. ln(Calc ECa) Correlation Structure and ln(Calc ECa) v.s. z1-signal Correlation Structure

	depth specific ln(Calc ECa) sample depth levels 30.00	60.00	90.00	120.00	ave
ave ln(Calc ECa)	0.976	0.992	0.990	0.987	1.000
z1-signal data	0.901	0.899	0.877	0.873	0.899

II. Bulk ave ln(Calc ECa) v.s. bulk ave Pri/Sec Soil Variable Correlations

Column Labels:
0. ln(Calc ECa)
1. ln(ECe)
2. SP
3. Vol H2o
4. Bulk Den

5. %H2o | FC

	0	1	2	3	4	5
0	1.000	0.962	0.899	0.818	-0.899	-0.685
1	0.962	1.000	0.757	0.715	-0.757	-0.548
2	0.899	0.757	1.000	0.843	-1.000	-0.776
3	0.818	0.715	0.843	1.000	-0.843	-0.361
4	-0.899	-0.757	-1.000	-0.843	1.000	0.776
5	-0.685	-0.548	-0.776	-0.361	0.776	1.000

IV. ECe <-> Calc ECa Signal Deterioration: by depth

depth level	% Signal Deterioration
30.00	2.8
60.00	6.8
90.00	15.2
120.00	19.1
ave	10.0

V. Observed bulk ave & depth specific Pri/Sec Soil Variables v.s. z1-signal Correlations

Pri/Sec Soil Variable	sample depth levels 30.00	60.00	90.00	120.00	ave
ln(ECe)	0.902	0.871	0.857	0.868	0.891
SP	0.815	0.825	0.727	0.745	0.785
Vol H2o	0.668	0.914	0.781	0.864	0.875
Bulk Den	-0.815	-0.825	-0.727	-0.745	-0.785
%H2o | FC	-0.118	0.021	-0.355	-0.532	-0.369

VI. Predicted v.s. observed Bulk ave Pri/Sec Soil Variable / z1-signal Correlation Estimates

DPPC Model Correlation: 0.899

Pri/Sec Soil Variable	Calc CECa Corr	Prd ECa Corr	95% CI	Obs ECa Corr
ln(ECe)	0.962	0.865	0.792 to 0.937	0.891
SP	0.899	0.808	0.692 to 0.924	0.785
Vol H2o	0.818	0.735	0.583 to 0.887	0.875
Bulk Den	-0.899	-0.808	-0.924 to -0.692	-0.785
%H2o | FC	-0.685	-0.616	-0.808 to -0.423	-0.369

Field 10-6 (Fall 2017)

I. ln(Calc ECa) Correlation Structure and

ln(Calc ECa) v.s. z1-signal Correlation Structure

	depth specific ln(Calc ECa) sample depth levels				
	30.00	60.00	90.00	120.00	ave
ave ln(Calc ECa)	0.948	0.981	0.983	0.933	1.000
z1-signal data	0.850	0.849	0.876	0.882	0.897

II. Bulk ave ln(Calc ECa) v.s. bulk ave Pri/Sec Soil Variable Correlations

Column Labels:

0. ln(Calc ECa)
1. ln(ECe)
2. SP
3. Vol H2o
4. Bulk Den
5. %H2o | FC

	0	1	2	3	4	5
0	1.000	0.941	0.785	0.840	-0.785	-0.315
1	0.941	1.000	0.535	0.685	-0.535	-0.061
2	0.785	0.535	1.000	0.842	-1.000	-0.666
3	0.840	0.685	0.842	1.000	-0.842	-0.203
4	-0.785	-0.535	-1.000	-0.842	1.000	0.666
5	-0.315	-0.061	-0.666	-0.203	0.666	1.000

IV. ECe <-> Calc ECa Signal Deterioration: by depth

depth level	% Signal Deterioration
30.00	4.3
60.00	10.8
90.00	23.1
120.00	28.7
ave	12.7

V. Observed bulk ave & depth specific Pri/Sec Soil Variables v.s. z1-signal Correlations

Pri/Sec Soil Variable	sample depth levels 30.00	60.00	90.00	120.00	ave
ln(ECe)	0.793	0.742	0.809	0.889	0.827
SP	0.767	0.761	0.713	0.671	0.742
Vol H2o	0.750	0.897	0.796	0.544	0.879
Bulk Den	-0.767	-0.761	-0.713	-0.671	-0.742
%H2o | FC	0.459	0.266	-0.286	-0.361	-0.126

VI. Predicted v.s. observed Bulk ave Pri/Sec Soil

Variable / z1-signal Correlation Estimates

DPPC Model Correlation: 0.897

Pri/Sec Soil Variable	Calc CECa Corr	Prd ECa Corr	95% CI	Obs ECa Corr
ln(ECe)	0.941	0.844	0.754 to 0.934	0.827
SP	0.785	0.704	0.539 to 0.869	0.742
Vol H2o	0.840	0.754	0.609 to 0.898	0.879
Bulk Den	-0.785	-0.704	-0.869 to -0.539	-0.742
%H2o | FC	-0.315	-0.283	-0.536 to -0.030	-0.126

Field 13-1 (Spring 2016)

I. ln(Calc ECa) Correlation Structure and ln(Calc ECa) v.s. z1-signal Correlation Structure

	depth specific ln(Calc ECa) sample depth levels 30.00	60.00	90.00	120.00	ave
ave ln(Calc ECa)	0.805	0.827	0.849	0.755	1.000
z1-signal data	0.624	0.794	0.826	0.519	0.868

II. Bulk ave ln(Calc ECa) v.s. bulk ave Pri/Sec Soil Variable Correlations

Column Labels:
0. ln(Calc ECa)
1. ln(ECe)
2. SP
3. Vol H2o
4. Bulk Den
5. Calc ECa

	0	1	2	3	4	5
0	1.000	0.991	0.217	0.435	-0.217	0.998
1	0.991	1.000	0.102	0.342	-0.102	0.986
2	0.217	0.102	1.000	0.317	-1.000	0.234
3	0.435	0.342	0.317	1.000	-0.317	0.437
4	-0.217	-0.102	-1.000	-0.317	1.000	-0.234
5	0.998	0.986	0.234	0.437	-0.234	1.000

IV. ECe <-> Calc ECa Signal Deterioration: by depth

depth level	% Signal Deterioration
30.00	7.1
60.00	1.8

90.00	1.3
120.00	1.9
ave	1.7

V. Observed bulk ave & depth specific Pri/Sec Soil Variables v.s. z1-signal Correlations

Pri/Sec Soil Variable	sample depth levels 30.00	60.00	90.00	120.00	ave
ln(ECe)	0.523	0.777	0.842	0.545	0.854
SP	0.425	-0.367	0.206	-0.303	0.035
Vol H2o	0.545	0.522	0.453	0.314	0.653
Bulk Den	-0.425	0.367	-0.206	0.303	-0.035
Calc ECa	0.627	0.782	0.809	0.515	0.855

VI. Predicted v.s. observed Bulk ave Pri/Sec Soil Variable / z1-signal Correlation Estimate

DPPC Model Correlation: 0.868

Pri/Sec Soil Variable	Calc CECa Corr	Prd ECa Corr	95% CI	Obs ECa Corr
ln(ECe)	0.991	0.860	0.819 to 0.901	0.854
SP	0.217	0.188	-0.104 to 0.480	0.035
Vol H2o	0.435	0.377	0.108 to 0.647	0.653
Bulk Den	-0.217	-0.188	-0.480 to 0.104	-0.035
Calc ECa	0.998	0.866	0.847 to 0.885	0.855

Field 13-1 (Fall 2016)

I. ln(Calc ECa) Correlation Structure and ln(Calc ECa) v.s. z1-signal Correlation Structure

	depth specific ln(Calc ECa) sample depth levels 30.00	60.00	90.00	120.00	ave
ave ln(Calc ECa)	0.927	0.958	0.916	0.955	1.000
z1-signal data	0.175	0.088	0.363	0.184	0.216

II. Bulk ave ln(Calc ECa) v.s. bulk ave Pri/Sec Soil Variable Correlations

Column Labels:
0. ln(Calc ECa)
1. ln(ECe)
2. SP
3. Vol H2o

4. Bulk Den

	0	1	2	3	4
0	1.000	0.994	0.723	0.707	-0.723
1	0.994	1.000	0.644	0.653	-0.644
2	0.723	0.644	1.000	0.686	-1.000
3	0.707	0.653	0.686	1.000	-0.686
4	-0.723	-0.644	-1.000	-0.686	1.000

IV. ECe <-> Calc ECa Signal Deterioration: by depth

depth level	% Signal Deterioration
30.00	2.6
60.00	3.7
90.00	1.4
120.00	1.2
ave	1.4

V. Observed bulk ave & depth specific Pri/Sec Soil Variables v.s. z1-signal Correlations

Pri/Sec Soil Variable	sample depth levels 30.00	60.00	90.00	120.00	ave
ln(ECe)	0.134	0.026	0.323	0.161	0.172
SP	0.174	0.301	0.387	0.197	0.358
Vol H2o	0.438	0.359	0.337	0.267	0.423
Bulk Den	-0.174	-0.301	-0.387	-0.197	-0.358

VI. Predicted v.s. observed Bulk ave Pri/Sec Soil Variable / z1-signal Correlation Estimate

DPPC Model Correlation: 0.216

Pri/Sec Soil Variable	Calc CECa Corr	Prd ECa Corr	95% CI	Obs ECa Corr
ln(ECe)	0.994	0.215	0.148 to 0.281	0.172
SP	0.723	0.156	-0.250 to 0.562	0.358
Vol H2o	0.707	0.153	-0.263 to 0.568	0.423
Bulk Den	-0.723	-0.156	-0.562 to 0.250	-0.358

Field 13-1 (Spring 2017)

I. ln(Calc ECa) Correlation Structure and ln(Calc ECa) v.s. z1-signal Correlation Structure

	depth specific ln(Calc ECa) sample depth levels				
	30.00	60.00	90.00	120.00	ave
ave ln(Calc ECa)	0.910	0.975	0.939	0.925	1.000
z1-signal data	0.918	0.843	0.841	0.737	0.878

II. Bulk ave ln(Calc ECa) v.s. bulk ave Pri/Sec Soil Variable Correlations

Column Labels:
0. ln(Calc ECa)
1. ln(ECe)
2. SP
3. Vol H2o
4. Bulk Den
5. %H2o | FC

	0	1	2	3	4	5
0	1.000	0.997	0.744	0.304	-0.744	0.028
1	0.997	1.000	0.706	0.277	-0.706	0.015
2	0.744	0.706	1.000	0.013	-1.000	-0.331
3	0.304	0.277	0.013	1.000	-0.013	0.939
4	-0.744	-0.706	-1.000	-0.013	1.000	0.331
5	0.028	0.015	-0.331	0.939	0.331	1.000

IV. ECe <-> Calc ECa Signal Deterioration: by depth

depth level	% Signal Deterioration
30.00	1.5
60.00	1.4
90.00	0.7
120.00	3.3
ave	0.6

V. Observed bulk ave & depth specific Pri/Sec Soil Variables v.s. z1-signal Correlations

Pri/Sec Soil Variable	sample depth levels 30.00	60.00	90.00	120.00	ave
ln(ECe)	0.913	0.820	0.819	0.686	0.861
SP	0.371	0.414	0.503	0.524	0.640
Vol H2o	0.206	0.528	0.535	0.541	0.606
Bulk Den	-0.371	-0.414	-0.503	-0.524	-0.640
%H2o | FC	0.077	0.336	0.344	0.253	0.351

VI. Predicted v.s. observed Bulk ave Pri/Sec Soil Variable / z1-signal Correlation Estimates

DPPC Model Correlation: 0.878

Pri/Sec Soil Variable	Calc CECa Corr	Prd ECa Corr	95% CI	Obs ECa Corr
ln(ECe)	0.997	0.876	0.855 to 0.897	0.861
SP	0.744	0.653	0.461 to 0.846	0.640
Vol H2o	0.304	0.267	-0.007 to 0.541	0.606
Bulk Den	-0.744	-0.653	-0.846 to -0.461	-0.640
%H2o | FC	0.028	0.025	-0.263 to 0.312	0.351

Field 13-1 (Fall 2017)

I. ln(Calc ECa) Correlation Structure and ln(Calc ECa) v.s. z1-signal Correlation Structure

	depth specific ln(Calc ECa) sample depth levels 30.00	60.00	90.00	120.00	ave
ave ln(Calc ECa)	0.789	0.950	0.909	0.939	1.000
z1-signal data	0.683	0.483	0.476	0.433	0.536

II. Bulk ave ln(Calc ECa) v.s. bulk ave Pri/Sec Soil Variable Correlations

Column Labels:

0. ln(Calc ECa)
1. ln(ECe)
2. SP
3. Vol H2o
4. Bulk Den
5. %H2o | FC

	0	1	2	3	4	5
0	1.000	0.994	0.705	0.118	-0.705	-0.098
1	0.994	1.000	0.637	0.072	-0.637	-0.121
2	0.705	0.637	1.000	-0.072	-1.000	-0.367
3	0.118	0.072	-0.072	1.000	0.072	0.954
4	-0.705	-0.637	-1.000	0.072	1.000	0.367
5	-0.098	-0.121	-0.367	0.954	0.367	1.000

IV. ECe <-> Calc ECa Signal Deterioration: by depth

depth level	% Signal Deterioration
30.00	7.0
60.00	2.6
90.00	2.7

120.00	4.6
ave	1.4

V. Observed bulk ave & depth specific Pri/Sec Soil Variables v.s. z1-signal Correlations

Pri/Sec Soil Variable	sample depth levels 30.00	60.00	90.00	120.00	ave
ln(ECe)	0.664	0.436	0.365	0.389	0.491
SP	0.266	0.296	0.701	0.336	0.579
Vol H2o	-0.274	0.516	0.616	0.519	0.253
Bulk Den	-0.266	-0.296	-0.701	-0.336	-0.579
%H2o | FC	-0.290	0.365	0.279	0.356	0.067

VI. Predicted v.s. observed Bulk ave Pri/Sec Soil Variable / z1-signal Correlation Estimates

DPPC Model Correlation: 0.536

Pri/Sec Soil Variable	Calc CECa Corr	Prd ECa Corr	95% CI	Obs ECa Corr
ln(ECe)	0.994	0.532	0.475 to 0.590	0.491
SP	0.705	0.378	0.017 to 0.738	0.579
Vol H2o	0.118	0.063	-0.441 to 0.568	0.253
Bulk Den	-0.705	-0.378	-0.738 to -0.017	-0.579
%H2o | FC	-0.098	-0.053	-0.559 to 0.453	0.067

Field 13-2 (Spring 2016)

I. ln(Calc ECa) Correlation Structure and ln(Calc ECa) v.s. z1-signal Correlation Structure

	depth specific ln(Calc ECa) sample depth levels 30.00	60.00	90.00	120.00	ave
ave ln(Calc ECa)	0.881	0.898	0.809	0.926	1.000
z1-signal data	0.893	0.893	0.559	0.905	0.905

II. Bulk ave ln(Calc ECa) v.s. bulk ave Pri/Sec Soil Variable Correlations

Column Labels:

0. ln(Calc ECa)
1. ln(ECe)

2. SP
3. Vol H2o
4. Bulk Den

	0	1	2	3	4
0	1.000	0.991	0.834	-0.178	-0.834
1	0.991	1.000	0.759	-0.230	-0.759
2	0.834	0.759	1.000	-0.174	-1.000
3	-0.178	-0.230	-0.174	1.000	0.174
4	-0.834	-0.759	-1.000	0.174	1.000

IV. ECe <-> Calc ECa Signal Deterioration: by depth

depth level	% Signal Deterioration
30.00	1.9
60.00	3.1
90.00	1.9
120.00	5.7
ave	1.8

V. Observed bulk ave & depth specific Pri/Sec Soil Variables v.s. z1-signal Correlations

Pri/Sec Soil Variable	sample depth levels 30.00	60.00	90.00	120.00	ave
ln(ECe)	0.888	0.844	0.541	0.935	0.915
SP	0.630	0.660	0.575	0.501	0.699
Vol H2o	0.436	-0.152	-0.232	-0.475	-0.288
Bulk Den	-0.630	-0.660	-0.575	-0.501	-0.699

VI. Predicted v.s. observed Bulk ave Pri/Sec Soil Variable / z1-signal Correlation Estimates

DPPC Model Correlation: 0.905

Pri/Sec Soil Variable	Calc CECa Corr	Prd ECa Corr	95% CI	Obs ECa Corr
ln(ECe)	0.991	0.897	0.862 to 0.932	0.915
SP	0.834	0.755	0.614 to 0.896	0.699
Vol H2o	-0.178	-0.161	-0.413 to 0.091	-0.288
Bulk Den	-0.834	-0.755	-0.896 to -0.614	-0.699

Field 13-2 (Fall 2016)

I. ln(Calc ECa) Correlation Structure and

ln(Calc ECa) v.s. z1-signal Correlation Structure

	depth specific ln(Calc ECa) sample depth levels				
	30.00	60.00	90.00	120.00	ave
ave ln(Calc ECa)	0.881	0.974	0.888	0.938	1.000
z1-signal data	0.694	0.817	0.748	0.641	0.788

II. Bulk ave ln(Calc ECa) v.s. bulk ave Pri/Sec Soil Variable Correlations

Column Labels:

0. ln(Calc ECa)
1. ln(ECe)
2. SP
3. Vol H2o
4. Bulk Den

	0	1	2	3	4
0	1.000	0.930	0.765	0.672	-0.765
1	0.930	1.000	0.485	0.502	-0.485
2	0.765	0.485	1.000	0.628	-1.000
3	0.672	0.502	0.628	1.000	-0.628
4	-0.765	-0.485	-1.000	-0.628	1.000

IV. ECe <-> Calc ECa Signal Deterioration: by depth

depth level	% Signal Deterioration
30.00	4.0
60.00	4.8
90.00	19.1
120.00	45.0
ave	13.5

V. Observed bulk ave & depth specific Pri/Sec Soil Variables v.s. z1-signal Correlations

Pri/Sec Soil Variable	sample depth levels 30.00	60.00	90.00	120.00	ave
ln(ECe)	0.630	0.766	0.578	0.252	0.660
SP	0.648	0.546	0.757	0.696	0.761
Vol H2o	0.654	0.645	0.239	-0.238	0.492
Bulk Den	-0.648	-0.546	-0.757	-0.696	-0.761

VI. Predicted v.s. observed Bulk ave Pri/Sec Soil

Variable / z1-signal Correlation Estimates

DPPC Model Correlation: 0.788

Pri/Sec Soil Variable	Calc CECa Corr	Prd ECa Corr	95% CI	Obs ECa Corr
ln(ECe)	0.930	0.733	0.597 to 0.869	0.660
SP	0.765	0.603	0.364 to 0.841	0.761
Vol H2o	0.672	0.529	0.254 to 0.804	0.492
Bulk Den	-0.765	-0.603	-0.841 to -0.364	-0.761

Field 13-2 (Spring 2017)

I. ln(Calc ECa) Correlation Structure and
ln(Calc ECa) v.s. z1-signal Correlation Structure

	depth specific ln(Calc ECa) sample depth levels 30.00	60.00	90.00	120.00	ave
ave ln(Calc ECa)	0.958	0.967	0.962	0.978	1.000
z1-signal data	0.947	0.914	0.867	0.955	0.949

II. Bulk ave ln(Calc ECa) v.s. bulk ave Pri/Sec Soil Variable Correlations

Column Labels:
0. ln(Calc ECa)
1. ln(ECe)
2. SP
3. Vol H2o
4. Bulk Den
5. %H2o | FC

	0	1	2	3	4	5
0	1.000	0.992	0.886	-0.190	-0.886	-0.641
1	0.992	1.000	0.825	-0.212	-0.825	-0.623
2	0.886	0.825	1.000	-0.276	-1.000	-0.750
3	-0.190	-0.212	-0.276	1.000	0.276	0.835
4	-0.886	-0.825	-1.000	0.276	1.000	0.750
5	-0.641	-0.623	-0.750	0.835	0.750	1.000

IV. ECe <-> Calc ECa Signal Deterioration: by depth

depth level	% Signal Deterioration
30.00	4.3
60.00	1.2
90.00	6.8

120.00	10.6
ave	1.6

V. Observed bulk ave & depth specific Pri/Sec Soil Variables v.s. z1-signal Correlations

Pri/Sec Soil Variable	sample depth levels 30.00	60.00	90.00	120.00	ave
ln(ECe)	0.929	0.917	0.851	0.892	0.937
SP	0.889	0.790	0.651	0.795	0.884
Vol H2o	0.029	-0.062	-0.367	-0.643	-0.350
Bulk Den	-0.889	-0.790	-0.651	-0.795	-0.884
%H2o | FC	-0.201	-0.584	-0.543	-0.849	-0.738

VI. Predicted v.s. observed Bulk ave Pri/Sec Soil Variable / z1-signal Correlation Estimates

DPPC Model Correlation: 0.949

Pri/Sec Soil Variable	Calc CECa Corr	Prd ECa Corr	95% CI	Obs ECa Corr
ln(ECe)	0.992	0.941	0.917 to 0.966	0.937
SP	0.886	0.840	0.752 to 0.929	0.884
Vol H2o	-0.190	-0.181	-0.367 to 0.006	-0.350
Bulk Den	-0.886	-0.840	-0.929 to -0.752	-0.884
%H2o | FC	-0.641	-0.608	-0.754 to -0.463	-0.738

Field 13-2 (Fall 2017)

I. Calc ECa Correlation Structure and Calc ECa v.s. z1-signal Correlation Structure

	depth specific Calc ECa sample depth levels 30.00	60.00	90.00	120.00	ave
ave Calc ECa	0.785	0.804	0.770	0.906	1.000
z1-signal data	0.926	0.600	0.598	0.622	0.812

II. Bulk ave Calc ECa v.s. bulk ave Pri/Sec Soil Variable Correlations

Column Labels:

0. Calc ECa
1. ECe
2. SP

3. Vol H2o
4. Bulk Den
5. %H2o | FC

	0	1	2	3	4	5
0	1.000	0.941	0.856	-0.232	-0.856	-0.778
1	0.941	1.000	0.637	-0.477	-0.637	-0.839
2	0.856	0.637	1.000	0.107	-1.000	-0.576
3	-0.232	-0.477	0.107	1.000	-0.107	0.741
4	-0.856	-0.637	-1.000	-0.107	1.000	0.576
5	-0.778	-0.839	-0.576	0.741	0.576	1.000

IV. ECe <-> Calc ECa Signal Deterioration: by depth

depth level	% Signal Deterioration
30.00	4.4
60.00	4.4
90.00	15.5
120.00	29.0
ave	11.7

V. Observed bulk ave & depth specific Pri/Sec Soil Variables v.s. z1-signal Correlations

Pri/Sec Soil Variable	sample depth levels 30.00	60.00	90.00	120.00	ave
ECe	0.901	0.544	0.403	0.251	0.644
SP	0.748	0.567	0.717	0.785	0.882
Vol H2o	0.201	0.006	0.020	-0.088	0.049
Bulk Den	-0.748	-0.567	-0.717	-0.785	-0.882
%H2o | FC	-0.115	-0.291	-0.537	-0.601	-0.552

VI. Predicted v.s. observed Bulk ave Pri/Sec Soil Variable / z1-signal Correlation Estimates

DPPC Model Correlation: 0.812

Pri/Sec Soil Variable	Calc CECa Corr	Prd ECa Corr	95% CI	Obs ECa Corr
ECe	0.941	0.764	0.645 to 0.883	0.644
SP	0.856	0.695	0.513 to 0.877	0.882
Vol H2o	-0.232	-0.188	-0.530 to 0.154	0.049
Bulk Den	-0.856	-0.695	-0.877 to -0.513	-0.882
%H2o | FC	-0.778	-0.631	-0.852 to -0.410	-0.552

Field 13-6 (Spring 2016

I. ln(Calc ECa) Correlation Structure and
ln(Calc ECa) v.s. z1-signal Correlation Structure

	depth specific ln(Calc ECa) sample depth levels				
	30.00	60.00	90.00	120.00	ave
ave ln(Calc ECa)	0.958	0.943	0.972	0.870	1.000
z1-signal data	0.846	0.748	0.741	0.670	0.790

II. Bulk ave ln(Calc ECa) v.s. bulk ave Pri/Sec Soil Variable Correlations

Column Labels:
0. ln(Calc ECa)
1. ln(ECe)
2. SP
3. Vol H2o
4. Bulk Den

	0	1	2	3	4
0	1.000	0.982	0.813	-0.107	-0.813
1	0.982	1.000	0.693	-0.144	-0.693
2	0.813	0.693	1.000	-0.120	-1.000
3	-0.107	-0.144	-0.120	1.000	0.120
4	-0.813	-0.693	-1.000	0.120	1.000

IV. ECe <-> Calc ECa Signal Deterioration: by depth

depth level	% Signal Deterioration
30.00	2.5
60.00	6.1
90.00	11.8
120.00	6.0
ave	3.6

V. Observed bulk ave & depth specific Pri/Sec Soil Variables v.s. z1-signal Correlations

Pri/Sec Soil Variable	sample depth levels 30.00	60.00	90.00	120.00	ave
ln(ECe)	0.858	0.674	0.618	0.636	0.742
SP	0.308	0.718	0.708	0.535	0.709
Vol H2o	0.123	0.387	0.093	-0.070	0.219
Bulk Den	-0.308	-0.718	-0.708	-0.535	-0.709

VI. Predicted v.s. observed Bulk ave Pri/Sec Soil
Variable / z1-signal Correlation Estimates

DPPC Model Correlation: 0.790

Pri/Sec Soil Variable	Calc CECa Corr	Prd ECa Corr	95% CI	Obs ECa Corr
ln(ECe)	0.982	0.775	0.705 to 0.845	0.742
SP	0.813	0.642	0.427 to 0.857	0.709
Vol H2o	-0.107	-0.085	-0.452 to 0.282	0.219
Bulk Den	-0.813	-0.642	-0.857 to -0.427	-0.709

Field 13-6 (Fall 2016)

I. ln(Calc ECa) Correlation Structure and
ln(Calc ECa) v.s. z1-signal Correlation Structure

	depth specific ln(Calc ECa) sample depth levels 30.00	60.00	90.00	120.00	ave
ave ln(Calc ECa)	0.793	0.873	0.946	0.875	1.000
z1-signal data	0.765	0.686	0.737	0.781	0.844

II. Bulk ave ln(Calc ECa) v.s. bulk ave Pri/Sec Soil Variable Correlations

Column Labels:
0. ln(Calc ECa)
1. ln(ECe)
2. SP
3. Vol H2o
4. Bulk Den

	0	1	2	3	4
0	1.000	0.969	0.867	-0.138	-0.867
1	0.969	1.000	0.720	-0.220	-0.720
2	0.867	0.720	1.000	-0.061	-1.000
3	-0.138	-0.220	-0.061	1.000	0.061
4	-0.867	-0.720	-1.000	0.061	1.000

IV. ECe <-> Calc ECa Signal Deterioration: by depth

depth level	% Signal Deterioration
30.00	7.8
60.00	6.6
90.00	7.9
120.00	6.2

ave 6.2

V. Observed bulk ave & depth specific Pri/Sec Soil Variables v.s. z1-signal Correlations

Pri/Sec Soil Variable	sample depth levels 30.00	60.00	90.00	120.00	ave
ln(ECe)	0.684	0.580	0.671	0.725	0.784
SP	0.272	0.722	0.752	0.773	0.788
Vol H2o	0.158	0.169	0.205	-0.189	0.082
Bulk Den	-0.272	-0.722	-0.752	-0.773	-0.788

VI. Predicted v.s. observed Bulk ave Pri/Sec Soil Variable / z1-signal Correlation Estimates

DPPC Model Correlation: 0.844

Pri/Sec Soil Variable	Calc CECa Corr	Prd ECa Corr	95% CI	Obs ECa Corr
ln(ECe)	0.969	0.818	0.737 to 0.898	0.784
SP	0.867	0.731	0.570 to 0.893	0.788
Vol H2o	-0.138	-0.117	-0.437 to 0.203	0.082
Bulk Den	-0.867	-0.731	-0.893 to -0.570	-0.788

Field 13-6 (Spring 2017)

I. ln(Calc ECa) Correlation Structure and ln(Calc ECa) v.s. z1-signal Correlation Structure

	depth specific ln(Calc ECa) sample depth levels 30.00	60.00	90.00	120.00	ave
ave ln(Calc ECa)	0.922	0.973	0.975	0.935	1.000
z1-signal data	0.862	0.903	0.945	0.966	0.963

II. Bulk ave ln(Calc ECa) v.s. bulk ave Pri/Sec Soil Variable Correlations

Column Labels:
0. ln(Calc ECa)
1. ln(ECe)
2. SP
3. Vol H2o
4. Bulk Den
5. %H2o | FC

	0	1	2	3	4	5
0	1.000	0.991	0.892	0.383	-0.892	-0.621
1	0.991	1.000	0.823	0.310	-0.823	-0.611
2	0.892	0.823	1.000	0.488	-1.000	-0.648
3	0.383	0.310	0.488	1.000	-0.488	0.344
4	-0.892	-0.823	-1.000	-0.488	1.000	0.648
5	-0.621	-0.611	-0.648	0.344	0.648	1.000

IV. ECe <-> Calc ECa Signal Deterioration: by depth

depth level	% Signal Deterioration
30.00	4.5
60.00	1.7
90.00	6.3
120.00	6.2
ave	2.0

V. Observed bulk ave & depth specific Pri/Sec Soil Variables v.s. z1-signal Correlations

Pri/Sec Soil Variable	sample depth levels 30.00	60.00	90.00	120.00	ave
ln(ECe)	0.780	0.894	0.942	0.975	0.951
SP	0.820	0.748	0.616	0.827	0.872
Vol H2o	-0.089	0.421	0.451	0.159	0.344
Bulk Den	-0.820	-0.748	-0.616	-0.827	-0.872
%H2o | FC	-0.715	-0.351	-0.203	-0.578	-0.644

VI. Predicted v.s. observed Bulk ave Pri/Sec Soil Variable / z1-signal Correlation Estimates

DPPC Model Correlation: 0.963

Pri/Sec Soil Variable	Calc CECa Corr	Prd ECa Corr	95% CI	Obs ECa Corr
ln(ECe)	0.991	0.954	0.932 to 0.976	0.951
SP	0.892	0.859	0.786 to 0.932	0.872
Vol H2o	0.383	0.369	0.220 to 0.518	0.344
Bulk Den	-0.892	-0.859	-0.932 to -0.786	-0.872
%H2o | FC	-0.621	-0.598	-0.725 to -0.472	-0.644

Field 13-6 (Fall 2017)

I. ln(Calc ECa) Correlation Structure and ln(Calc ECa) v.s. z1-signal Correlation Structure

	depth specific sample depth levels				
	30.00	60.00	90.00	120.00	ave
ave ln(Calc ECa)	0.899	0.936	0.975	0.931	1.000
z1-signal data	0.857	0.851	0.873	0.863	0.917

II. Bulk ave ln(Calc ECa) v.s. bulk ave Pri/Sec Soil Variable Correlations

Column Labels:
0. ln(Calc ECa)
1. ln(ECe)
2. SP
3. Vol H2o
4. Bulk Den
5. %H2o | FC

	0	1	2	3	4	5
0	1.000	0.967	0.838	-0.015	-0.838	-0.774
1	0.967	1.000	0.675	-0.077	-0.675	-0.647
2	0.838	0.675	1.000	0.017	-1.000	-0.914
3	-0.015	-0.077	0.017	1.000	-0.017	0.388
4	-0.838	-0.675	-1.000	-0.017	1.000	0.914
5	-0.774	-0.647	-0.914	0.388	0.914	1.000

IV. ECe <-> Calc ECa Signal Deterioration: by depth

depth level	% Signal Deterioration
30.00	9.3
60.00	6.9
90.00	9.3
120.00	3.7
ave	6.5

V. Observed bulk ave & depth specific Pri/Sec Soil Variables v.s. z1-signal Correlations

Pri/Sec Soil Variable	sample depth levels 30.00	60.00	90.00	120.00	ave
ln(ECe)	0.841	0.831	0.886	0.908	0.927
SP	0.335	0.616	0.655	0.783	0.703
Vol H2o	0.548	-0.054	-0.231	-0.665	-0.187
Bulk Den	-0.335	-0.616	-0.655	-0.783	-0.703
%H2o | FC	0.384	-0.483	-0.662	-0.816	-0.724

VI. Predicted v.s. observed Bulk ave Pri/Sec Soil

Variable / z1-signal Correlation Estimates

DPPC Model Correlation: 0.917

Pri/Sec Soil Variable	Calc CECa Corr	Prd ECa Corr	95% CI	Obs ECa Corr
ln(ECe)	0.967	0.887	0.826 to 0.948	0.927
SP	0.838	0.768	0.637 to 0.899	0.703
Vol H2o	-0.015	-0.014	-0.254 to 0.226	-0.187
Bulk Den	-0.838	-0.768	-0.899 to -0.637	-0.703

APPENDIX C: AVERAGE SOIL SALINITY ECE (DS/M), STANDARD DEVIATION AND RANGE FOR EACH DEPTH FOR THE 12 SAMPLED LOCATIONS IN EACH FIELD

	Spring 2016		Fall 2016		Spring 2017		Fall 2017	
Field 10-6 (TWG)								
Depth (cm)	**Mean**	**Range**	**Mean**	**Range**	**Mean**	**Range**	**Mean**	**Range**
0-30	11.2	3.4- 22.4	15.6	5.8 - 41.5	12.1	5.0 - 28.9	14.3	2.9 - 27.3
30-60	14.2	3.0- 27.7	16.4	4.2 - 30.4	15.1	4.8 - 32.1	16.2	4.1 - 24.9
60-90	12.5	3.4- 21.0	17.3	5.2 - 26.6	15.8	4.7 - 24.9	15.9	4.3 - 22.5
90-120	13.0	3.4- 27.8	15.7	4.6 - 23.2	15.3	4.6 - 23.5	14.3	3.9 - 25.4
[0-120]	**12.7**	**3.0- 27.8**	**16.2**	**4.2 - 41.5**	**14.6**	**4.6 - 32.1**	**15.2**	**2.9 - 27.3**
Field 13-1 (TWG)								
0-30	13.3	8.6- 18.3	14.4	9.6 - 22.4	12.2	8.3 - 18.1	13.6	10.3 - 18.2
30-60	19.9	10.9- 25.9	19.0	13.7 - 25.4	16.8	11.0 - 26.1	19.9	14.3 - 25.1
60-90	21.2	14.3- 30.2	19.6	13.4 - 28.9	18.9	11.5 - 26.7	20.6	14.7 - 30.1
90-120	23.6	17.8- 30.8	22.2	12.1 - 32.7	18.9	13.0 - 28.8	21.4	14.9 - 26.9
[0-120]	**19.5**	**8.6- 30.8**	**18.8**	**9.6 - 32.7**	**16.7**	**8.3 - 28.8**	**18.9**	**10.3 - 26.9**
Field 13-2 (ALF)								
0-30	10.0	5.4- 19.7	8.2	5.1 - 12.6	7.20	4.2 - 13.3	7.10	4.5 - 9.3
30-60	14.3	7.0- 18.2	12.1	7.7 - 15.7	11.8	5.1 - 20.1	13.8	10.4 - 16.9
60-90	17.1	11.9- 27.4	15	11.2 - 21.4	14.3	7.7 - 18.7	16.3	13.5 - 18.7
90-120	17.5	11.6- 24.9	15.3	10.5 - 19.7	15.4	9.3 - 24.6	15.9	11.2 - 20.4
[0-120]	**14.7**	**5.4- 27.4**	**12.6**	**5.1 - 21.4**	**12.2**	**4.2 - 24.6**	**13.3**	**4.5 - 20.4**
Field 13-6 (ALF)								
0-30	5.70	2.9- 8.31	7.36	5.2 - 11.3	5.21	2.5 - 9.1	6.80	4.7 - 9.0
30-60	9.10	4.2- 14.1	10.6	6.2 - 15.5	10.2	4.5 - 22.7	10.6	6.1 - 15.5
60-90	10.8	6.2- 14.5	12.3	9.1 - 16.4	12.1	5.7 - 20.6	12.5	6.8 - 17.2
90-120	10.4	4.6- 15.6	11.3	7.5 - 17.2	10.9	6.6 - 16.2	12.0	8.1 - 15.5
[0-120]	**9.02**	**2.9- 15.6**	**10.4**	**5.2 - 17.2**	**9.6**	**2.5 - 22.7**	**10.5**	**4.7 - 17.2**

APPENDIX D: FORAGE DATA

Field 10-6

```
Pearson's product-moment correlation
data:  Forage_10_6S$`Ave Forage wt.` and Forage_10_6S$`Ave Na conc.`
t = -0.041083, df = 10, p-value = 0.968
alternative hypothesis: true correlation is not equal to 0
95 percent confidence interval:
 -0.5825491  0.5651243
sample estimates:
        cor  -0.01299053


Pearson's product-moment correlation
data:  Forage_10_6S$`Ave Forage wt.` and Forage_10_6S$`ECe(avg)`
t = -2.269, df = 10, p-value = 0.04665
alternative hypothesis: true correlation is not equal to 0
95 percent confidence interval:
 -0.86685504 -0.01364252
sample estimates:
       cor  -0.5829797
```

Field 13-1

```
Pearson's product-moment correlation

data:  Forage_13_1S17$`Ave Forage dry wt.` and Forage_13_1S17$`Ave Na
conc.`
t = -1.8676, df = 10, p-value = 0.09137
alternative hypothesis: true correlation is not equal to 0
95 percent confidence interval:
 -0.83789292  0.09232005
```

```
sample estimates:
       cor  -0.5085245


      Pearson's product-moment correlation

data:  Forage_13_1S17$`Ave Forage dry wt.` and Forage_13_1S17$`Soil Ece
(ave)`
t = 0.39756, df = 10, p-value = 0.6993
alternative hypothesis: true correlation is not equal to 0
95 percent confidence interval:
 -0.4837974  0.6519670
sample estimates:
     cor  0.124738
```

Field 13-2

```
      Pearson's product-moment correlation

data:  Forage_13_2S$`Ave Forage dry wt` and Forage_13_2S$`Avg Na conc.`
t = -2.6878, df = 10, p-value = 0.02278
alternative hypothesis: true correlation is not equal to 0
95 percent confidence interval:
 -0.8905411 -0.1173488
sample estimates:
       cor  -0.6476344


      Pearson's product-moment correlation

data:  Forage_13_2S$`Ave Forage dry wt` and Forage_13_2S$Ece
t = -4.5576, df = 10, p-value = 0.001046
alternative hypothesis: true correlation is not equal to 0
```

```
95 percent confidence interval:
 -0.9483418 -0.4686977
sample estimates:
       cor  -0.8216001
```

Field 13-6

```
      Pearson's product-moment correlation

data:  Forage_13_6S17$`Ave Forage dry wt.` and Forage_13_6S17$`Avg. Na
conc.`
t = -1.4094, df = 10, p-value = 0.189
alternative hypothesis: true correlation is not equal to 0
95 percent confidence interval:
 -0.7952107  0.2176564
sample estimates:
       cor -0.4070971

      Pearson's product-moment correlation

data:  Forage_13_6S17$`Ave Forage dry wt.` and Forage_13_6S17$`Ece ave`
t = -3.3236, df = 10, p-value = 0.0077
alternative hypothesis: true correlation is not equal to 0
95 percent confidence interval:
 -0.917076 -0.257728
sample estimates:
       cor -0.7244725
```